

A GENERALIZED TREATMENT OF THE ORDER-DISORDER
TRANSFORMATION IN ALLOYS
AND ITS EFFECT ON THEIR MAGNETIC PROPERTIES

Thesis by

Michael Baskes

In Partial Fulfillment of the Requirements

For the Degree of
Doctor of Philosophy

California Institute of Technology

Pasadena, California 91109

1970

(Submitted December 12, 1969)

ACKNOWLEDGMENTS

I wish to express my sincere gratitude to Professor F. S. Buffington who suggested the problems treated in this dissertation and offered valuable guidance in this research.

I would like to acknowledge the financial support of the National Science Foundation and the John and Fannie Hertz Foundation.

I also would like to thank Mrs. Vivian Davies for her help in typing the thesis.

Abstract

A theory of the order-disorder transformation is developed in complete generality. The general theory is used to calculate long range order parameters, short range order parameters, energy, and phase diagrams for a face centered cubic binary alloy. The theoretical results are compared to the experimental determination of the copper-gold system. Values for the two adjustable parameters are obtained.

An explanation for the behavior of magnetic alloys is developed. Curie temperatures and magnetic moments of the first transition series elements and their alloys in both the ordered and disordered states are predicted. Experimental agreement is excellent in most cases. It is predicted that the state of order can effect the magnetic properties of an alloy to a considerable extent in alloys such as Ni_3Mn . The values of the adjustable parameter used to fix the level of the Curie temperature, and the adjustable parameter that expresses the effect of ordering on the Curie temperature are obtained.

TABLE OF CONTENTS

	PAGE
I. Introduction	1
II. Calculation of the Free Energy of an Alloy	5
A. Energy	5
B. Entropy	19
C. Free Energy Minimization	21
III. Application of the Order-Disorder Theory	24
IV. Magnetism in Alloys	41
A. Magnetic Properties of Disordered Alloys	51
B. Magnetic Properties of Ordered Alloys	67
1. Saturation moment	67
2. Curie Temperature	69
V. Conclusion	94
VI. References	97
Appendix I	100
Values of $N(H, i, I, k, J, j)/N_{IH}^i$ for various lattice structures and sublattices.	
Appendix II	104
Energy of a binary alloy on two sublattices.	
Appendix III	109
Entropy of a binary alloy on two sublattices.	
Appendix IV	111
Minimization on the free energy of short range order.	

LIST OF TABLES

TABLE		PAGE
I	Values of w for various lattice structures and superlattices	15
II	Order parameters for a f.c.c. AB_3 stoichiometric alloy for $p = 0$	26
III	Values of m, J, u, g, B, n_0, T_C , and θ_0 for the first series transition elements	49
IV	Number of electrons element contributes to a nickel alloy	52
V	Number of electrons element contributes to cobalt alloys	59
VI	Number of electrons element contributes to iron alloys	66

LIST OF FIGURES

FIGURE		PAGE
1	The Slater-Pauling curve	3
2	Relationships between distances and sites used to define $N(H, i, l, k, J, j)$.	6
3	Relationships between atoms and sites used to define $p_i(\beta l \alpha H)$.	7
4	Long range (S) and short range ($\sigma_i, q/q_L$) order coefficients for the f.c.c. AB_3 stoichiometric alloy $q = q_{AB} = q_{BB}$	29
5	Long range (S) and short range ($\sigma_i, q/q_L$) order coefficients for the f.c.c. AB_3 stoichiometric alloy $q = q_{AB} = q_{BB}$	30
6	Long range (S) and short range (σ_1) order coefficients for f.c.c. AB alloys of various compositions	31
7	Energy of the f.c.c. AB_3 stoichiometric alloy for various values of p	32
8	Energy of the f.c.c. AB_3 alloy for various compositions	33
9	Energy of the f.c.c. AB alloy for various compositions	34
10	Partial phase diagram for $p = 0$ with no lattice parameter variation	35
11	Partial phase diagram for $p = .025$ with no lattice parameter variation	36
12	Partial phase diagram for $p = -.025$ with no lattice parameter variation	37
13	Partial phase diagram for $p = 0$ including lattice parameter variation	38
14	Partial phase diagram for $p = -.025$ including lattice parameter variation	39
15	Experimental phase diagram of the copper-gold system	40
16	Comparison of the values of B_β commonly used and the values used in this treatment	47

List of Figures (Cont'd.)

FIGURE		PAGE
17	Saturation moments and Curie temperatures of nickel alloys	73
18	Saturation moments and Curie temperatures for the nickel-cobalt alloys	74
19	Curie temperature of iron-nickel alloys under various assumptions specified in the text	75
20	Saturation moments in iron-nickel alloys	76
21	Curie temperature of iron-nickel alloys	77
22	Saturation moments of nickel-manganese alloys under various assumptions specified in the text	78
23	Saturation moments of disordered nickel-manganese alloys	79
24	Curie temperature of disordered nickel-manganese alloys	80
25	Saturation moments and Curie temperatures for the iron-cobalt alloys	81
26	Saturation moments and Curie temperatures of cobalt alloys	82
27	Saturation moment and Curie temperature of iron alloys	83
28	Saturation moments and Curie temperatures for the iron-chromium alloys	84
29	Saturation moments and Curie temperatures of iron-vanadium alloys	85
30	Theoretical values of the saturation moments of nickel-manganese alloys for various degrees of long range order, S , and short range order, q_{AA_1} , q_{AB_1} , q_{BB_1} , $q_1 = q_{AA_1} = q_{AB_1} = q_{BB_1}$	86
31	Saturation magnetization of nickel manganese alloys quenched from various temperatures, T	87
32	Curie temperatures of nickel alloys with various degrees of long range order, S	88

List of Figures (Cont'd.)

FIGURE		PAGE
33	Curie temperatures of nickel alloys with various degrees of long range order, S	89
34	Curie temperatures of fully ordered nickel alloys for various values of the magnetic interaction parameter, λ_1	90
35	Curie temperatures of nickel manganese alloys with various degrees of long range order, S	91
36	Curie temperatures of nickel manganese alloys with various degrees of long range order, S	92
37	Curie temperatures of fully ordered nickel manganese alloys for various values of the magnetic interaction parameter, λ_1	93

Introduction

It was first proposed by Tammann¹ that the atoms in an alloy may arrange themselves in an ordered structure. The first use of x-rays to show the presence of an ordered structure was made by Johansson and Linde². Nix et al³ used neutron scattering to show the presence of order in alloys whose components had almost identical x-ray scattering factors. It is also possible to use electron diffraction⁴ to determine the presence of order in alloys.

The experimental evidence implies the existence of an ordered structure in which like atoms tend to surround themselves with as many unlike atoms as possible. Consideration of the free energy leads to the prediction that an alloy ordered at low temperatures will disorder at high temperatures where the temperature times entropy term becomes more important. Experimental evidence^{5,6} also implies that there are two kinds of ordering, long range order and short range order. If long range order exists each type of atom migrates to a designated atomic site forming a superlattice.

There were many early theoretical attempts^{7,8,9,10} to explain the order-disorder transformation in alloys. Bragg and Williams¹¹ introduced the most famous of these theories. Their treatment considered only long range order, the AB type of superlattice, binary alloys of stoichiometric composition, and ignored atomic interactions other than those with first nearest neighbors. Their method was refined and extended by Bethe¹², Peierls¹³, Chang¹⁴, Easthope¹⁵ and others to include the short range order of first nearest neighbors, the

AB_3 type of superlattice, and non-stoichiometric compositions. The extension to non-stoichiometric compositions, however, was incorrect as it did not predict a maximum critical temperature of long range order around the AB_3 stoichiometric composition contrary to experimental evidence.

Cowley¹⁶ and Fournet¹⁷ considered interactions with other than first nearest neighbor by assuming a small but arbitrary contribution from the second and third nearest neighbors. The contribution was determined by those values that fit the experimental data best. Cowley's¹⁶ theory of short range order is quite good. In extending it to long range order, however, he erroneously considers only those atoms on a simple cubic lattice in taking the limit of the short range order parameters. He also errs in assuming that the superlattice sites are always available in the same ratio as the compositions of the atoms. This assumption leads to an incorrect dependence on composition.

The major deficiencies of the above theories are 1) insufficient generality in treating all crystal structures and superlattices; 2) improper treatment at the variations with composition; 3) incomplete treatment of the interaction of neighbors other than the first nearest; 4) inability to treat more than two components; and 5) inability to treat the combination and interaction of long and short range order.

Ordering in alloys can have rather dramatic effects on their magnetic properties. As one example, the ordered stoichiometric alloy Ni_3Mn has a Curie temperature that is 600° higher than the disordered alloy. Grabbe¹⁸ has shown that ordering increases the saturation magnetization of iron-nickel alloys with the largest increase near Ni_3Fe .

The variation in the saturation magnetization in disordered alloys is usually explained by considering the electron concentration. The Slater-Pauling curve¹⁹ (Fig. 1) shows that this relationship is usually valid, although there are some prominent exceptions (Co-Cr, Co-Mn, Ni-Mn, Ni-Cr, Ni-V).

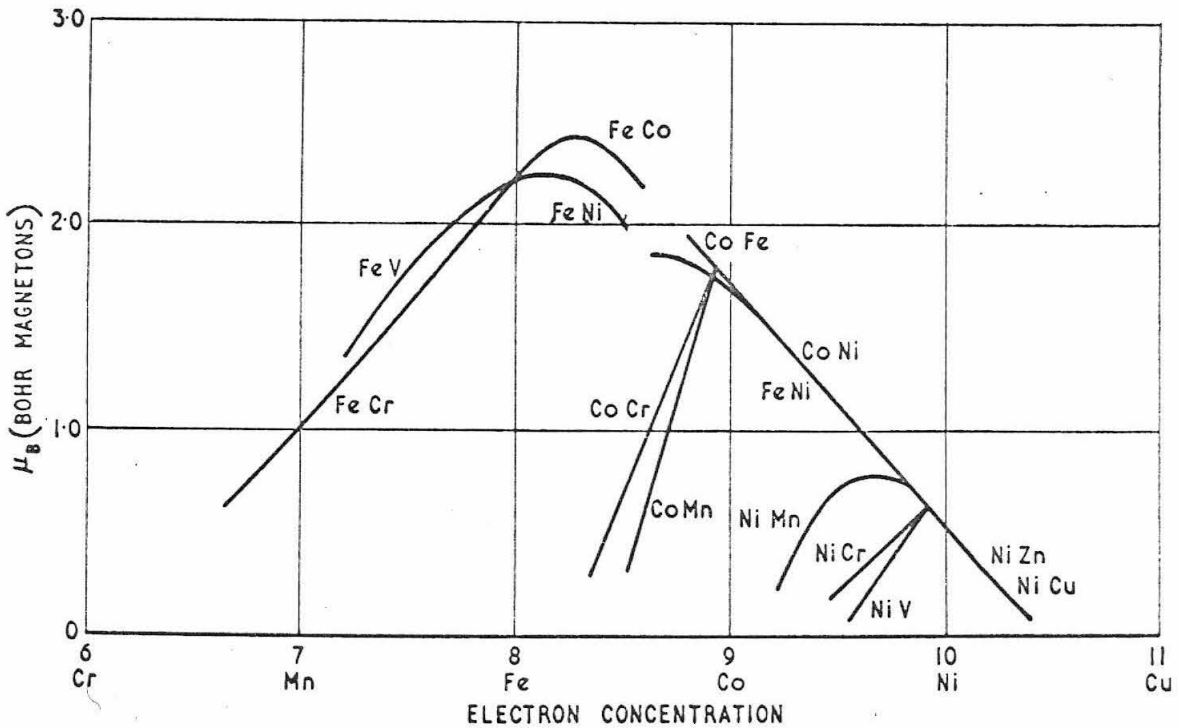


Fig. 1. The Slater-Pauling curve²⁰

Goldman and Smoluchowski²¹ have considered the saturation magnetization to be determined by the local electron concentration rather than the average electron concentration. Smoluchowski²² applied this idea to iron-cobalt alloys with good success. The application to other alloy systems has not been fruitful.

Sato²³ and Muto et al.²⁴ have made theoretical studies on the effect of order on magnetic properties without much success in developing a working theory. Bell, Lavis, and Fairburn²⁵ have made a theoretical study on the equilibrium behavior of ordered magnetic alloys. Their results are of a very qualitative nature and virtually impossible to compare with experiment without making simplifying assumptions that render the theory practically useless.

There has been little success in obtaining a comprehensive theory of magnetic behavior of alloys in either the disordered or ordered states.

The objectives of this study are 1) to derive a theory of the order-disorder transformation in sufficient generality so that it may be applied to any crystal structure or superlattice, multicomponent systems, and nonstoichiometric compositions; 2) to examine the behavior and interaction of long and short range order; 3) to determine the effect of the interaction of neighbors other than first nearest; and 4) to explain the magnetic behavior of alloys and how it is influenced by ordering.

Calculation of the Free Energy of an Alloy

Energy

Consider a space lattice of N sites. Divide this lattice into sublattices of types designated by A, B, C, \dots . Let $H, I,$ or J be dummy indices each of which may be equal to A, B, C, \dots . Define $n_H(n_I, n_J)$ as the fraction of sites contained in the H th(I th, J th) sublattice. Since all sites are included in one or another sublattice:

$$\sum_H n_H = 1, \quad \sum_I n_I = 1, \quad \sum_J n_J = 1 \quad (1)$$

Define N_{IH}^i as the number of I sites that are a distance r_i from an H site, where $i = 1, 2, 3, \dots$. The number of I sites a distance r_i from all H sites equals $n_H N_{IH}^i$. Similarly the number of H sites a distance r_i from all I sites equals $n_I N_{HI}^i$. Since the number of I - H pairs at distance r_i must equal the number of H - I pairs at distance r_i :

$$n_H N_{IH}^i = n_I N_{HI}^i. \quad (2)$$

For example, a body centered cubic structure may be divided into two interpenetrating simple cubic sublattices where $n_A = \frac{1}{2}$, $n_B = \frac{1}{2}$, $N_{AA}^1 = 0$, $N_{BB}^1 = 0$, $N_{AB}^1 = 8$, $N_{BA}^1 = 8$, $N_{AA}^2 = 6$, $N_{BB}^2 = 6$, $N_{AB}^2 = 0$, $N_{BA}^2 = 0$, etc.

Consider an H site. (Fig. 2) Look at all I sites at a distance

r_i from this H site. Define the number of J sites a distance r_k ($k = 1, 2, 3, \dots$). From these I sites and a distance r_j ($j = 1, 2, 3, \dots$). From the H site as $N(H, i, I, k, J, j)$. Then by symmetry:
 $N(H, i, I, k, J, j) = N(H, j, J, k, I, i)$.

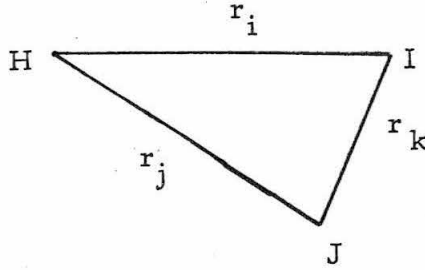


Fig. 2. Relationships between distances and sites used to define $N(H, i, I, k, J, j)$.

The values of $N(H, i, I, k, J, j)$ for various lattice structure and superlattices are given in Appendix I.

An atom of types designated by a, b, c, \dots , is located at each site of the space lattice. Vacant sites may be considered by assuming one type of atom to be vacancies. Let α, β , or γ be dummy indices each of which may be equal to a, b, c, \dots . Define m_α (m_β, m_γ) as the fraction of the α th (β th, γ th) type of atom. Clearly:

$$\sum_{\alpha} m_{\alpha} = 1, \quad \sum_{\beta} m_{\beta} = 1, \quad \sum_{\gamma} m_{\gamma} = 1. \quad (3)$$

Let the total number of α atoms on the H sites be given by

$$n_H N X_{\alpha}(H)$$

where $X_\alpha(H)$ is the probability of finding an α atom on an H site.
 Since each site is occupied

$$\sum_{\alpha} X_{\alpha}(H) = 1 \quad \text{for } H = A, B, C, \dots \quad (4)$$

Since the composition of each component is fixed

$$\sum_{\alpha} n_H X_{\alpha}(H) = m_{\alpha} \quad \text{for } \alpha = a, b, c, \dots \quad (5)$$

Let $p_i(\beta I | \alpha H)$ be the probability of finding a β atom on an I site given that there is an α atom on an H site that is a distance r_i from the I site. (Fig. 3).

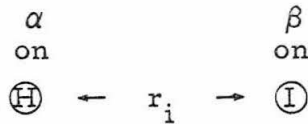


Fig. 3. Relationships between atoms and sites
 used to define $p_i(\beta I | \alpha H)$.

Since each site is occupied

$$\sum_{\beta} p_i(\beta I | \alpha H) = 1 \quad \text{for } \begin{array}{l} H, I = A, B, C, \dots \\ \alpha = a, b, c, \dots \\ i = 1, 2, 3, \dots \end{array} \quad (6)$$

The total energy, E , may be calculated by considering each atom successively as the origin and then adding the energies of all atom pairs. The energy so calculated must be divided by $2N$ as each interaction has been counted $2N$ times. If $E_{\beta\gamma}(r_k)$ is the interaction energy between a β and γ atom separated by a distance r_k ,

$$E = \frac{1}{2N} \sum_{\substack{ljk\alpha\beta\gamma HIJ}} n_H N X_{\alpha} (H) N(H, i, I, k, J, j) \quad (7)$$

$$E_{\beta\gamma}(r_k) p_i(\beta I | \alpha H) p_j(\gamma J | \alpha H)$$

The total energy may also be calculated by the classical method of considering successively one site of each sublattice as the origin and adding the energies of interaction of all atoms with the atom at the origin. In this way

$$E = \frac{1}{2} \sum_{k\beta\gamma IJ} n_I N X_{\beta} (I) N_{JI}^k p_k(\gamma J | \beta I) E_{\beta\gamma}(r_k) \quad (7a)$$

The factor of $\frac{1}{2}$ is due to counting each interaction twice.

The energy may be separated into two parts, E_{LRO} , the contribution from long range order only, and E_{SRO} the remainder.

Let

$$p_i(\beta I | \alpha H) = X_{\beta} (I) (1 + q_i(\beta I | \alpha H)) \quad (8a)$$

and similarly

$$p_j(\gamma J | \alpha H) = X_{\gamma} (J) (1 + q_j(\gamma J | \alpha H)) \quad (8b)$$

The set of q_i and q_j so defined are a quantitative measure of the short range order. They are equal to zero in the absence of short range order. The set of X 's are a quantitative measure of the long range order.

Equations (4), (6), and (8) yield:

$$\sum_{\beta} X_{\beta}(I) q_i(\beta I | \alpha H) = 0 \quad (9a)$$

and
$$\sum_{\alpha} X_{\gamma}(J) q_j(\gamma J | \alpha H) = 0 \quad (9b)$$

Since the number of α - β atom pairs at a distance r_i is equal to the number of β - α atom pairs at a distance r_i :

$$\sum_{HI} n_H X_{\alpha}(H) p_i(\beta I | \alpha H) N_{IH}^i = \sum_{IH} n_I X_{\beta}(I) p_i(\alpha H | \beta I) N_{HI}^i$$

From equation (2) $n_H N_{IH}^i = n_I N_{HI}^i$ which with equation (8a) yields:

$$\sum_{HI} n_H N_{IH}^i X_{\alpha}(H) X_{\beta}(I) [q_i(\beta I | \alpha H) - q_i(\alpha H | \beta I)] = 0$$

For

$$\begin{aligned} n_H N_{IH}^i X_{\alpha}(H) X_{\beta}(I) &\neq 0 \\ q_i(\beta I | \alpha H) &= q_i(\alpha H | \beta I) \end{aligned} \quad (10a)$$

Similarly

$$q_j(\gamma J | \alpha H) = q_j(\alpha H | \gamma J) \quad (10b)$$

Equations (10a, b) are also valid for the trivial case

$n_H N_{IH}^i X_\alpha(H) X_\beta(I) = 0$. Using equations (8a, b) in equation (7):

$$E = \frac{1}{2} \sum_{ijk\alpha\beta\gamma HIJ} n_H X_\alpha(H) N(H, i, I, k, J, j) E_{\beta\gamma}(r_k) X_\beta(I) X_\gamma(J) \\ \left[1 + q_i(\beta I | \alpha H) + q_j(\gamma J | \alpha H) + q_i(\beta I | \alpha H) q_j(\gamma J | \alpha H) \right]$$

The summation over α of the second and third terms in brackets above may be written:

$$\sum_{\alpha} X_\alpha(H) \left[q_i(\beta I | \alpha H) + q_j(\gamma J | \alpha H) \right] \\ = \sum_{\alpha} X_\alpha(H) \left[q_i(\alpha H | \beta I) + q_j(\alpha H | \gamma J) \right] \\ = \sum_{\beta} X_\beta(I) q_i(\beta I | \alpha H) + \sum_{\gamma} X_\alpha(J) q_j(\gamma J | \alpha H) = 0$$

where equations (9a, b) and (10a, b) have been used and the dummy indices have been changed.

Equation (7) may now be written:

$$E = E_{LRO} + E_{SRO}$$

where

$$E_{LRO} = \frac{1}{2} \sum_{ijk\alpha\beta\gamma HIJ} n_H X_\alpha(H) N(H, i, I, k, J, j) E_{\beta\gamma}(r_k) X_\beta(I) X_\gamma(J) \quad (11)$$

$$E_{\text{SRO}} = \frac{1}{2} \sum_{ijka\beta\gamma HIJ} n_H X_\alpha^{(H)} N(H, i, I, k, J, j) E_{\beta\gamma}(r_k) X_\beta^{(I)} X_\gamma^{(J)} q_i(\beta I | \alpha H) q_j(\gamma J | \alpha H) \quad (12)$$

Similarly we may separate equation (7a) into two parts.

$$E_{\text{LRO}} = \frac{1}{2} N \sum_{k\beta\gamma IJ} n_I N_{JI}^k X_\beta^{(I)} X_\gamma^{(J)} E_{\beta\gamma}(r_k) \quad (11a)$$

$$E_{\text{SRO}} = \frac{1}{2} N \sum_{k\beta\gamma IJ} n_I N_{JI}^k X_\beta^{(I)} X_\gamma^{(J)} q_k(\gamma J | \beta I) E_{\beta\gamma}(r_k) \quad (12a)$$

Equation (11) may be simplified considerably. Consideration of the summations over α , j , i , and H yields: ¹

$$\begin{aligned} & \sum_H n_H \sum_i \sum_j N(H, i, I, k, J, j) \sum_\alpha X_\alpha^{(H)} \\ &= \sum_H n_H \sum_i \sum_j N(H, i, I, k, J, j) \\ &= \sum_H n_H \sum_i N_{IH}^i N_{JI}^k \\ &= \sum_H n_H n_I N N_{JI}^k = n_I N N_{JI}^k \end{aligned}$$

¹ The summation over j may be performed by first considering one I site a distance r_i from the H site. The number of J sites a distance r_k from this I site and any (\sum_j) distance from the H site is simply N_{JI}^k . Now simply multiply by the number of I sites a distance r_i from the H site, i.e. N_{IH}^i .

Equation (11) may now be written

$$E_{\text{LRO}} = \frac{1}{2}N \sum_{k\beta\gamma IJ} n_I N_{JI}^k X_{\beta}^{(I)} X_{\gamma}^{(J)} E_{\beta\gamma}(r_k)$$

which is identical to equation (11a) which was calculated by the classical method.

Next, consider the summation over k in equation (11a).

Ordinarily approximations have been introduced at this stage such as the Bragg-Williams approximation of considering only the contribution from the first nearest neighbors, i.e. $k = 1$. Others have attempted to include the effect of second nearest neighbors by assuming a small, arbitrary contribution from them. The complexity introduced by considering other neighbors was usually assumed to be too much to handle. This investigation was undertaken, in part, to determine if the above approximations were indeed necessary. The development that follows leads to the conclusion that in many cases of interest the symmetry of the lattice is sufficient to insure that none of these limiting assumptions need be made.

Let N_I^k be the number of sites that are a distance r_k from an I site.

$$N_I^k = \sum_J N_{JI}^k$$

Let $c_{JI}^k = N_{JI}^k / N_I^k$ which implies $\sum_J c_{JI}^k = 1$. For each r_k there is a set of c_{JI}^k . Some of these sets of c_{JI}^k may be identical for different values of k . Each such group of sets shall be designated

by k_n ($n=1, 2, \dots$). The characteristic set of $c_{JI}^{k_n}$ shall be designated by w_{JI}^n . From above

$$\sum_J w_{JI}^n = 1 \quad (13)$$

The summation over k in equation (11a) now becomes:

$$\sum_k N_{JI}^k E_{\beta\gamma}(r_k) = \sum_n \sum_{k_n} c_{JI}^{k_n} N_I^{k_n} E_{\beta\gamma}(r_{k_n}) = \sum_n w_{JI}^n \sum_{k_n} N_I^{k_n} E_{\beta\gamma}(r_{k_n})$$

If the crystal symmetry is sufficient to insure that the number of k th neighbors to a site is independent of the site, i.e. $N_I^k = N^k$ then the summation over k in equation (11a) becomes

$$\sum_n w_{JI}^n E_{\beta\gamma}^n \quad (14)$$

where $E_{\beta\gamma}^n = \sum_{k_n} N^{k_n} E_{\beta\gamma}(r_{k_n}) = E_{\gamma\beta}^n$ equation (11a) becomes:

$$E_{LRO} = \frac{1}{2}N \sum_{n\beta\gamma IJ} n_I X_{\beta}(I) X_{\gamma}(J) w_{JI}^n E_{\beta\gamma}^n \quad (15)$$

The value of replacing the summation over k by the summation over n may be seen by considering a brief example. In the face-centered cubic AB structure there are only two sets of w_{JI}^n . For

$$k_1 = 1, 3, 5, \dots \quad w_{AB}^1 = w_{BA}^1 = \frac{2}{3}, \quad w_{AA}^1 = w_{BB}^1 = \frac{1}{3}$$

$$k_2 = 2, 4, 6, \dots \quad w_{AB}^2 = w_{BA}^2 = 0, \quad w_{AA}^2 = w_{BB}^2 = 1.$$

A similar result is found for the simple cubic AB structure, tetragonal AB structure, body centered tetragonal structure, face centered cubic AB₃ structure and the body centered cubic AB structure (Table 1). In the above cases the summation over n in equation (15) is therefore over only two values of n. For the face centered tetragonal AB₂C structure, the summation is over three values of n (Table I).

It is interesting to compare the above example with the approximation of k = 1, 2 (second neighbor) of equation (11a). For equation (11a) the summation over k becomes:

$$N_{JI}^1 E_{\beta\gamma}(r_1) + N_{JI}^2 E_{\beta\gamma}(r_2)$$

while in equation (15) the summation over n becomes:

$$w_{JI}^1 E_{\beta\gamma}^1 + w_{JI}^2 E_{\beta\gamma}^2$$

The mathematical complexity of the exact equation (14) is no more complicated than using the second neighbor approximation, yet equation (15) considers all atomic interactions.

It must be remembered that $E_{\beta\gamma}^1$ and $E_{\beta\gamma}^2$ are the weighted sums of all atomic interactions, while $E_{\beta\gamma}(r_1)$, $E_{\beta\gamma}(r_2)$, $E_{\beta\gamma}(r_3)$, ... represent the interactions at first, second, third, ... neighbor distances.

Equation (12a) may be simplified in a manner similar to that used in the simplification of equation (11a) above. Let r_n be the smallest of r_{k_n} . The summation over k in equation (12a) may be written:

$$\begin{aligned}
 \sum_k N_{JI}^k q_k(\gamma J|\beta I) E_{\beta\gamma}(r_k) &= \sum_n \sum_{k_n} c_{JI}^{k_n} N_I^{k_n} q_{k_n}(\gamma J|\beta I) E_{\beta\gamma}(r_{k_n}) \\
 &= \sum_n w_{JI}^n q_n(\gamma J|\beta I) \sum_{k_n} N^{k_n} E_{\beta\gamma}(r_{k_n}) \\
 &\quad + \sum_n w_{JI}^n \sum_{k_n} N^{k_n} E_{\beta\gamma}(r_{k_n}) (q_{k_n}(\gamma J|\beta I) - q_n(\gamma J|\beta I)) \\
 &= \sum_n w_{JI}^n q_n(\gamma J|\beta I) E_{\beta\gamma}^n + \sum_n w_{JI}^n \sum_{k_n \neq n} N^{k_n} E_{\beta\gamma}(r_{k_n}) (q_{k_n}(\gamma J|\beta I) - q_n(\gamma J|\beta I))
 \end{aligned}$$

Since $|E_{\beta\gamma}(r_k)|$ decreases rapidly with increasing r_k , it is safe to assume $|E_{\beta\gamma}(r_{k_n})| \ll |E_{\beta\gamma}(r_n)|$ $k_n \neq n$ and to ignore the second summation. This approximation is better than the usual second neighbor approximation for three reasons:

- 1) This approximation is made in the short range order energy term, while the usual approximation is made in both the long and short range order energy terms. Usually the energy of short range order is much less than that of long range order thus the above error is correspondingly less.
- 2) In the case of a large amount of short range order $q_{k_n} \rightarrow q_n$ thereby reducing the error.
- 3) For some structures the energy assumption is lessened. In the face-centered cubic case the third neighbor interactions are

regarded small compared to the first neighbor, rather than the second neighbor interactions.

Equation (12) may now be written:

$$E_{\text{SRO}} = \frac{1}{2}N \sum_{n\beta\gamma IJ} n_I w_{JI}^n X_{\beta}^{(I)} X_{\gamma}^{(J)} q_n(\gamma J | \beta I) E_{\beta\gamma}^n \quad (16)$$

The model used in this development considers the order in an alloy as a state of uniform long range order on which is superimposed overlapping clusters of short range order. Equation (16) would give the value of the energy of short range order were it not for the regions of overlap. It is convenient to define the regions of overlap as regions that do not contribute to the energy of short range order. If f is defined as the fraction of atoms found in the regions of overlap, and E'_{SRO} as the actual contribution to the energy:

$$E'_{\text{SRO}} = \frac{1}{2}N(1-f) \sum_{n\beta\gamma IJ} n_I w_{JI}^n X_{\beta}^{(I)} X_{\gamma}^{(J)} q_n(\gamma J | \beta I) E_{\beta\gamma}^n \quad (17)$$

It is possible to determine f by comparing the energies of an atom in a cluster of short range order and that of an atom in a region of overlap. In the former case the energy is $E_{\text{LRO}} + E_{\text{SRO}}$, while in the latter it is E_{LRO} . Therefore, f may be written as the Boltzmann factor:

$$f = e^{E_{\text{SRO}}/kT} \quad (18)$$

The equations obtained are completely general and permit treating systems with many components. However, it is instructive to

consider the order-disorder transformation in binary alloy systems. Specific consideration will be given to lattice structures that may be decomposed into two sublattices, such as the face-centered cubic and body-centered cubic systems. For the above special case equations (15), (12) and (17) become (Appendix II).

$$E_{LRO} = N \left\{ m_a E_{aa} + m_b E_{bb} - m_a m_b \Delta E_{ab} + (X_a(A) - m_a)(m_a - X_a(B)) \sum_n \Delta E_{ab}^n (w_{AA}^n - w_{AB}^n) \right\} \quad (19)$$

$$E_{SRO} = 2 \sum_{iIJ} n_J N_{IJ}^i X_a(I) X_a(J) q_{IJ}^i \frac{\Delta E_{ab}(r_i)}{N^i} + \sum_{ijkHIJ} n_H N(H, i, I, k, J, j) \frac{X_a(H)}{X_b(H)} X_a(I) X_a(J) q_{IH}^i q_{JH}^j \frac{\Delta E_{ab}(r_k)}{N^k} \quad (20)$$

$$E'_{SRO} = N(1-f) \sum_{nIJ} n_I w_{JI}^n X_a(I) X_a(J) q_{IJ}^n \Delta E_{ab}^n \quad (21)$$

where \sum' is over $i, j, k > 0$ $q_{IJ}^i = q_i(aI|aJ)$

E_{aa} = energy of an "a" atom in pure "a"

E_{bb} = energy of a "b" atom in pure "b"

E_{ab} = energy of a "b" atom in pure "a"

or energy of an "a" atom in pure "b"

$$\Delta E_{ab} = (E_{aa} + E_{bb} - 2E_{ab})$$

$$\Delta E_{ab}(r_i) = \frac{1}{2}(E_{aa}(r_i) + E_{bb}(r_i) - 2E_{ab}(r_i)) N^i$$

$$\Delta E_{ab}^n = \sum_{k_n} \Delta E_{ab}(r_{k_n})$$

The above derivation is given^{kⁿ} in Appendix II.

Entropy

Consider the entropy contribution from the long and short range order of all atoms that are separated by a distance r_i .

The number of I sites at a distance r_i from an α atom on an H site is

$$N_{IH}^i X_{\alpha}^{(H)} n_H N.$$

The number of β atoms on these I sites is

$$p_i(\beta I | \alpha H) N_{IH}^i X_{\alpha}^{(H)} n_H N.$$

The number of ways of arranging these β atoms on these I sites is

$$\binom{N_{IH}^i X_{\alpha}^{(H)} n_H N}{p_i(\beta I | \alpha H) N_{IH}^i X_{\alpha}^{(H)} n_H N}.$$

where $\binom{n}{k} = \frac{n!}{n!(n-k)!}$.

The number of ways of arranging all β atoms at a distance r_i from any atom on any site is

$$\prod_{\alpha HI} \binom{N_{IH}^i X_{\alpha}^{(H)} n_H N}{p_i(\beta I | \alpha H) N_{IH}^i X_{\alpha}^{(H)} n_H N}$$

The number of ways of arranging the β atoms after the γ atoms have been arranged on I sites is

$$\prod_{\alpha HI} \left(\begin{array}{c} N_{IH}^i X_{\alpha}^{(H)} n_H N (1 - p_i(\gamma I | \alpha H)) \\ p_i(\beta I | \alpha H) N_{IH}^i X_{\alpha}^{(H)} n_H N \end{array} \right)$$

The number of ways of arranging all atoms at a distance r_i from any site is:

$$W = \prod_{i\alpha\beta HI} \left(\begin{array}{c} N_{IH}^i X_{\alpha}^{(H)} n_H N \left(1 - \sum_{\gamma=1}^{\beta-1} p_i(\gamma I | \alpha H) \right) \\ p_i(\beta I | \alpha H) N_{IH}^i X_{\alpha}^{(H)} n_H N \end{array} \right) \quad (22)$$

The entropy, S , is obtained from

$$S = \kappa \ln W$$

where κ is Boltzmann's constant.

In the special case of a binary alloy on two sublattices, the entropy takes the form (Appendix III):

$$S = -\kappa \sum_{iIJ} N_{IJ}^i n_J \left\{ X_a^{(J)} G \left[X_a^{(I)} (1 + q_{IJ}^i) \right] + X_b^{(J)} G \left[X_a^{(I)} \left(1 - \frac{X_a^{(J)}}{X_b^{(J)}} q_{IJ}^i \right) \right] \right\} \quad (23)$$

where

$$q_{IJ}^i = q_i(aI|aJ)$$

$$G(x) = x \ln x + (1-x) \ln(1-x)$$

The derivation of (23) is given in Appendix III.

It is useful to obtain the form of the entropy in which $q_{IJ}^i = q_{IJ}^{i*}$ for all i .

The value of i^* is the lowest value of i which yields the correct entropy in the limit of perfect short range order. For b.c.c. $i^*=1$, for f.c.c. $i^*=2$. In this case:

$$S = -Nk \sum_{IJ} n_I n_J \left\{ X_a(J) G\left(X_a(I)(1-q_{IJ}^{i*})\right) + X_b(J) G\left(X_a(I)\left(1 - \frac{X_a(J)}{X_b(J)} q_{IJ}^{i*}\right)\right) \right\} \quad (24)$$

Free Energy Minimization

First consider the free energy dependence on short range order. Using the general formula

$$F = E - TS$$

where F is the free energy, E , the energy, T the absolute temperature, and S , the entropy, minimize the free energy with respect to the short range order parameters. E is obtained from equation (20) and S from equation (23). The resulting set of equations is given below for each I, J, i :

$$\begin{aligned}
& \frac{2\Delta E_{ab}(r_i)}{N^i kT} + \ln \frac{\left(1 + q_{IJ}^i\right) \left(1 + \frac{X_a(I)}{X_b(I)} \frac{X_a(J)}{X_b(J)} q_{IJ}^i\right)}{\left(1 - \frac{X_a(I)}{X_b(I)} q_{IJ}^i\right) \left(1 - \frac{X_a(J)}{X_b(J)} q_{IJ}^i\right)} \\
& + \sum'_{jkH} \frac{\Delta E_{ab}(r_k)}{N^k kT} X_a(H) \left[\frac{N(J, i, I, k, H, j)}{N_{IJ}^i} \frac{q_{JH}^i}{X_b(J)} + \frac{N(I, i, J, k, H, j)}{N_{JI}^i} \frac{q_{IH}^i}{X_b(I)} \right] \\
& = 0 \tag{25}
\end{aligned}$$

The derivation of equation (25) is given in Appendix IV.

The set of equations (25) may be solved by the following iterative procedure: Let

$$\begin{aligned}
\ln D = & \frac{2\Delta E_{ab}(r_i)}{N^i kT} + \sum_{jkH} \frac{\Delta E_{ab}(r_k)}{N^k kT} X_a(H) \left[\frac{N(J, i, I, k, H, j)}{N_{IJ}^i} \frac{q_{JH}^i}{X_b(J)} \right. \\
& \left. + \frac{N(I, i, J, k, H, j)}{N_{JI}^i} \frac{q_{IH}^i}{X_b(I)} \right],
\end{aligned}$$

$$X = \frac{X_a(I)}{X_b(I)}, \quad Y = \frac{X_a(J)}{X_b(J)}, \quad Q = q_{IJ}^i$$

Equation (25) may be written:

$$\ln D + \ln \frac{(1+Q)(1+XYQ)}{(1-XQ)(1-YQ)} = 0$$

Solving for Q:
$$Q = \frac{(1+XY)D + X + Y - \sqrt{[(1+XY)D + X + Y]^2 - 4XY(D-1)^2}}{2XY(1-D)}$$

A set of q_{IJ}^i is assumed ($q_{IJ}^i = 0$ is a good starting point). For a

given X, Y, and $\frac{\Delta E_{ab}(r_i)}{N^i kT}$, D is calculated. Next, Q is

calculated and the old value of q_{IJ}^i is replaced by the new one. The procedure is repeated until the calculated Q is as near to the trial Q as desired.

It is now possible to calculate a set of q_{IJ}^i for any given long range order and temperature. To minimize the free energy with respect to the long range order parameter, use the set of q_{IJ}^i determined above along with the energy of equations (19) and (21) and the entropy of equation (24). Values of the long range order parameter are assumed and the free energy is calculated until a minimum is obtained.

Application of the Order-Disorder Theory

The following assumptions have been made to facilitate the calculations:

(1) Short range order parameters for shells greater than a distance of 10th nearest neighbors are set equal to zero.

(2) To avoid the choice of numerous arbitrary constants, the following energy values are assumed in the calculation of short range order parameters:

$$\Delta E_{ab}(r_1) = \Delta E_{ab}^1, \quad \Delta E_{ab}(r_2) = \Delta E_{ab}^2$$

$$\Delta E_{ab}(r_k) = 0 \quad k > 2,$$

i. e. the ΔE values at first and second neighbor positions are given by the ΔE values for the odd and even shells respectively. Assumption (1) has very little effect on the results obtained below since the short range order parameters for shells greater than 10th nearest neighbors are small (Table II). In addition, the effects of the atoms in these distant shells frequently cancel. Assumption (2) has little effect on the results obtained below except perhaps for a small effect on the values of the short range order parameters in the shells greater than 2nd nearest neighbors. For example, if $\Delta E_{ab}(r_3) \neq 0$ there is a change in the short range order parameters of the third shell. For $|\Delta E_{ab}(r_3)| \ll |\Delta E_{ab}(r_1)|$, however, the effect is not great. It therefore seems reasonable as a first approximation to ignore $\Delta E_{ab}(r_k)$ for $k > 2$.

Use of the dimensionless quantity $\kappa T / \Delta E_{ab}^1$ permits the

determination of ΔE_{ab}^1 by comparison with the experimental critical temperature. The remaining energy ΔE_{ab}^2 will be used in the form $\Delta E_{ab}^2 / \Delta E_{ab}^1 = p$. The behavior of an alloy system will be examined as a function of p . A long range order parameter, S , may be defined as:

$$S = \frac{X_a(A) - m_a}{n_B}$$

This parameter reduces to the Bragg-Williams S for stoichiometric compositions. A short range order parameter, σ_i , for each shell may be defined as:

$$\sigma_i = \frac{N_{aa}^i(S, q) - N_{aa}^i(S, 0)}{N_{aa}^i(0, q_L) - N_{aa}^i(0, 0)}$$

where $N_{aa}^i(S, q)$ is the number of a-a atom pairs at distance r_i with long range order S and short range order q given by q_{AA}^i , q_{AB}^i , q_{BB}^i and q_L is the maximum short range order possible. The parameter σ_i is equal to zero for no short range order and equal to one for maximum short range order.

For structures such as face centered cubic, with $m_a > .25$, the fully ordered structure has some a-a first neighbor pairs. The limiting values of q determined above yield no a-a first neighbor pairs, i.e. $q \rightarrow -1$. It is therefore necessary to multiply the q values determined above by $\frac{1}{3} \frac{m_b}{m_a}$ for $m_a > .25$. This procedure gives the proper q_L values.

Table II shows typical order parameters for an AB_3 stoichiometric alloy. Figures 4-6 show S , σ_i , and q/q_L as a function of

TABLE II

$kT/\Delta E_{ab}^1$	i	q_{AA}^i	q_{AB}^i	q_{BB}^i	S
$1/12$	1	-	-.1527	-.7564	.9513
	2	.0006	-	.5203	
	3	-	.0031	.3370	
	4	.0001	-	.0671	
	5	-	-.0029	-.1202	
	6	-.0000	-	-.0911	
	7	-	-.0022	-.1308	
	8	.0000	-	.0367	
	9	-	-.0023	-.1333	
	10	-	-.0024	-.1353	
	11	.0000	-	.1417	
$1/8$	1		-.5741		0
	2		.8071		
	3		.0898		
	4		.2046		
	5		-.2459		
	6		-.0731		
	7		.0032		
	8		.2269		
	9		-.0846		
	10		.0331		
	11		.0666		

Order parameters for a f.c.c. AB_3 stoichiometric alloy for $p = 0$.

T/T_t and p for various compositions and lattice structures, where T_t is the highest temperature at which long range order exists. Figures 7-9 show the energy as a function of T/T_t and p for various compositions and lattice structures. Figures 10, 11, and 12 show partial phase diagrams for different values of p . The two phase regions were determined by the common tangent method.

In the phase diagrams the disordered regions represent alloys with no long range order, but with a varying degree of short range order. The A_3B , AB , and AB_3 regions represent alloys with varying amounts of long range order based on the respective superlattice plus a varying amount of short range order.

For $p = 0$, i.e. $\Delta E_{ab}^2 = 0$, three maxima (25%, 50%, 75%) are observed. For the case of no lattice parameter variation, two eutectoids occur at a temperature 67.5% of the critical temperature for the AB stoichiometric alloy (Fig. 10). For $p = .025$ the three maxima are again observed, however no eutectoids occur (Fig. 11). For $p = -.025$ one maximum (50%) is observed (Fig. 12). For the case of no lattice parameter variation, there are two peritectoids at a temperature 89% of the critical temperature for the AB stoichiometric alloy.

The effect of p as seen above is to stabilize long range order for $p < 0$ and to stabilize short range order for $p > 0$. For perfect long range order, there are many like second neighbor pairs. A negative value of p gives this configuration a lower energy than a positive p .

It is possible to include the effect of lattice parameter changes

by allowing $\Delta E'_{ab}$ to be a function of composition. This effect influences T_t through a simple shift in the temperature scale. Figs. 13 and 14 show the effect of a small linear variation in $\Delta E'_{ab}$. The experimental phase diagram (Fig. 15) for the copper-gold system is quite similar to the theoretical phase diagram shown in Fig. 13 for $p = 0$, $\Delta E^2_{ab} = 0$. The experimental phase diagram shows that it is likely that there is a peritectoid for $m_{Cu} = .25$. If so, a value of p slightly less than zero would produce a eutectoid at $m_{Cu} = .75$ and a peritectoid at $m_{Cu} = .25$. A value of p slightly less than zero would also give good agreement with the experimental measurements of long range order at the critical temperature, short range order just above the critical temperature, and energy as a function of temperature.

It is estimated that p is between $-.005$ and $-.01$. This value of p would represent a contribution of the even shells of $.5$ to 1.0 percent of the contribution of the odd shells. The negative value of p implies that the even shells favor like atoms as neighbors while the odd shells favor unlike atoms. The value of $\Delta E'_{ab} (m_{Cu} = .5) / \kappa$ is determined to be 4430°K .

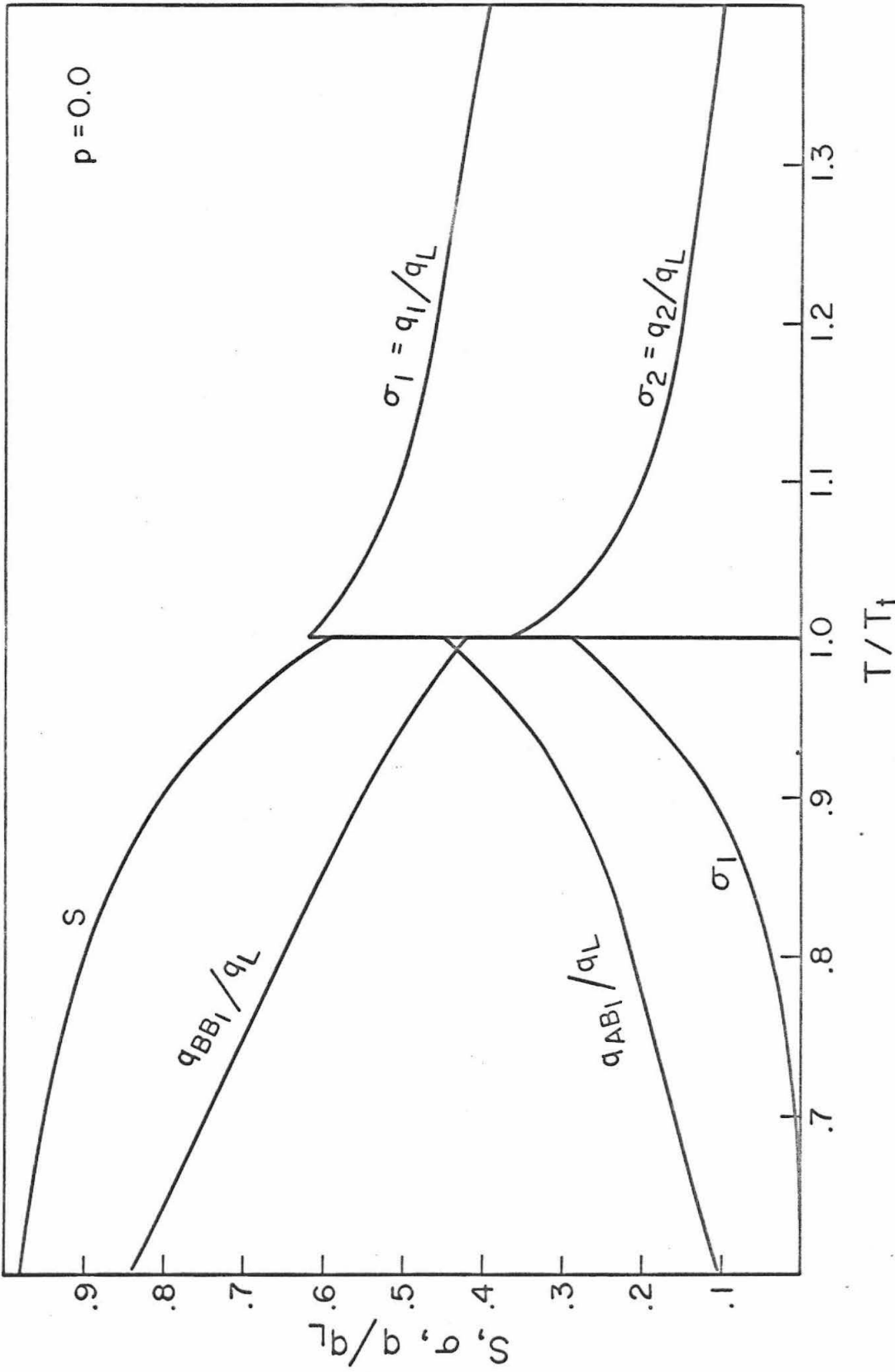


Fig. 4. Long range (S) and short range ($\sigma_i, q/q_L$) order coefficients for the f.c.c. AB_3 stoichiometric alloy

$$q = q_{AB} = q_{BB}$$

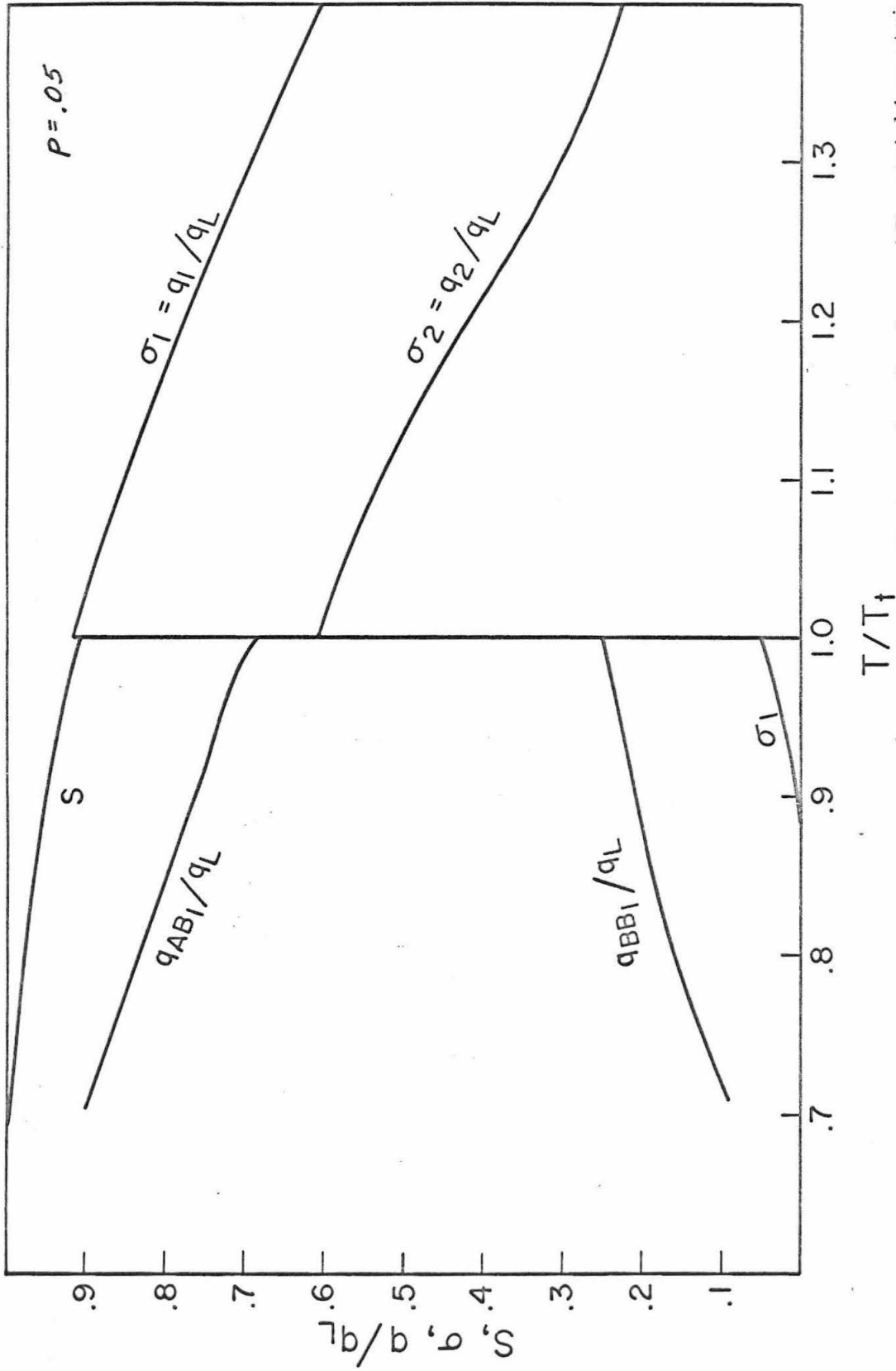


Fig. 5. Long range (S) and short range ($\sigma_i, q/q_L$) order coefficients for the f.c.c. AB_3 stoichiometric alloy
 $q = q_{AB} = q_{BB}$

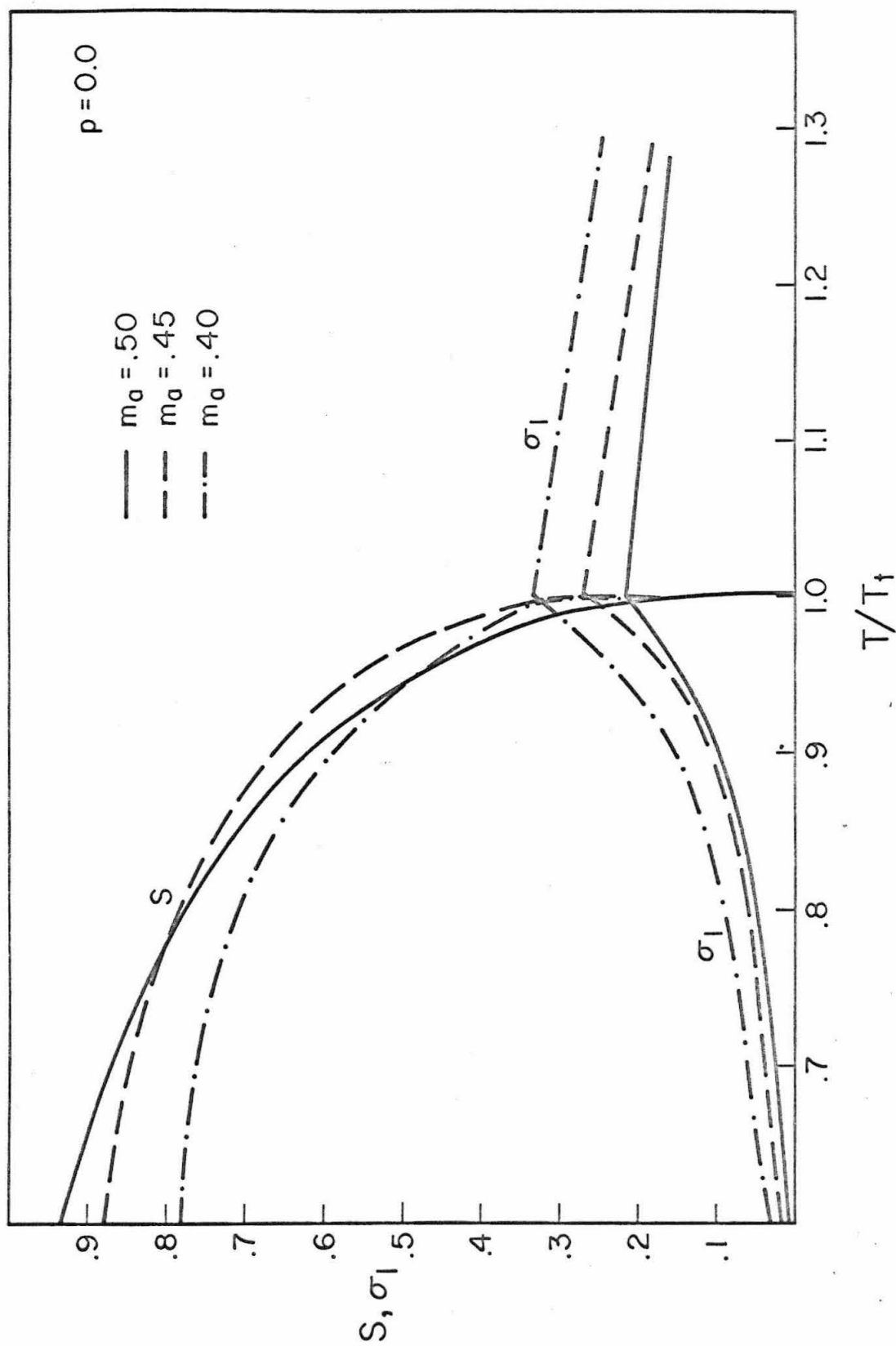


Fig. 6. Long range (S) and short range (σ_1) order coefficients for f.c.c. AB alloys of various compositions

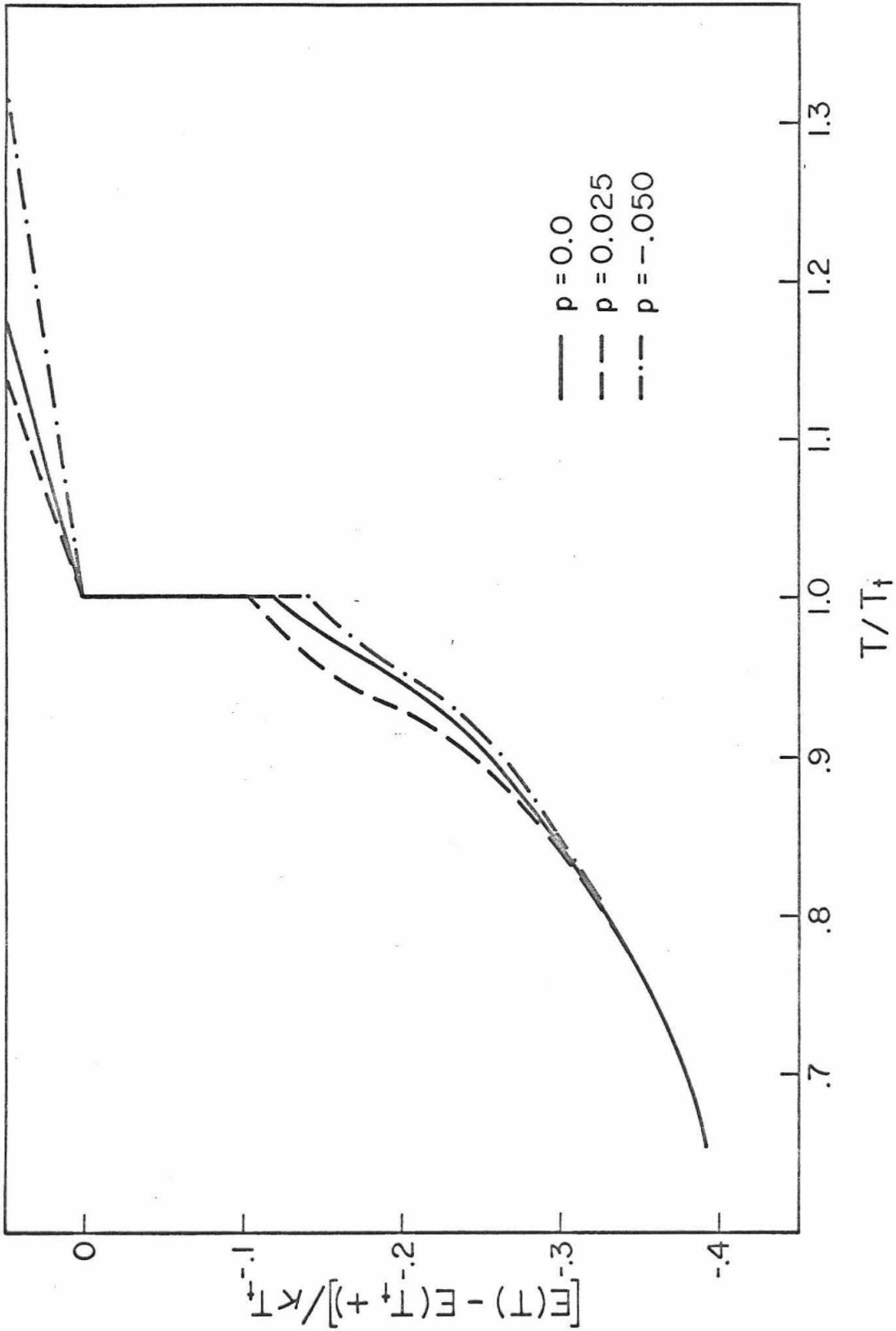


Fig. 7. Energy of the f. c. c. AB_3 stoichiometric alloy for various values of p

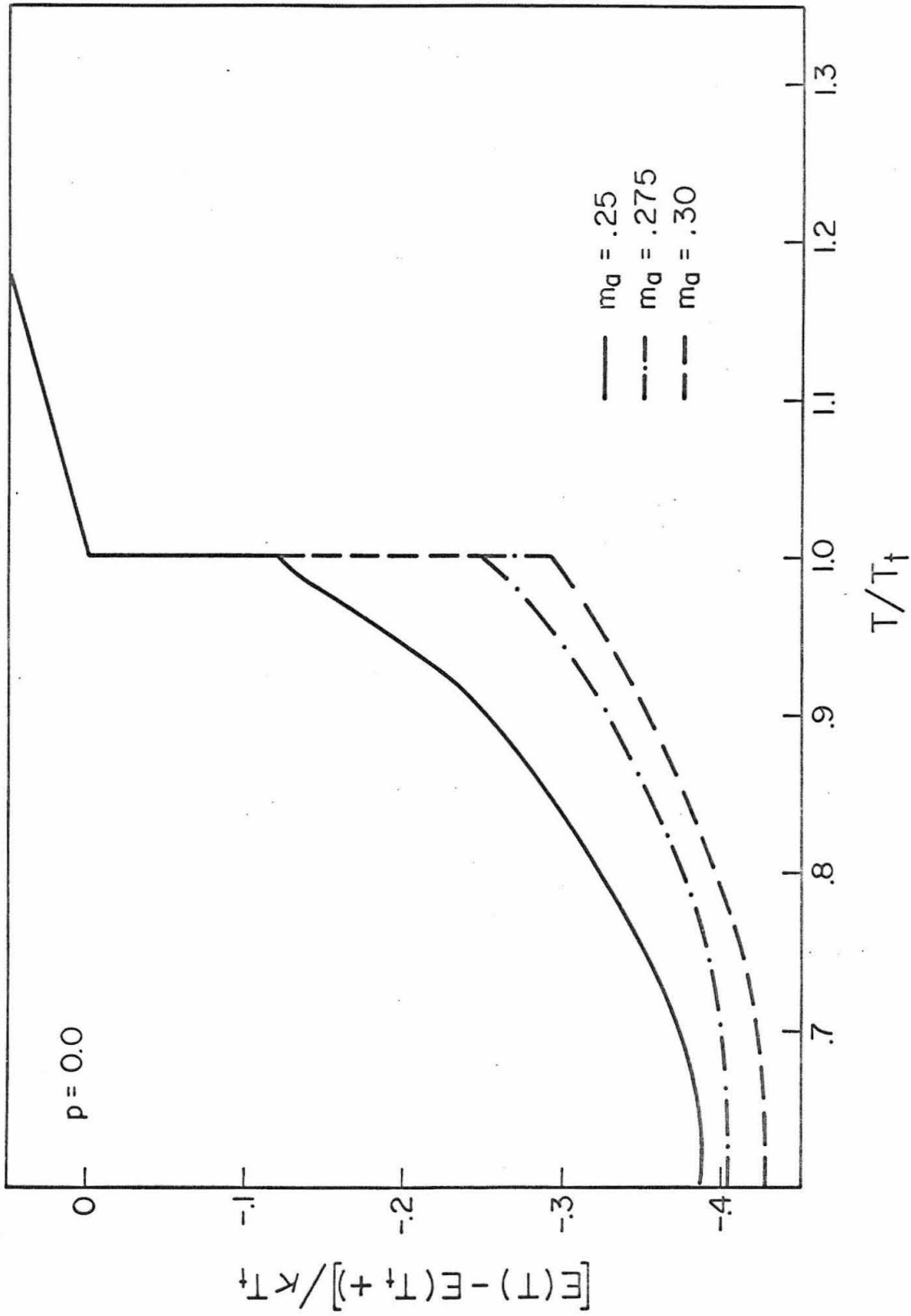


Fig. 8. Energy of the f.c.c. AB_3 alloy for various compositions

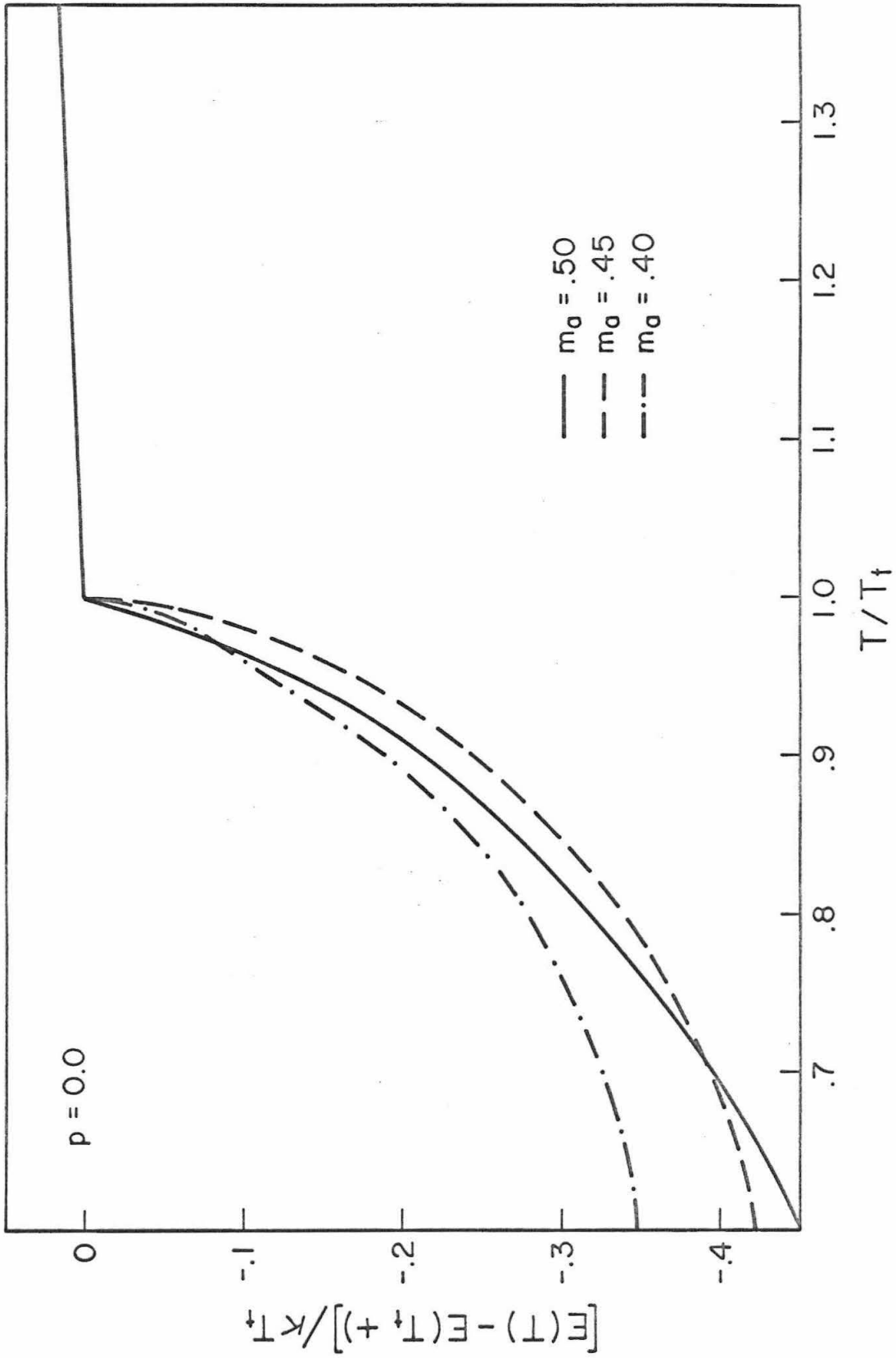


Fig. 9. Energy of the f. c. c. AB alloy for various compositions

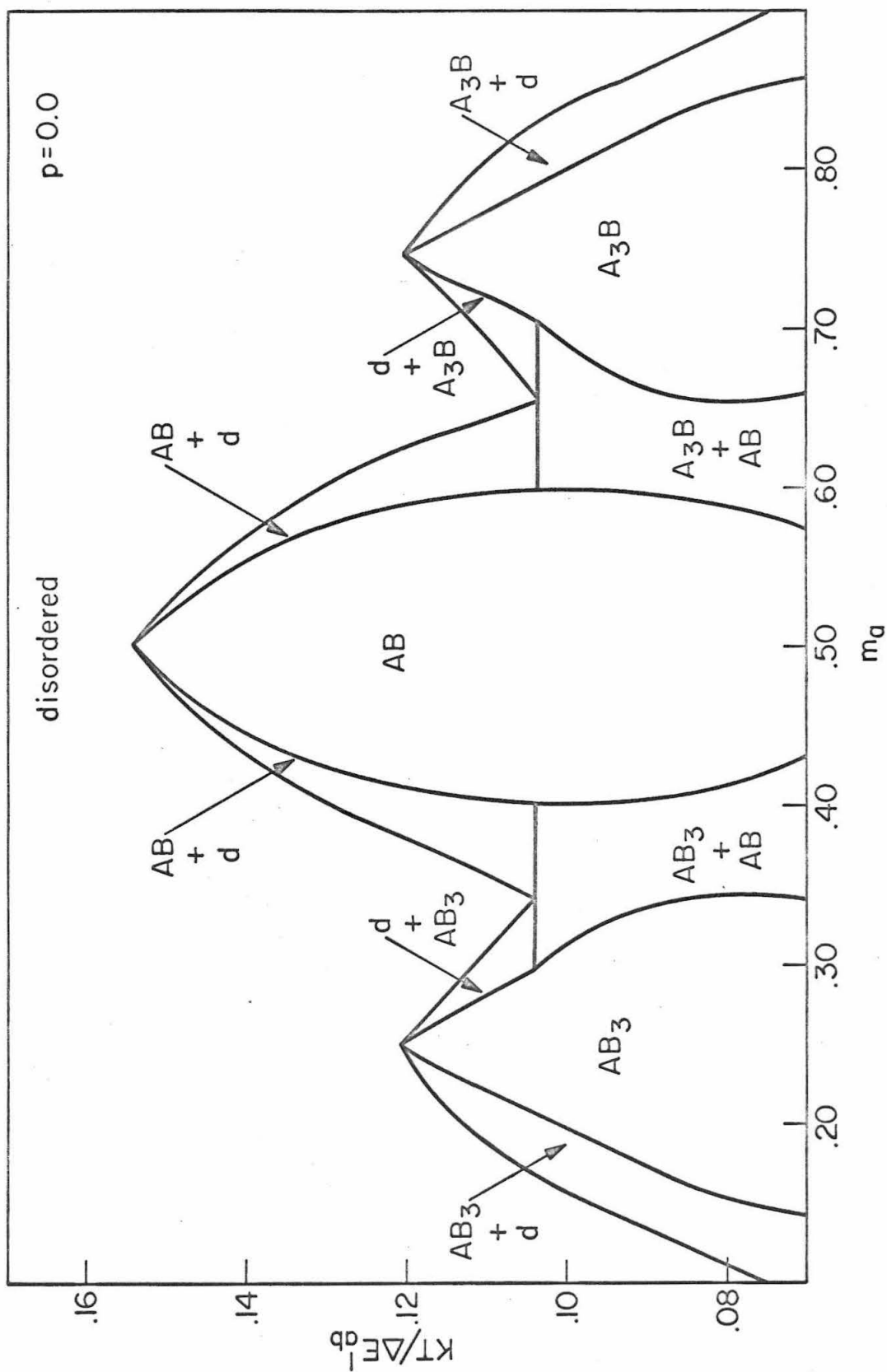


Fig. 10. Partial phase diagram for $p = 0$ with no lattice parameter variation

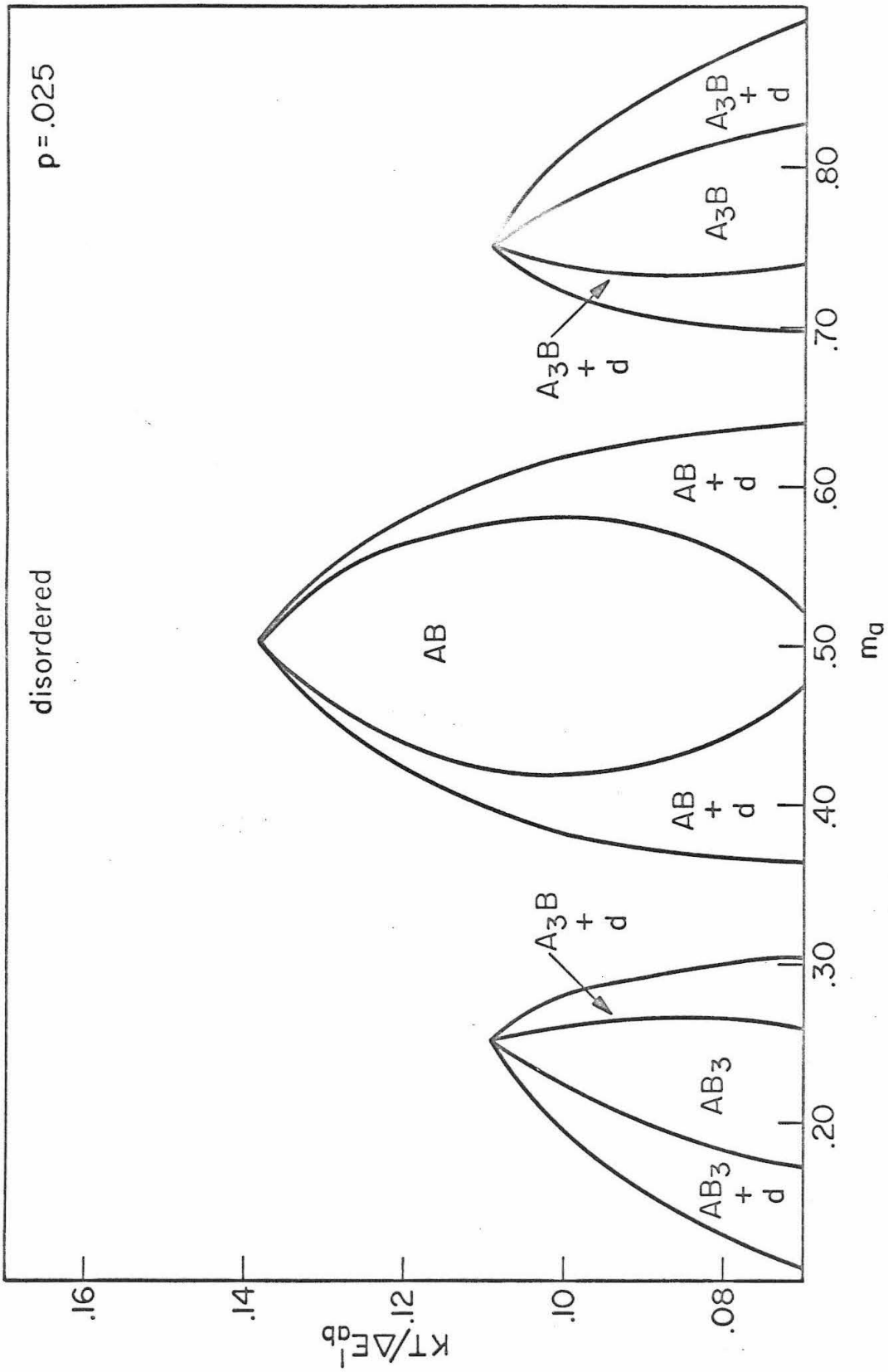


Fig. 11. Partial phase diagram for $p = .025$ with no lattice parameter variation

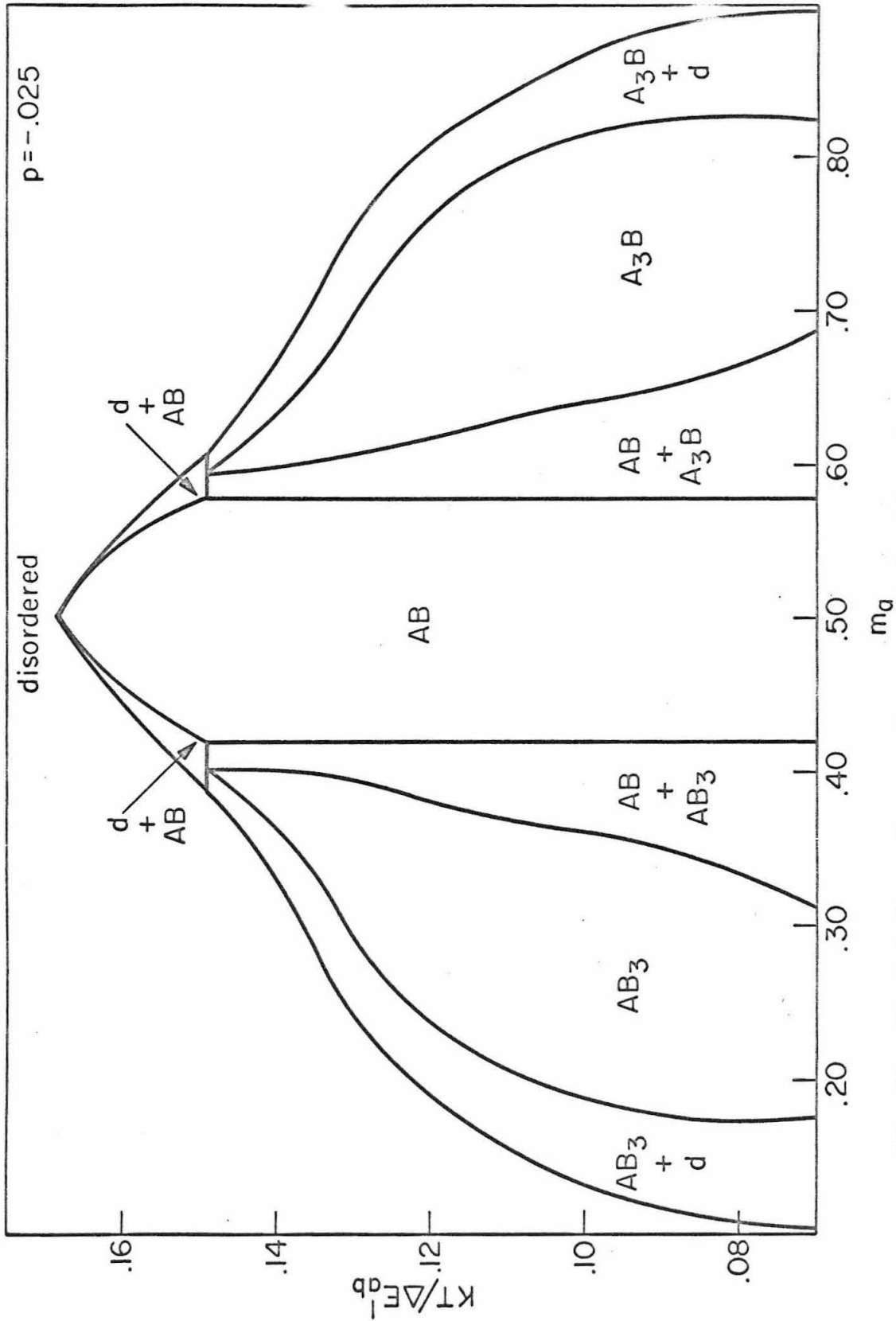


Fig. 12. Partial phase diagram for $p = -.025$ with no lattice parameter variation

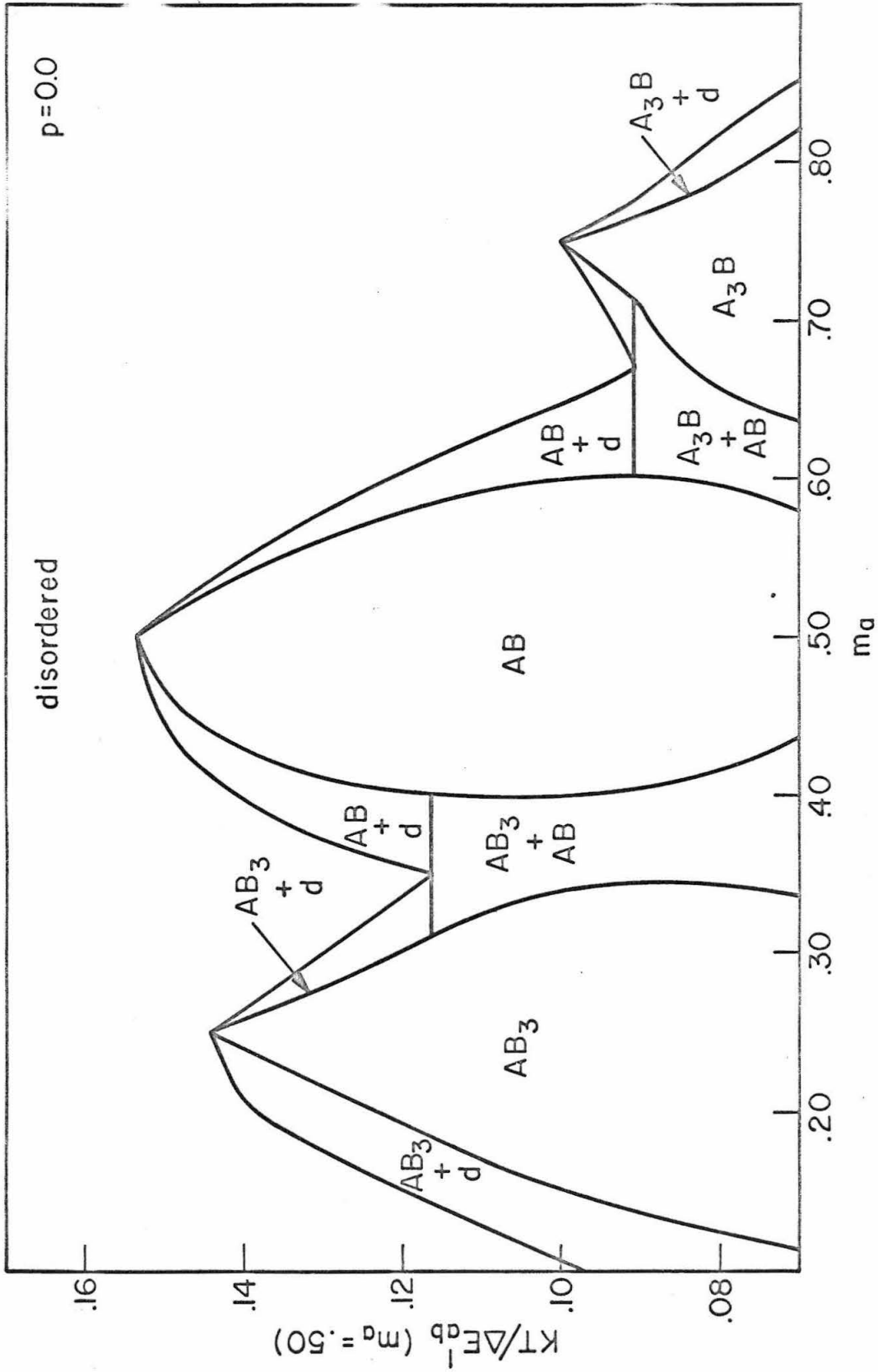


Fig. 13. Partial phase diagram for $p = 0$ including lattice parameter variation

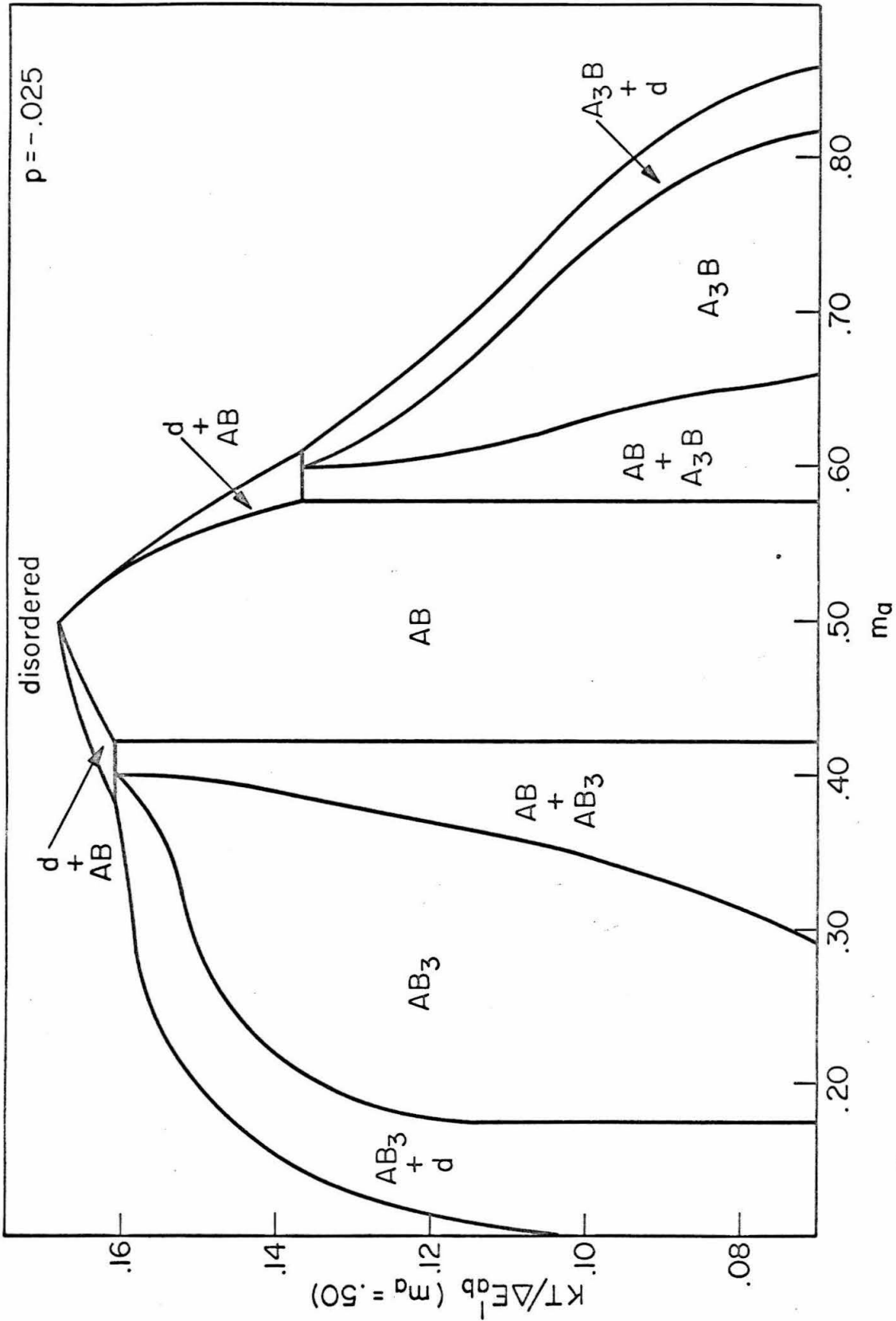


Fig. 14. Partial phase diagram for $p = -.025$ including lattice parameter variation

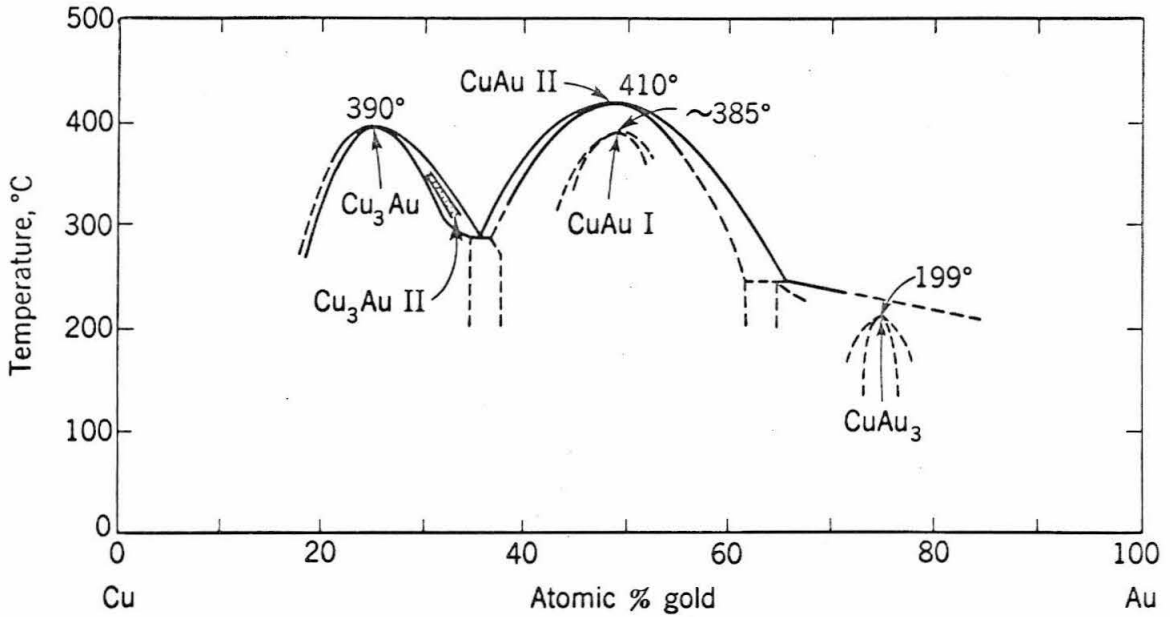


Fig. 15. Experimental phase diagram
of the copper-gold system.

Barrett, C. S., and Massalski, J. B., Structure of Metals,
McGraw-Hill Book Co., 1966.

Magnetism in Alloys

Consider the magnetic properties of alloys under the molecular field approximation. Assume the contribution to the molecular field from a β type ion may be written:

$$\bar{H}_{\beta}(r_i) = \bar{A}_{\beta} \lambda(r_i) \quad (1)$$

where \bar{A} depends only on the type of ion and λ depends only on the distance r_i from that ion.

Let $\sigma(\beta I)$ be the relative magnetization of β ions on I sites. The contribution to the molecular field from a β ion on an I site is given by:

$$H_{\beta I}(r_i) = A_{\beta} \lambda(r_i) \sigma(\beta I) \quad (2)$$

where $A_{\beta} = |\bar{A}_{\beta}|$.

The field acting on an α ion on an H site, $H(\alpha H)$, is given by the sum of the contributions of the surrounding ions.

$$H(\alpha H) = \sum_{i, \beta, I} N_{IH}^i p_i(\beta I | \alpha H) H_{\beta I}(r_i) \quad (3)$$

where N_{IH}^i is the number of I sites a distance r_i from an H site and $p_i(\beta I | \alpha H)$ is the probability of finding a β ion on an I site given an α ion on an H site.

Let J_α be the total angular momentum quantum number of an α ion, g_α the Landé spectroscopic g-factor of an α ion, and μ_B , the Bohr magneton. Calculating $\sigma(\alpha H)$ from simple statistical mechanics:

$$\sigma(\alpha H) = B_{J_\alpha} \left(\frac{g_\alpha J_\alpha \mu_B H(\alpha H)}{\kappa T} \right) \quad (4)$$

where $B_J(x) = \frac{2J+1}{2J} \coth \frac{2J+1}{2J} x - \frac{1}{2J} \coth \frac{1}{2J} x$ is the Brillouin function. The Curie temperature, T_c , may be determined by solving the set of equations obtained in the limit $\sigma \rightarrow 0$, $T \rightarrow T_c$.

$$\sigma(\alpha H) = \frac{J_\alpha + 1}{3J_\alpha} \frac{g_\alpha J_\alpha \mu_B H(\alpha H)}{\kappa T_c} \quad \sigma \rightarrow 0 \quad (5)$$

Solutions of equation (3) for some special cases are given in the following sections.

Case of Complete Disorder.

$p_i(\beta I | \alpha H) = m_\beta$, the composition of β ions. From equations (2) and (3):

$$\begin{aligned} H(\alpha H) &= \sum_{i\beta I} N_{IH}^i m_\beta A_\beta \lambda(r_i) \sigma(\beta I) \\ &= \sum_i N^i \lambda(r_i) \sum_\beta m_\beta A_\beta \sigma(\beta H) \end{aligned}$$

Where N^i is the number of i th neighbors to a site. Since $H(\alpha H)$ is

independent of α , equation (5) yields:

$$\frac{\sigma(\beta H)}{\sigma(\alpha H)} = \frac{(J_\beta + 1) g_\beta}{(J_\alpha + 1) g_\alpha}$$

and

$$H(\alpha H) = \Lambda \sum_{\beta} m_{\beta} A_{\beta} \left[\frac{g_{\beta} (J_{\beta} + 1)}{g_{\alpha} (J_{\alpha} + 1)} \right] \sigma(\alpha H)$$

where $\Lambda = \sum_i N_i^{\lambda} \lambda(r_i)$.

Equation (5) yields:

$$T_c = \theta_0 \sum_{\beta} m_{\beta} B_{\beta} \quad (6)$$

where $\theta_0 = \frac{2\mu_B^2 \Lambda}{3K}$ and $B_{\beta} = A_{\beta} (J_{\beta} + 1) g_{\beta} / 2\mu_B$

Case of Long Range Order Only.

$$p_i(\beta I | \alpha H) = X_{\beta}(I)$$

From equations (2) and (3):

$$\begin{aligned} H(\alpha H) &= \sum_{i\beta I} N_{IH}^i X_{\beta}(I) A_{\beta} \lambda(r_i) \sigma(\beta I) \\ &= \sum_{n\beta I} w_{IH}^n X_{\beta}(I) A_{\beta} \Lambda_n \sigma(\beta I) \end{aligned}$$

where w_{IH}^n are defined above and $\Lambda_n = \sum_i \lambda(r_{i_n}) N_i^n$. The reduction

to a summation over n is mathematically equivalent to the treatment of order-disorder above. Since $H(\alpha H)$ is independent of α , equation (5) yields:

$$\frac{\sigma(\beta I)}{\sigma(\alpha I)} = \frac{(J_\beta + 1) g_\beta}{(J_\alpha + 1) g_\alpha}$$

and

$$\begin{aligned} H(\alpha H) &= \sum_{n\beta i} w_{IH}^n X_\beta(I) A_\beta \Lambda_n \left[\frac{g_\beta^{(J_\beta + 1)}}{g_\alpha^{(J_\alpha + 1)}} \right] \sigma(\alpha I) \\ &= 2\mu_B \Lambda \sum_I W_{IH} U_I \frac{\sigma(\alpha I)}{g_\alpha^{(J_\alpha + 1)}} \end{aligned}$$

where $W_{IH} = \sum_n w_{IH}^n \Lambda_n / \Lambda$ and $U_I = \sum_\beta X_\beta(I) B_\beta$. Equation (5) yields:

$$\sigma(\alpha H) = \frac{\theta_0}{T_c} \sum_I W_{IH} U_I \sigma(\alpha I) \quad \sigma \rightarrow 0$$

In the case of two sublattices, eliminating the σ 's yields:

$$T_c = \frac{\theta_0}{2} \left[U_A W_{AA} + U_B W_{BB} + \sqrt{(U_A W_{AA} - U_B W_{BB})^2 + 4W_{AB} W_{BA} U_A U_B} \right] \quad (7)$$

Case of Short Range Order Only.

$$p_i(\beta I | \alpha H) = m_\beta (1 + q_i(\beta | \alpha))$$

From equations (2) and (3):

$$\begin{aligned} H(\alpha H) &= \sum_{i \in I} N_{IH}^i m_{\beta} (1 + q_i(\beta | \alpha)) A_{\beta} \lambda(r_i) \sigma(\beta) \\ &= \Lambda \sum_{\beta} m_{\beta} A_{\beta} \sigma(\beta) [1 + \lambda_{\beta \alpha}] \end{aligned}$$

where

$$\lambda_{\beta \alpha} = \sum_i N^i q_i(\beta | \alpha) \lambda(r_i) / \Lambda$$

Equation (5) yields:

$$\sigma(\alpha) = \frac{J_{\alpha} + 1}{3kT_c} \Lambda g_{\alpha} \mu_B \sum_{\beta} m_{\beta} A_{\beta} \sigma(\beta) [1 + \lambda_{\beta \alpha}] \sigma \rightarrow 0$$

or

$$\frac{\sigma(\alpha)}{(J_{\alpha} + 1) g_{\alpha}} = \frac{\theta_0}{T_c} \sum_{\beta} m_{\beta} B_{\beta} \left[\frac{\sigma(\beta)}{(J_{\beta} + 1) g_{\beta}} \right] [1 + \lambda_{\beta \alpha}] \sigma \rightarrow 0 \quad (8)$$

For the case of a small amount of short range order, i.e. $q(\beta | \alpha) \ll 1$,

$\lambda_{\beta \alpha} \ll 1$. In this case:

$$T_c / \theta_0 = \sum_{\beta} m_{\beta} B_{\beta} + \sum_{\alpha \beta} m_{\alpha} m_{\beta} B_{\alpha} B_{\beta} \lambda_{\beta \alpha} / \sum_{\beta} m_{\beta} B_{\beta} + \dots \quad (8a)$$

In order to examine the affect of ordering on magnetic properties it is necessary to know more about \bar{A}_{β} of equation (1). As an example consider the first transition series of elements. It is commonly assumed that the 3d shell is split into two subshells that are displaced

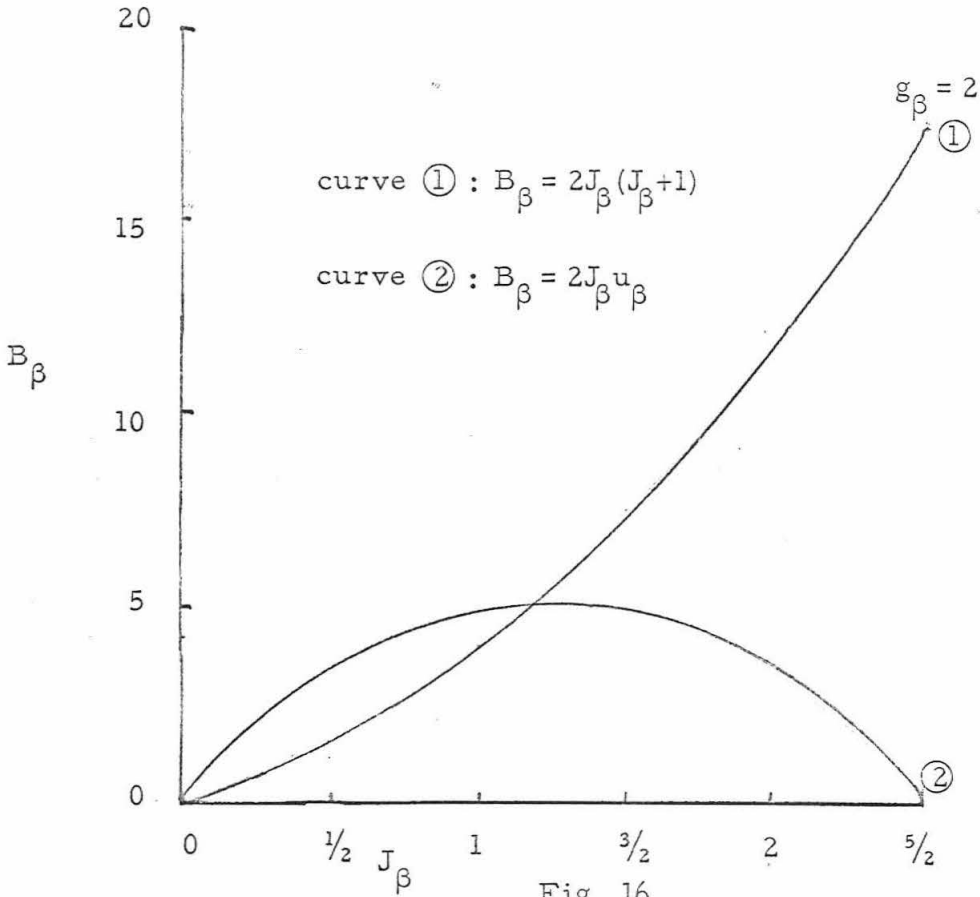
in energy. The subshell with the lower energy states is said to contain electrons with + spin, while the other subshell is said to contain electrons with - spin. The difference in occupation levels of the subshells gives rise to a magnetic moment. It is commonly assumed that $A_{\beta} = \mu_B J_{\beta} g_{\beta}$, i.e. the molecular field is proportional to the average magnetic moment per ion. This assumption would yield a value of $B_{\beta} = J_{\beta}(J_{\beta}+1) g_{\beta}^2 / 2$. It is indeed reasonable to assume that the magnetic moment is one factor involved in the mechanism producing the molecular field, but quite limiting to assume that it is the only ion dependent factor. Anderson⁴⁷ considers the number of electrons in the $3d^{-}$ subshell in his formulation of a theory of the origin of localized magnetic moments. In this treatment his correlation Hamiltonian is proportional to u_{β} , the number of electrons in the $3d^{-}$ subshell. Following this reasoning the internal field here is assumed to be proportional to u_{β} . It has been assumed in the derivation of equation (4) that the molecular field is independent of m_J , the projection of J along the z -axis. This assumption leads to the factor $J_{\beta}+1$ in B_{β} . If the molecular field is allowed to depend on m_J , the values of B_{β} would depend critically on the assumptions made about the behavior of the molecular field. It is assumed here that the dependence is such that the new B_{β} is given by

$$B_{\beta} = J_{\beta} u_{\beta} g_{\beta}^2 / 2 \quad (9)$$

The difference between the B_{β} used here and the B_{β} commonly used may be seen in Fig. 16 for ions with a filled $3d^{+}$ subshell.

The important difference in behavior occurs for those ions that have an almost completely unfilled $3d^{-}$ subshell. The B_{β} commonly used gives a much larger contribution to the magnetic interaction from these ions than

the B_β used in this paper.



Comparison of the values of B_β commonly used
and the values used in this treatment.

Using equation (9) for B_β yields two different values for $\sum_{\beta} m_{\beta} B_{\beta}$ depending on whether the time average or instantaneous values of B_β are used. For example, in pure nickel if $g = 2$, the time average value of B_{Ni} is approximately $(.6)(4.4) = 2.64$. The instantaneous value of B_{Ni} is obtained by allowing only integer number of electrons. In pure nickel approximately .6 of the ions have $B_{Ni_1} = 4$ while the remaining ions have $B_{Ni_2} = 0$ which yields $B_{Ni} = .6(4) = 2.4$. In the

following development the instantaneous value of B_β will be used. In addition, it is assumed that an ion with both $3d^+$ and $3d^-$ subshells unfilled has a $B = 0$. The number of electrons in each of the subshells of a β ion will be represented by $\beta \left(\begin{smallmatrix} \# \text{ electrons in } 3d^+ \\ \# \text{ electrons in } 3d^- \end{smallmatrix} \right)$, e.g. $\text{Ni} \left(\begin{smallmatrix} 5 \\ 4 \end{smallmatrix} \right)$ denotes a nickel ion with five $3d^+$ electrons and four $3d^-$ electrons.

To determine the m_β for a pure element assume there is a resonance of the $3d^-$ electrons. If the probability for an ion to change from a state with u_β $3d^-$ electrons is proportional to u_β , detailed balance requires $m_{\beta_1} u_{\beta_1} = m_{\beta_1} u_{\beta_2} = m_{\beta_3} u_{\beta_3} = \dots$. In iron, $\text{Fe} \left(\begin{smallmatrix} 5 \\ 3 \end{smallmatrix} \right)$, $\text{Fe} \left(\begin{smallmatrix} 5 \\ 2 \end{smallmatrix} \right)$, and $\text{Fe} \left(\begin{smallmatrix} 4 \\ 3 \end{smallmatrix} \right)$ are present; in cobalt, $\text{Co} \left(\begin{smallmatrix} 5 \\ 4 \end{smallmatrix} \right)$ and $\text{Co} \left(\begin{smallmatrix} 5 \\ 3 \end{smallmatrix} \right)$ are present; and in nickel, $\text{Ni} \left(\begin{smallmatrix} 5 \\ 5 \end{smallmatrix} \right)$ and $\text{Ni} \left(\begin{smallmatrix} 5 \\ 4 \end{smallmatrix} \right)$ are present. Table III gives the resultant values of m_β along with the values of J, u, g, B, n_0, T_c , and θ_0 . It is assumed that the g values for each ion species of an element are the same and equal to the experimental value for that element. B is calculated from equation (9). The saturation moment in Bohr magnetons, n_0 , is given by:

$$n_0 = \sum_{\beta} m_{\beta} g_{\beta} J_{\beta} \quad (10)$$

The agreement with the experimental values is excellent. θ_0 is calculated from equation (6).

Since the values of θ_0 are so close together it seems that the differences in structure and lattice parameter are relatively unimportant in determining the Curie temperature and perhaps other magnetic properties. A further investigation was therefore undertaken to explore the possibility that the arrangement of atoms is a dominant factor in determining the magnetic properties of alloys.

Table III

Ion Species	m	J	u	¹ g (exp)	B	n ₀	² n ₀ (exp)	² T _C (exp)	θ ₀
Fe(⁵ ₃)	2/7	1	3	2.070	6.43	2.218	2.218	1043	227
Fe(⁵ ₂)	3/7	3/2	2	2.070	6.43				
Fe(⁴ ₃)	2/7	1/2	3	2.070	0				
Co(³ ₄)	3/7	1/2	4	2.170	4.71	1.705	1.714	1403	232
Co(⁵ ₃)	4/7	1	3	2.170	7.06				
Ni(⁵ ₅)	4/9	0	5	2.190	0	.6083	.604	631	236
Ni(⁵ ₄)	5/9	1/2	4	2.190	4.80				

Values of m, J, u, g, B, n₀, T_C, and θ₀ for the first series transition elements

m = composition

J = ionic spin

u = number of 3d⁻ electrons/atom

g = Landé g factor

B given by equation (9)

n₀ = saturation moment given by equation (10)

T_C = Curie temperature

θ₀ given by equation (6)

¹ Calculated from g' in D. H. Martin, Magnetism in Solids, M.I.T. Press, 1967, p. 22.

² R. M. Bozorth, Ferromagnetism, D. Van Nostrand Co., 1951.

Let T be any element in the first transition series. Let t_T be the average number of electrons in the $3d^-$ subshell of a T ion with a filled $3d^+$ subshell. For example, pure nickel contains $Ni(5)$ and $Ni(4)$ ion species in the ratio of 4/9: 5/9 and $t_{Ni} = \frac{40}{9}$. Similarly, $t_{Co} = \frac{24}{7}$. For iron $t_{Fe} = \frac{12}{5}$ since only $Fe(3)$ and $Fe(2)$ have a filled $3d^+$ subshell. For manganese only $Mn(2)$ exists and $t_{Mn} = 2$. Let z be any element that is able to contribute b_z electrons to the $3d$ subshell. The average number of electrons in the unfilled $3d$ subshell is

$$\sum_T' m_T t_T + \sum_z m_z b_z$$

where m_T and m_z are the compositions of the respective elements and \sum' is over those ions with filled $3d^+$ subshells.

But this average number of electrons is also given by

$$\sum_{\beta}' m_{\beta} u_{\beta}$$

Therefore

$$\sum_{\beta}' m_{\beta} u_{\beta} = \sum_T' m_T t_T + \sum_z m_z b_z \quad (11)$$

Use of equations (6), (9), (10), and (11) along with the knowledge of the electron distribution of an impurity ion as it enters a host lattice allows calculation of n_0 and T_c/θ_0 in the alloys of the elements of the first transition series. The electron distribution of an ion is frequently dependent upon its surroundings. Below it is assumed for simplicity

that only first nearest neighbors determine the electron distribution.

Magnetic Properties of Disordered Alloys.

A list of transition alloy behavior in the disordered case follows. A comparison of the predicted and observed behavior is given at the end of this section. When necessary θ_0 is assumed to be a weighted average of the values in Table III.

Ni with Cu, Zn, Al, S₁, Sb, Cr, and V

In all cases the impurity contributes z electrons per atom to the alloy. If $5/9$ electrons per atom go into the $4s$ band $b_z = z - 5/9$. Equation (11) yields:

$$5m_{\text{Ni}(5)} + 4m_{\text{Ni}(4)} = \frac{40}{9} m_{\text{Ni}} + (z - 5/9) m_z$$

Since $m_{\text{Ni}(5)} + m_{\text{Ni}(9)} = m_{\text{Ni}} = 1 - m_z$, $m_{\text{Ni}(4)} = 5/9 - zm_z$, equation (10) yields

$$n_0 = .608 - 1.095 zm_z$$

This simple case was first explained in a similar manner by Stoner.²⁶ Equations (6) and (9) yield:

$$T_c/\theta_0 = 2.67 - 4.80 zm_z$$

The linear behavior of T_c was first noted in experiments by Marian.²⁷ A satisfactory explanation has not been given until this paper. The values of z that best fit the experimental curves of n_0 and T_c/θ_0 are given in Table IV. Comparison with experiment is given in Fig.17.

Table IV

element	z
Cu	1
Zn	2
Al	3
Si	4
Sb	5
Cr	4
V	5

Number of electrons element
contributes to a nickel alloy.

Ni with Co

Equation (11) yields:

$$5m_{\text{Ni}(5)} + 4m_{\text{Ni}(4)} + 4m_{\text{Co}(4)} + 3m_{\text{Co}(3)} = \frac{40}{9} m_{\text{Ni}} + \frac{24}{7} m_{\text{Co}}$$

Since

$$m_{\text{Ni}(5)} + m_{\text{Ni}(4)} = m_{\text{Ni}} = 1 - m_{\text{Co}} = 1 - m_{\text{Co}(3)} - m_{\text{Co}(4)},$$

$$m_{\text{Ni}(4)} + m_{\text{Co}(4)} + 2m_{\text{Co}(3)} = \frac{5}{9} m_{\text{Ni}} + \frac{11}{7} m_{\text{Co}}$$

If $g_{\text{Ni}} = g_{\text{Co}}$ it would be possible to calculate n_0 from equation (10), i.e. $n_0 = g/2 \left[\frac{5}{9} m_{\text{Ni}} + \frac{11}{7} m_{\text{Co}} \right]$, but since $g_{\text{Ni}} \neq g_{\text{Co}}$ it is necessary to make one further assumption to calculate n_0 and T_c/θ_0 . Assume simply that cobalt added to nickel enters the lattice as $\text{Co}(4)$ and similarly nickel added to cobalt enters the lattice as $\text{Ni}(4)$. Therefore

$$m_{\text{Co}(4)} = m_{\text{Co}} \quad m_{\text{Co}} \leq 7/16$$

$$m_{\text{Ni}(4)} = m_{\text{Ni}} \quad m_{\text{Co}} \geq 7/16$$

The limits are determined by the condition $m_{\text{Ni}(5)} \geq 0$, $m_{\text{Co}(3)} \geq 0$.

Equation (10) yields:

$$n_0 = \begin{cases} .608 + 1.102m_{Co} & m_{Co} \leq 7/16 \\ .613 + 1.092m_{Co} & m_{Co} \geq 7/16 \end{cases}$$

Equations (6) and (9) yield:

$$T_c/\theta_0 = \begin{cases} 2.67 + 4.78m_{Co} & m_{Co} \leq 7/16 \\ 3.75 + 2.30m_{Co} & m_{Co} \geq 7/16 \end{cases}$$

Comparison with experiment is given in Fig. 18.

Ni with Fe

In the case of iron added to nickel, the iron atoms enter the nickel lattice as $Fe(\frac{5}{3})$, the electron spin configuration most like nickel. If an iron ion has two or more iron nearest neighbors, $Fe(\frac{5}{3})$ transforms to $Fe(\frac{5}{2})$ such that the ratio of $Fe(\frac{5}{3})$ to $Fe(\frac{5}{2})$ is 2/5:3/5. This ratio is determined by the condition that the number of electrons in the unfilled subshell of each ion species be equal. If an iron ion has six or more iron nearest neighbors, all of the $Fe(\frac{5}{3})$ transforms to $Fe(\frac{5}{2})$. If an iron ion has eight or more iron nearest neighbors, it transforms to $Fe(\frac{4}{2})$.

Let f_n be the probability that n or more nearest neighbors are

iron. The compositions of the iron ion species are:

$$m_{\text{Fe}(3)}^{(5)} = m_{\text{Fe}} \left(1 - \frac{3}{5} f_2 - \frac{2}{5} f_6 \right)$$

$$m_{\text{Fe}(2)}^{(5)} = m_{\text{Fe}} \left(\frac{3}{5} f_2 + \frac{2}{5} f_6 - f_8 \right)$$

$$m_{\text{Fe}(2)}^{(4)} = m_{\text{Fe}} f_8$$

Equation (11) yields:

$$m_{\text{Ni}(4)}^{(5)} = \frac{5}{9} m_{\text{Ni}} + \frac{3}{5} m_{\text{Fe}} (1 - f_2) - \frac{2}{5} m_{\text{Fe}} (f_6 - f_8)$$

Equation (10) yields:

$$n_0 = .608 + 2.119 m_{\text{Fe}} - .036 m_{\text{Fe}} f_2 - .024 m_{\text{Fe}} f_6 - .597 m_{\text{Fe}} f_8$$

Equations (6) and (9) yield:

$$T_{\text{c}/\theta_0} = 2.67 + 6.64 m_{\text{Fe}} - 2.88 m_{\text{Fe}} f_2 - 1.92 m_{\text{Fe}} f_6 - 4.51 m_{\text{Fe}} f_8$$

It is interesting to observe (Fig. 19) the effect on T_{c/θ_0} of changing the assumptions made above about the iron ion species present. Curve ① shows the above equation for T_{c/θ_0} . Curve ② shows T_{c/θ_0} under the assumption that $\text{Fe}(3)^{(5)}$ transforms as above with one or more iron nearest neighbors. Curve ③ shows T_{c/θ_0} under the assumption that $\text{Fe}(3)^{(5)}$ transforms as above with three or more iron nearest neighbors.

Comparison with experiment is given in Figs. 20 and 21.

Ni with Mn

Manganese enters the nickel lattice as $\text{Mn}(\frac{5}{2})$. Since $\mu_{\text{Mn}} = 3.18$, $g_{\text{Mn}} = 2.12$, and $B_{\text{Mn}(\frac{5}{2})} = 6.74$. If a manganese ion has one manganese nearest neighbor it changes to $\text{Mn}(\frac{5}{0})$. If it has three or more manganese nearest neighbors it contributes four electrons per atom to the alloy. Of these electrons, $5/9$ electrons per atom go into the 4s band. Equation (11) yields:

$$m_{\text{Ni}(\frac{5}{4})} = \frac{5}{9} m_{\text{Ni}} - 2m_{\text{Mn}} f_1 - \frac{13}{9} m_{\text{Mn}} f_3$$

From above the compositions of the manganese ion species are:

$$m_{\text{Mn}(\frac{5}{2})} = m_{\text{Mn}} (1 - f_1)$$

$$m_{\text{Mn}(\frac{5}{0})} = m_{\text{Mn}} (f_1 - f_3)$$

Equation (10) yields:

$$n_0 = .608 + 2.572 m_{\text{Mn}} - 6.882 m_{\text{Mn}} f_3 - .07 m_{\text{Mn}} f_1$$

Equation (6) and (9) yield:

$$T_c/\theta_0 = 2.67 + 4.07 m_{\text{Mn}} - 16.34 m_{\text{Mn}} f_1 - 6.93 m_{\text{Mn}} f_3$$

It is again interesting to observe (Fig. 22) the effect on n_0 of

changing the assumptions made above about the manganese ion species present. Curve ① shows the above equation for n_0 . Curve ② shows n_0 under the assumption that $Mn(0)^5$ does not form, but instead manganese ions surrounded by one or more manganese ions contribute four electrons per atom to the alloy. Curve ③ shows n_0 under the assumption that $Mn(0)^5$ does not transform until it has four or more manganese nearest neighbors.

Comparison with experiment is given in Figs.23 and 24.

Co with Fe

The iron atoms enter the cobalt lattice as $Fe(3)^5$, $Fe(2)^5$, and $Fe(1)^4$ in the ratio of $\frac{2}{11} : \frac{3}{11} : \frac{6}{11}$. Equation (11) yields:

$$m_{Fe(3)^5} = \frac{2}{11} m_{Fe}$$

$$m_{Fe(2)^5} = \frac{3}{11} m_{Fe}$$

$$m_{Fe(1)^4} = \frac{6}{11} m_{Fe}$$

$$m_{Co(4)^5} = \frac{3}{7} m_{Co}$$

$$m_{Co(3)^5} = \frac{4}{7} m_{Co}$$

Equation (10) yields:

$$n_0 = 1.705 + 1.212 m_{Fe}$$

Equations (6) and (9) yield:

$$T_c/\theta_0 = 6.05 - 3.13 m_{Fe}$$

Comparison with experiment is given in Fig.25.

Co with Mn and Cr

In both cases the impurity contributes z electrons per atom to the alloy. If $4/7$ electrons per atom go into the $4s$ band, $b_z = z - 4/7$. Equation (11) yields:

$$5m_{Co(5)} + 4m_{Co(4)} + 3m_{Co(3)} = \frac{24}{7} m_{Co} + (z - \frac{4}{7})m_z$$

and

$$n_0 = 1.705 - 1.085(z+1)m_z$$

If the compositions are as follows:

$$m_{Co(4)} = \frac{3}{7} m_{Co} + (z - \frac{4}{7})m_z$$

$$m_{Co(3)} = \frac{4}{7} m_{Co} - (z - \frac{4}{7})m_z$$

$$m_z \leq \frac{4}{7z}$$

and

$$m_{\text{Co}}^{(5)} = (z - \frac{4}{7}) m_z - \frac{4}{7} m_{\text{Co}}$$

$$\frac{4}{7z} \leq m_z \leq \frac{11}{7(z+1)}$$

$$m_{\text{Co}}^{(4)} = \frac{11}{7} m_{\text{Co}} - (z - \frac{4}{7}) m_z$$

Equations (6) and (9) yield:

$$T_c/\theta_0 = \begin{cases} 6.05 - 4.71m_z - 2.35 m_z z & m_z \leq \frac{4}{7z} \\ 7.40 - 4.71m_z - 4.71 m_z z & \frac{4}{7z} \leq m_z \leq \frac{11}{7(z+1)} \end{cases}$$

The values of z that best fit the experimental values of n_0 and T_c/θ_0 are given in Table V. Comparison with experiment is given in Fig. 26.

Table V

element	z
Mn	4
Cr	5

Number of electrons element
contributes to cobalt alloys.

Fe with Ni

In the case of nickel added to iron, nickel atoms enter the iron lattice as $\text{Ni}(\frac{5}{4})$ and $\text{Ni}(\frac{5}{5})$ in the ratio of $\frac{4}{9} : \frac{5}{9}$. If an $\text{Fe}(\frac{4}{3})$ ion has one or more nickel neighbors it forms $\text{Fe}(\frac{4}{2})$ and $\text{Fe}(\frac{4}{1})$ in the ratio of $1/3 : 2/3$. Equation (11) yields:

$$m_{\text{Fe}(\frac{5}{3})} = \frac{2}{7} m_{\text{Fe}} \qquad m_{\text{Fe}(\frac{4}{1})} = \frac{4}{21} m_{\text{Fe}} f_1$$

$$m_{\text{Fe}(\frac{5}{2})} = \frac{3}{7} m_{\text{Fe}} \qquad m_{\text{Ni}(\frac{5}{5})} = \frac{4}{9} m_{\text{Ni}}$$

$$m_{\text{Fe}(\frac{4}{3})} = \frac{2}{7} m_{\text{Fe}} (1-f_1) \qquad m_{\text{Ni}(\frac{5}{4})} = \frac{5}{9} m_{\text{Ni}}$$

$$m_{\text{Fe}(\frac{4}{2})} = \frac{2}{21} m_{\text{Fe}} f_1$$

Equation (10) yields:

$$n_0 = 2.218 - 1.610 m_{\text{Ni}} + .493 (1-m_{\text{Ni}}) f_1$$

Equations (6) and (9) yield:

$$T_c/\theta_0 = 4.59 - 1.92 m_{\text{Ni}}$$

Comparison with experiment is given in Figs. 20 and 21. °

Fe with Co

Cobalt enters the iron lattice as $\text{Co}(\frac{5}{4})$ and $\text{Co}(\frac{5}{3})$ in the ratio of $3/7:4/7$. As with nickel the $\text{Fe}(\frac{4}{3})$ ions form $\text{Fe}(\frac{4}{2})$ when they have one cobalt nearest neighbor. There is an additional transformation shown below if the $\text{Fe}(\frac{4}{3})$ have more than one cobalt nearest neighbor. The following compositions satisfy equation (11):

$$m_{\text{Co}(\frac{5}{4})} = \frac{3}{7} m_{\text{Co}}$$

$$m_{\text{Co}(\frac{5}{3})} = \frac{4}{7} m_{\text{Co}}$$

$$m_{\text{Fe}(\frac{5}{3})} = \frac{2}{7} m_{\text{Fe}} + \frac{4}{35} m_{\text{Fe}}(f_2 - f_3)$$

$$m_{\text{Fe}(\frac{5}{2})} = \frac{3}{7} m_{\text{Fe}} + \frac{6}{35} m_{\text{Fe}}(f_2 - f_3)$$

$$m_{\text{Fe}(\frac{4}{3})} = \frac{2}{7} m_{\text{Fe}}(1 - f_1)$$

$$m_{\text{Fe}(\frac{4}{2})} = \frac{2}{7} m_{\text{Fe}}(f_1 - f_2)$$

$$m_{\text{Fe}(\frac{4}{1})} = \frac{2}{7} m_{\text{Fe}}(f_3 - f_4)$$

$$m_{\text{Fe}(\frac{4}{0})} = \frac{2}{7} m_{\text{Fe}} f_4$$

Equation (10) yields:

$$n_0 = 2.218 - .513m_{\text{Co}} + .296m_{\text{Fe}}f_1 + .178m_{\text{Fe}}f_2 + .118m_{\text{Fe}}f_3 + .296m_{\text{Fe}}f_4$$

Equations (6) and (9) yield:

$$T_{c/\theta_0} = 4.59 + 1.46m_{\text{Co}} + 1.84(1-m_{\text{Co}})(f_2 - f_3)$$

Comparison with experiment is given in Fig. 25.

Fe with Mn

In the case of manganese added to iron, manganese contributes one electron per atom to the alloy. If $5/7$ electrons per atom go into the 4s band, $\frac{2}{7}$ electrons per atom go into the 3d shell. Let

$$m_{\text{Fe}}^{(5)} = (A-1)m_{\text{Mn}}$$

$$m_{\text{Fe}}^{(3)} = \frac{2}{7}(1-Am_{\text{Mn}})$$

$$m_{\text{Fe}}^{(2)} = \frac{3}{7}(1-Am_{\text{Mn}})$$

$$m_{\text{Fe}}^{(4)} = \frac{2}{7}(1-Am_{\text{Mn}})$$

Equation (11) yields

$$A = \frac{37}{35}$$

$$n_0 = 2.218 \left(1 - \frac{37}{35} m_{\text{Mn}}\right)$$

Equations (6) and (9) yield:

$$T_c/\theta_0 = 4.59 \left(1 - \frac{37}{35} m_{\text{Mn}}\right)$$

Comparison with experiment is given in Fig. 27.

Fe with Cr

Chromium with a majority of iron nearest neighbors contributes two electrons per atom to the alloy while chromium with a majority of chromium nearest neighbors contributes one electron per atom to the alloy. Of these electrons $5/7$ electrons per atom go into the 4s band and $9/7$ electrons per atom go into the 3d shell. If there is a transformation of $\text{Fe}(\frac{4}{3})$ into iron ions with a filled 3d shell such that

$m_{\text{Fe}(\frac{4}{3})} = \frac{2}{7} m_{\text{Fe}} (1-f_2)$, equations (10) and (11) yield:

$$n_0 = 2.218 m_{\text{Fe}} - 1.331 m_{\text{Cr}} + .473 m_{\text{Fe}} f_2 + 1.035 m_{\text{Cr}} f_5$$

If the $\text{Fe}(\frac{4}{3})$ transforms into $\text{Fe}(\frac{5}{3})$ and $\text{Fe}(\frac{5}{2})$ as below, equations (6), (9), and (11) yield:

$$T_c/\theta_0 = (4.59 + 1.84 F_2) m_{\text{Fe}} - 1.38 m_{\text{Cr}} + 1.07 m_{\text{Cr}} f_5$$

The compositions of the ion species are:

$$m_{\text{Fe}(4)}^{(5)} = \frac{9}{14} m_{\text{Cr}} - \frac{1}{2} m_{\text{Cr}} f_5$$

$$m_{\text{Fe}(3)}^{(5)} = \frac{2}{7} m_{\text{Fe}} + \frac{4}{35} m_{\text{Fe}} f_2$$

$$m_{\text{Fe}(2)}^{(5)} = \frac{3}{7} m_{\text{Fe}} + \frac{6}{35} m_{\text{Fe}} f_2 - \frac{9}{14} m_{\text{Cr}} + \frac{1}{2} m_{\text{Cr}} f_5$$

$$m_{\text{Fe}(3)}^{(4)} = \frac{2}{7} m_{\text{Fe}} (1-f_2)$$

Comparison with experiment is given in Fig. 28.

Fe with V

Vanadium contributes four electrons per atom to the alloy of which $5/7$ electrons per atom go into the 4s band and $23/7$ electrons per atom go into the 3d shell. There is a transformation of $\text{Fe}(\frac{4}{3})$ into iron ions with a filled $3d^+$ shell such that $m_{\text{Fe}(\frac{4}{3})} = \frac{2}{7} m_{\text{Fe}} (1-f_1)$. Equations (10) and (11) yield:

$$n_0 = 2.218 m_{\text{Fe}} - 3.401 m_{\text{V}} + .473 m_{\text{Fe}} f_1 .$$

If the $\text{Fe}(\frac{4}{3})$ transforms into $\text{Fe}(\frac{5}{3})$ and $\text{Fe}(\frac{5}{2})$ as below, equations (6), (9), and (11) yield:

$$T_{c/\theta_0} = (4.59 + 1.84 f_1) m_{Fe} - 3.57 m_V$$

The compositions of the ion species are:

$$m_{Fe(4)}^{(5)} = \frac{23}{14} m_V$$

$$m_{Fe(3)}^{(5)} = \frac{2}{7} m_{Fe} + \frac{4}{35} m_{Fe} f_1$$

$$m_{Fe(2)}^{(5)} = \frac{3}{7} m_{Fe} + \frac{6}{35} m_{Fe} f_1 - \frac{23}{14} m_V$$

$$m_{Fe(3)}^{(4)} = \frac{2}{7} m_{Fe} (1-f_1)$$

Comparison with experiment is given in Fig. 29.

Fe with Al and Si

Each element contributes z electrons per atom to the alloy of which $5/7$ electrons per atom go into the $4s$ band and $z - \frac{5}{7}$ electrons per atom go into the $3d$ shell. There is a transformation of $Fe(3)^{(4)}$ into iron ions with a filled $3d^+$ shell such that $m_{Fe(3)}^{(4)} = \frac{2}{7} m_{Fe} (1-f_1)$. Equations (10) and (11) yield:

$$n_0 = 2.218 m_{Fe} - 1.035(z - \frac{5}{7}) m_z + .473 m_{Fe} f_1$$

If the $\text{Fe}_{(3)}^{(4)}$ transforms into $\text{Fe}_{(3)}^{(5)}$ and $\text{Fe}_{(2)}^{(5)}$ as below, equations (6), (9), and (11) yield:

$$T_{c/\theta_0} = (4.59 + 1.84 f_1) m_{\text{Fe}} - 2.14(z - \frac{5}{7}) m_z$$

The compositions of the ion species are:

$$m_{\text{Fe}_{(5)}^{(5)}} = \frac{1}{3} (z - \frac{5}{7}) m_z$$

$$m_{\text{Fe}_{(3)}^{(5)}} = \frac{2}{7} m_{\text{Fe}} + \frac{4}{35} m_{\text{Fe}} f_1$$

$$m_{\text{Fe}_{(2)}^{(5)}} = \frac{3}{7} m_{\text{Fe}} + \frac{6}{35} m_{\text{Fe}} f_1 - \frac{1}{3} (z - \frac{5}{7}) m_z$$

$$m_{\text{Fe}_{(3)}^{(4)}} = \frac{2}{7} m_{\text{Fe}} (1 - f_1)$$

The values of z that best fit the experimental curves for n_0 and T_{c/θ_0} are given in Table VI.

Table VI

element	z
Al	3
Si	4

Number of electrons element contributes to iron alloys.

Comparison with experiment is given in Fig.27.

Magnetic Properties of Ordered Alloys.

It is now possible to use equations (5) and (10) together with the information gained above about the behavior of the ion species to calculate the saturation moment and Curie temperature of an alloy with a specified degree of order. The effect of order on the magnetic properties may be seen by considering the special cases treated above, long range order only and short range order only. To determine the Curie temperature, equations (7) and (8a) are used instead of equation (5).

Saturation Moment.

Equation (10) for the saturation moment is valid for any degree of order. The only effect of order on the saturation moment is through a change in the compositions of the ion species. It may be seen from above that the alloys of nickel with copper, zinc, aluminum, silicon, antimony, chromium, vanadium and cobalt; the alloys of cobalt with manganese and chromium; and the iron manganese alloy do not have their saturation moments affected by ordering. The alloys systems where the saturation moment is affected by ordering are treated below.

Iron-Nickel.

For the fully ordered case in the nickel rich alloys, $f_6 = f_8 = 0$; $f_2 = 0$ for $m_{Fe} \leq 5/16$; $f_2 = 16(m_{Fe} - \frac{5}{16})$ for $5/16 \leq m_{Fe} \leq \frac{6}{16}$; and $f_2 = 1$ for $m_{Fe} \geq \frac{6}{16}$. In the iron rich alloys, $f_1 = 8m_{Ni}/m_{Fe}$ for $m_{Ni} \leq 1/9$ and $f_1 = 1$ for $m_{Ni} \geq \frac{1}{9}$. The theoretical curve is plotted in Fig. 20 . The values of n_0 for partially ordered states lie in between the fully ordered and disordered curves.

Nickel-Manganese

To obtain the values of n_0 for an arbitrary state of order, it is sufficient to use the equation for the disordered case with the modified probability of finding n manganese nearest neighbors given by:

$$m_{Mn} f_n^{ord} = n_A X_{Mn}(A) f_n \left(p_1(MnA | MnA) w_{AA}^1 + p_1(MnB | MnA) w_{BA}^1 \right) \\ + n_B X_{Mn}(B) f_n \left(p_1(MnA | MnB) w_{AB}^1 + p_1(MnB | MnB) w_{BB}^1 \right)$$

The theoretical values of n_0 for various states of order are given in Fig. 30 . The theoretical values of n_0 for alloys quenched from various temperatures are given in Fig. 31 . It is assumed that the free energy due to magnetism does not effect the state of order, $p = 0$, and only one phase is present. The discontinuities occur at the onset of long range order.

Iron-Cobalt.

For the fully ordered case in the iron rich alloys: .

$$m_{Co} \leq 1/9$$

$$1/9 \leq m_{Co} \leq \frac{17}{81}$$

$$\frac{17}{81} \leq m_{Co} \leq \frac{217}{729}$$

$$f_1 = 8m_{Co}/m_{Fe}$$

$$f_1 = 1$$

$$f_1 = 1$$

$$f_2 = 0$$

$$f_2 = 8(m_{Co} - 1/9)/m_{Fe}$$

$$f_2 = 1$$

$$f_3 = 0$$

$$f_3 = 0$$

$$f_3 = 8(m_{Co} - \frac{17}{81})/m_{Fe}$$

$$f_4 = 0$$

$$f_4 = 0$$

$$f_4 = 0$$

$$\frac{217}{729} \leq m_{\text{Co}} \leq \frac{2465}{6561}$$

$$m_{\text{Co}} \geq \frac{2465}{6561}$$

$$f_1 = 1$$

$$f_1 = 1$$

$$f_2 = 1$$

$$f_2 = 1$$

$$f_3 = 1$$

$$f_3 = 1$$

$$f_4 = 8(m_{\text{Co}} - \frac{217}{729})/m_{\text{Fe}}$$

$$f_4 = 1$$

The above values of f assume that the number of nearest neighbor cobalt atoms to each iron atom does not differ by more than one, i.e. if one iron atom has no cobalt nearest neighbors, another iron atom can not have two cobalt nearest neighbors. This assumption is not exact because of structure limitations, but it is a good approximation. The values for n_0 using the above assumption is given in Fig. 25. The values of n_0 for the partially ordered alloy lie in between the fully ordered and disordered curves. Comparison with experiment is also given in Fig. 25.

Iron-Chromium and Vanadium.

The values of f are the same as in the iron-cobalt case above. The curves for n_0 are plotted in Figs. 28 and 29.

Curie Temperature.

The alloys mentioned above in which the compositions of the ion species do not depend on the local environment still have a variation in Curie temperature with order due to the form of equations (7) or (8a). The variation of the Curie temperature with order is given below for a few typical systems.

Nickel-Copper, Zinc, Aluminum, Silicon, Antimony, Chromium, and Vanadium.

From above $m_{\text{Ni}(4)}^{(5)} = 5/9 - zm_z$, $u_A = 4.8(5/9 - zm_z)(1 - \frac{3S}{4m_{\text{Ni}}})$,

$u_B = 4.8(5/9 - zm_z)(1 + \frac{3S}{4m_{\text{Ni}}})$, $w_{AA} = \Lambda_2/\Lambda$, $w_{AB} = \frac{1}{3} \Lambda_1/\Lambda$, $w_{BA} = \Lambda_1/\Lambda$,

and $w_{BB} = (\frac{2}{3} \Lambda_1 + \Lambda_2)/\Lambda$ for the AB_3 superlattice. Let $\lambda_1 = \Lambda_1/\Lambda$, $\lambda_2 = \Lambda_2/\Lambda$, and $\lambda_1 + \lambda_2 = 1$. Using equation (7) it is possible to calculate the Curie temperature for various values of S , the long range order, and λ_1 , the magnetic interaction parameter. The ratio of the Curie temperatures of ordered and disordered alloys is given in Figs. 42, 43, and 44 as a function of S and λ_1 .

For the case of short range order only, it is not necessary to use the approximation to equation (8) since $\text{Ni}(4)^{(5)}$ is the only magnetic ion species present. Equation (8) yields:

$$T_c(\text{ord})/T_c(\text{dis}) = 1 + \lambda_{\text{NiNi}}$$

where $\lambda_{\text{NiNi}} = \sum_i^{\text{Ni}} q_i(\text{Ni}|\text{Ni}) \lambda(r_i)/\Lambda$. The behavior of $T_c/T_c(\text{dis})$ depends on both the amount of short range order, q_i , and the variation of $\lambda(r_i)$. In the case of a small amount of short range order with $|q_1| > |q_i|$ $i \neq 1$, if $q_1 > 0$ (Ni ions avoid each other) the Curie temperature will be lowered; if $q_1 < 0$ (segregation of Ni ions) the Curie temperature will be raised.

Nickel-Manganese

From above

$$m_{\text{Ni}(4)}^{(5)} = \frac{5}{9} m_{\text{Ni}} - 2m_{\text{Mn}} f_1 - \frac{13}{9} m_{\text{Mn}} f_3$$

$$m_{\text{Mn}(2)}^{(5)} = m_{\text{Mn}}(1-f_1)$$

The values of f are determined as above by using the modified probability of finding n manganese nearest neighbors, f_n^{ord} . The values of X for the AB_3 superlattice are:

$$X_{\text{Ni}(4)}^{(5)}(\text{A}) = m_{\text{Ni}(4)}^{(5)} \left(1 - \frac{3S}{4m_{\text{Ni}}}\right); \quad X_{\text{Ni}(4)}^{(5)}(\text{B}) = m_{\text{Ni}(6)}^{(5)} \left(1 + \frac{S}{4m_{\text{Ni}}}\right)$$

$$X_{\text{Mn}(2)}^{(5)}(\text{A}) = m_{\text{Nb}(2)}^{(5)} \left(1 + \frac{3S}{4m_{\text{Mn}}}\right); \quad X_{\text{Mn}(2)}^{(5)}(\text{B}) = m_{\text{Mn}(2)}^{(5)} \left(1 - \frac{S}{4m_{\text{Mn}}}\right)$$

$$X_{\text{Mn}(1)}^{(5)}(\text{A}) = m_{\text{Mn}(1)}^{(5)} \left(1 + \frac{3S}{4m_{\text{Mn}}}\right); \quad X_{\text{Mn}(1)}^{(5)}(\text{B}) = m_{\text{Mn}(2)}^{(5)} \left(1 - \frac{S}{4m_{\text{Mn}}}\right)$$

Equation (7) yields the values of T_c/θ_0 for various values of long range order, S . The results are given in Figs. 45 and 46 for $\lambda_1 = .5, 1$.

The values of T_c/θ_0 for the fully ordered alloy for various values of λ_1 are given in Fig. 47. It is clear that for Ni_3Mn T_c/θ_0 is a very sensitive function of order. For $\lambda_1 = 1$ there is a difference of 260°K between the Curie temperatures of the fully ordered alloy and the alloy with $S = .9$. It is therefore very difficult to determine λ_1 unless the degree of order is known quite well. The experimental measurements of Marchinkowski and Brown⁴⁵ yield $T_c/\theta_0 = 3.10$ for $m_{\text{Mn}} = .227$ in

what they consider a fully ordered alloy, i.e. $s = .91$. If it may be assumed that the order was slightly less than complete, $\lambda_1 = 1$ gives excellent agreement with the experimental value.

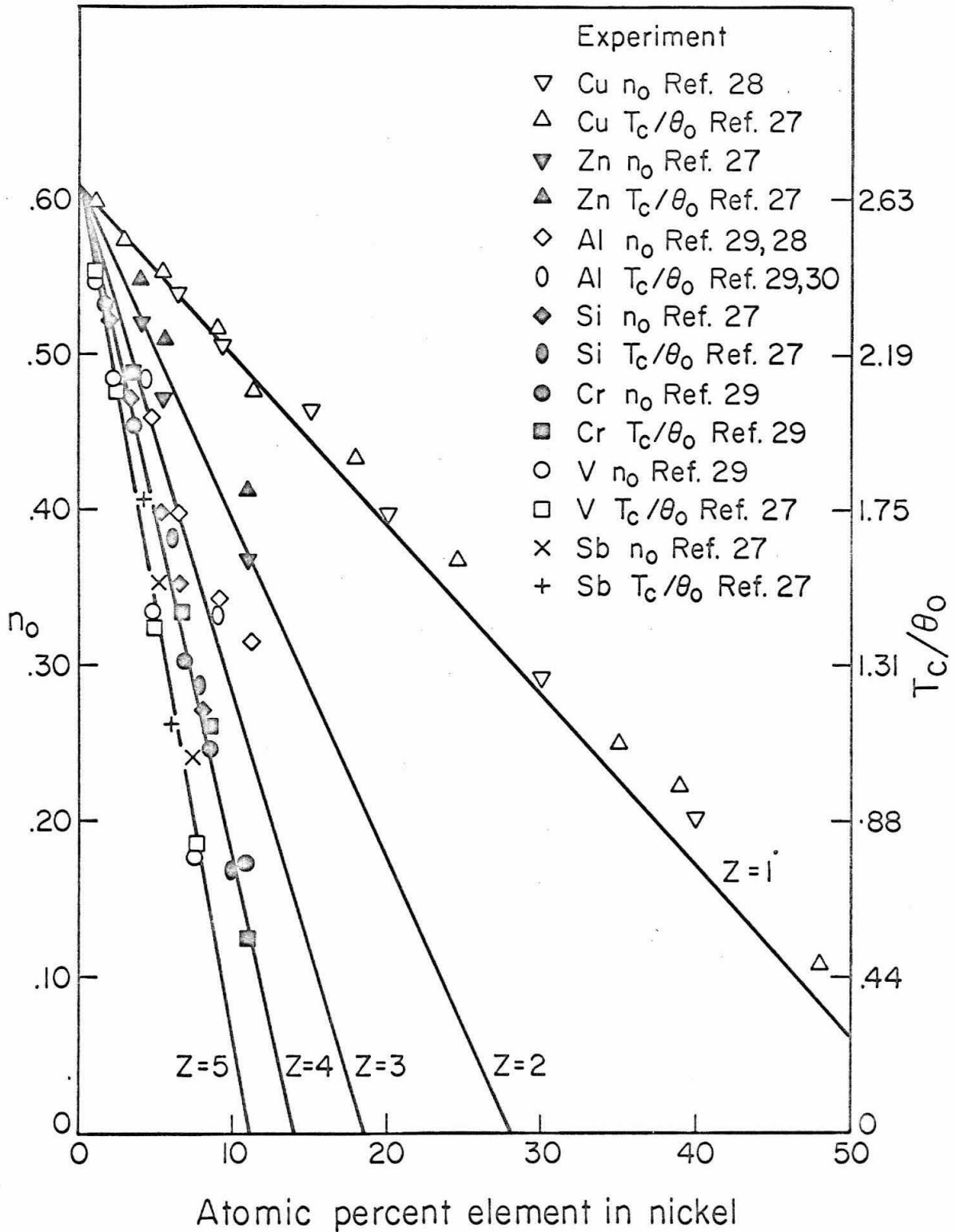
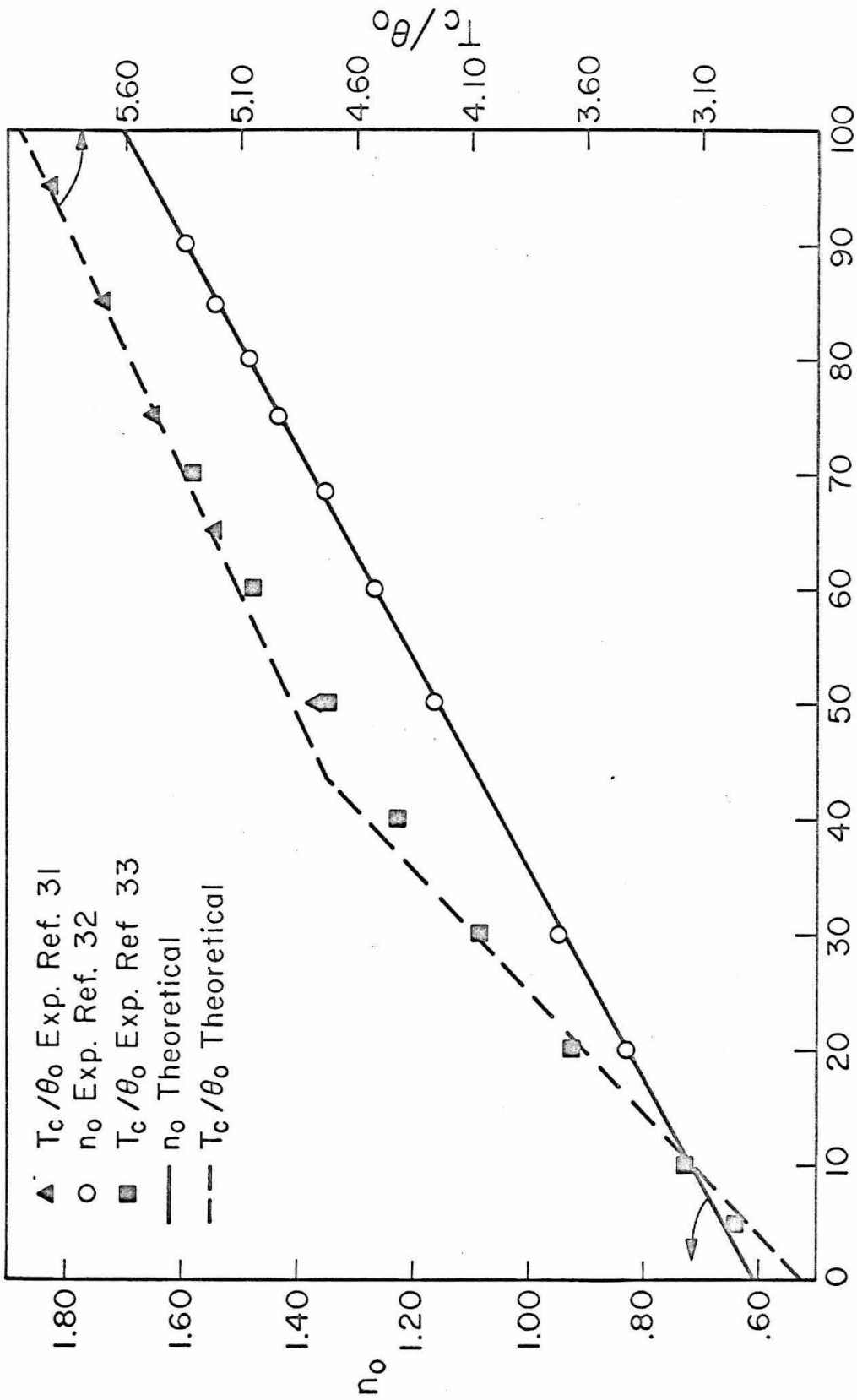
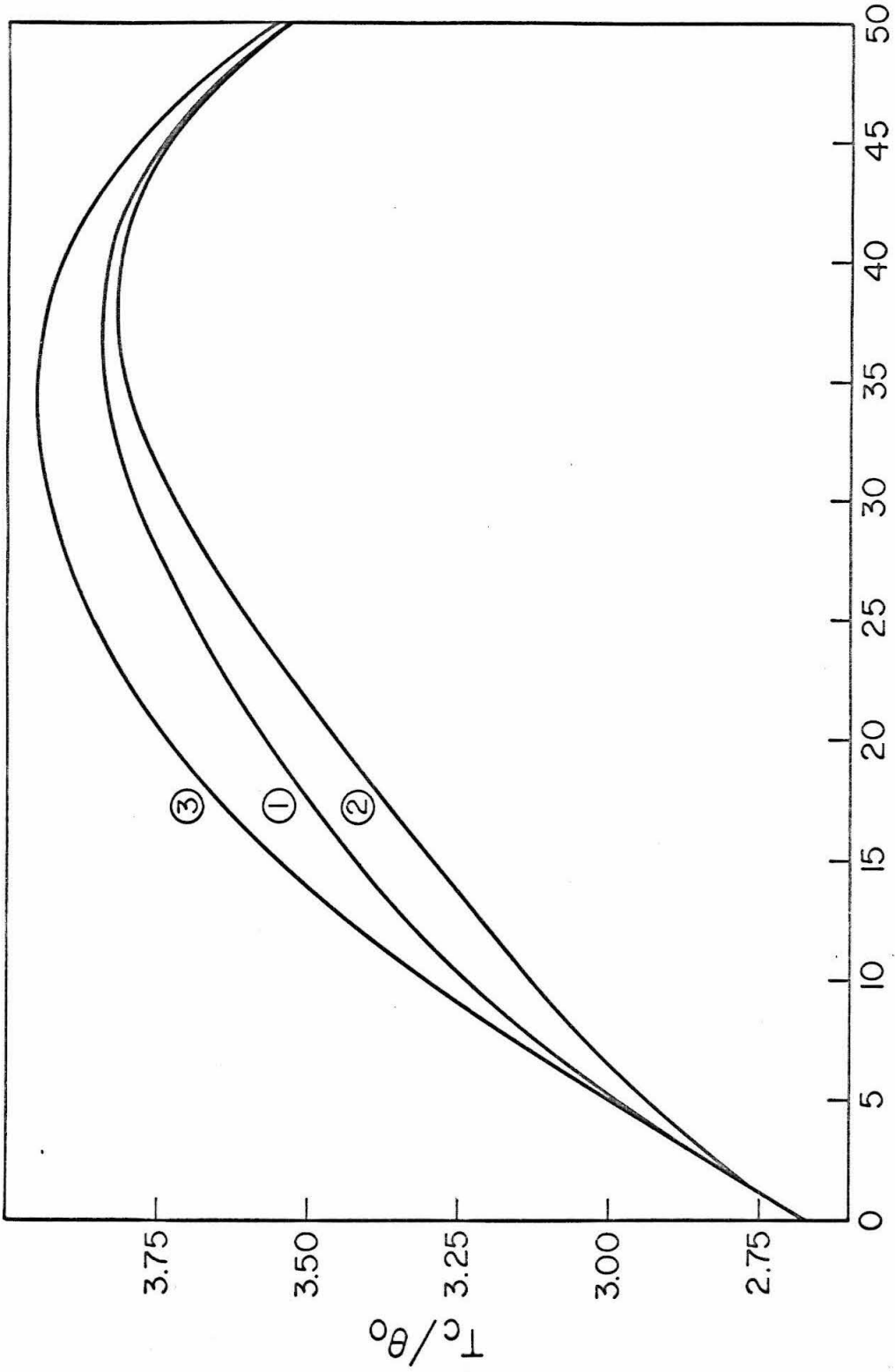


Fig.17. Saturation moments and Curie temperatures of nickel alloys



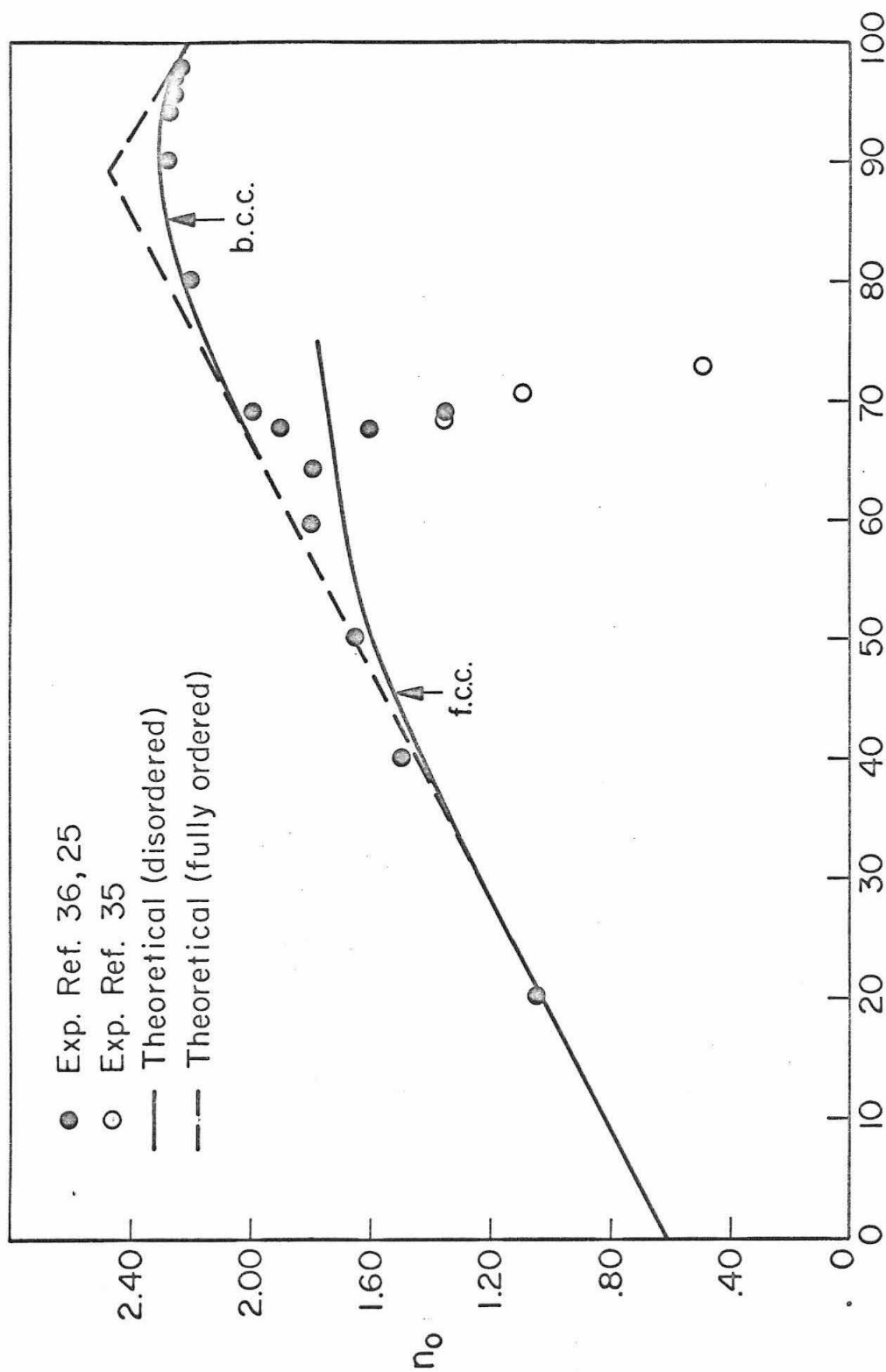
Atomic percent cobalt in nickel

Fig. 18. Saturation moments and Curie temperatures for the nickel-cobalt alloys



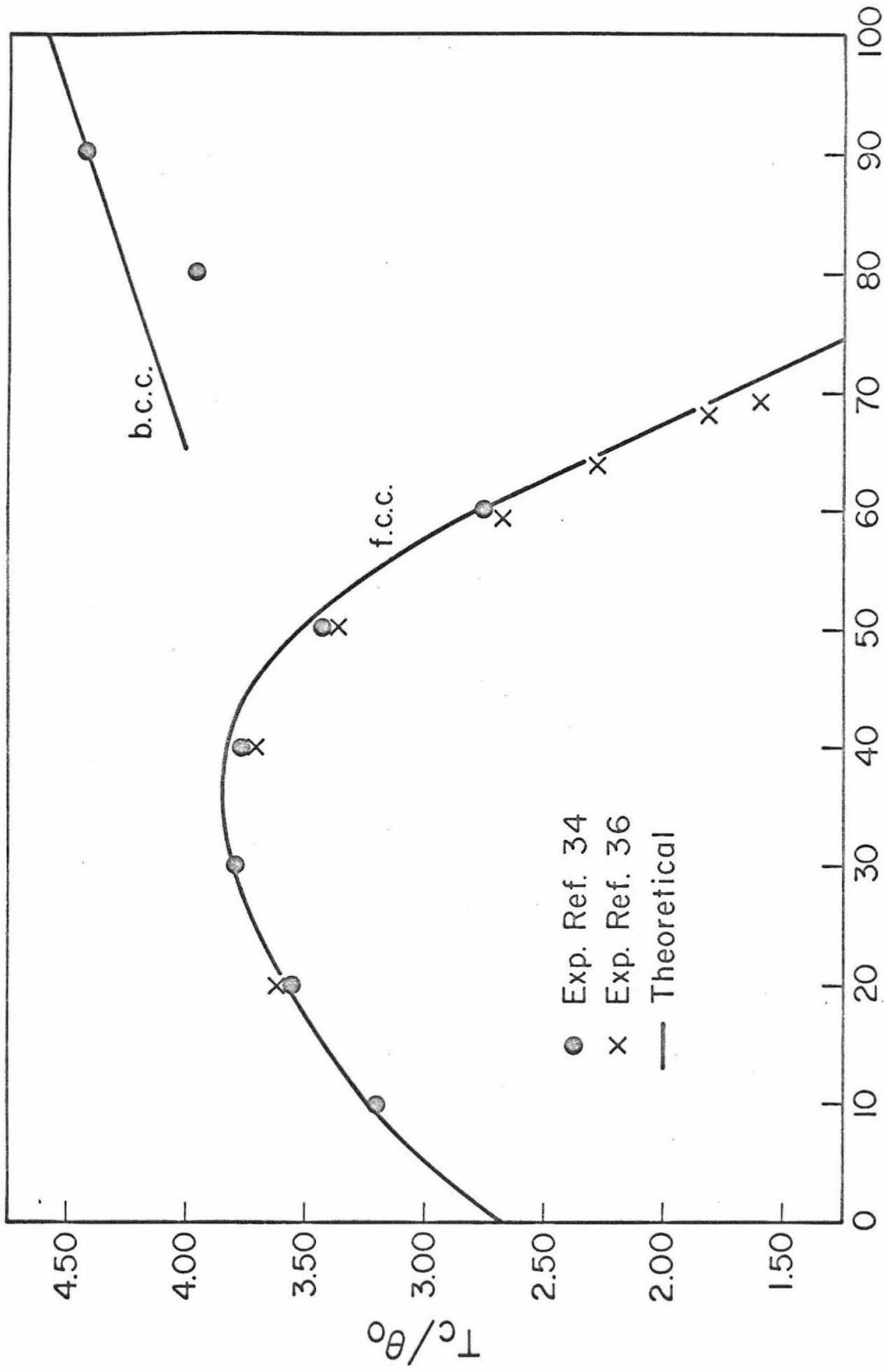
Atomic percent iron in nickel

Fig. 19. Curie temperature of iron-nickel alloys under various assumptions specified in the text



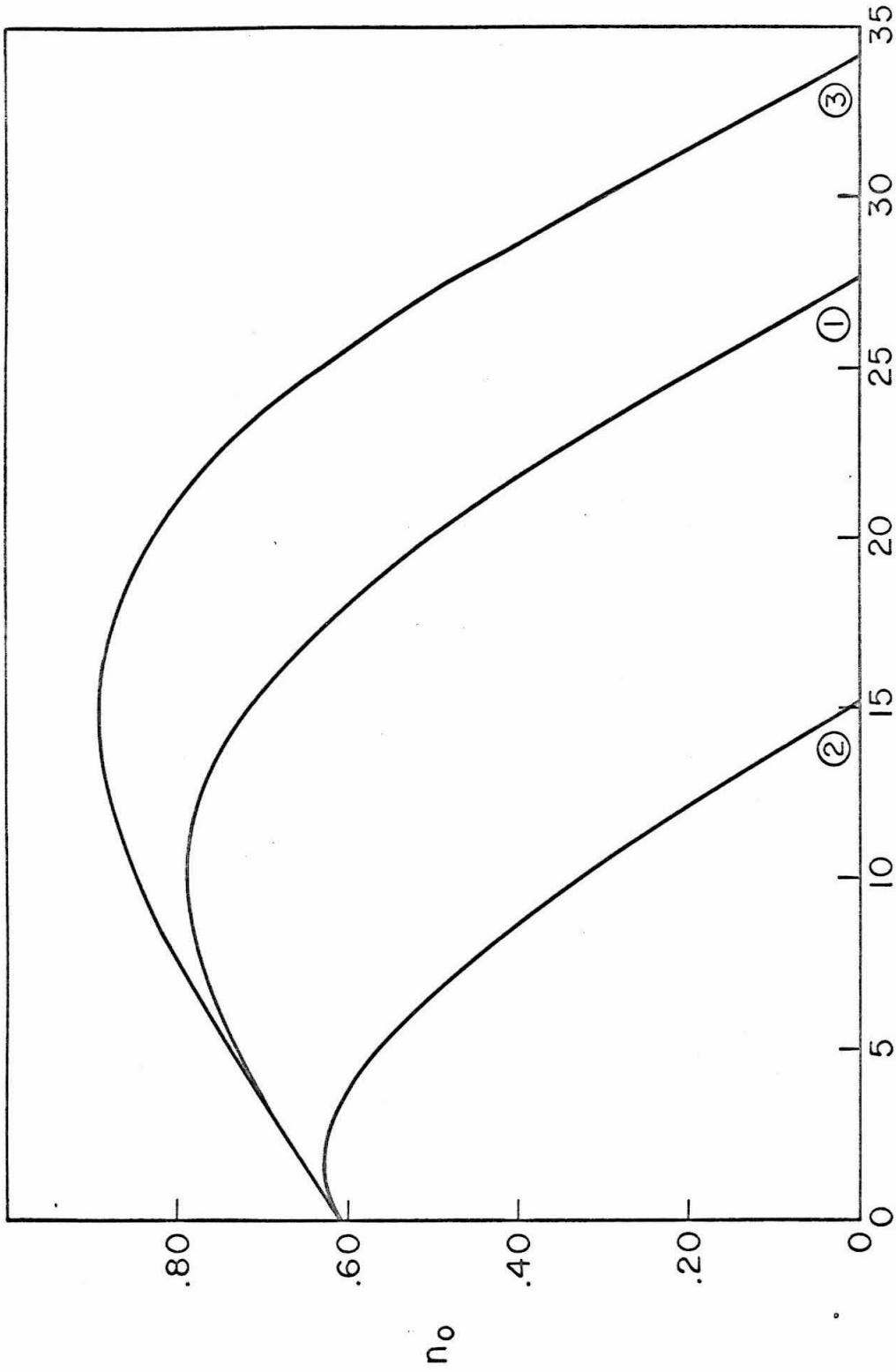
Atomic percent iron in nickel

Fig. 20. Saturation moments in iron-nickel alloys



Atomic percent iron in nickel

Fig. 21. Curie temperature of iron-nickel alloys



Atomic percent manganese in nickel

Fig. 22. Saturation moments of nickel-manganese alloys under various assumptions specified in the text

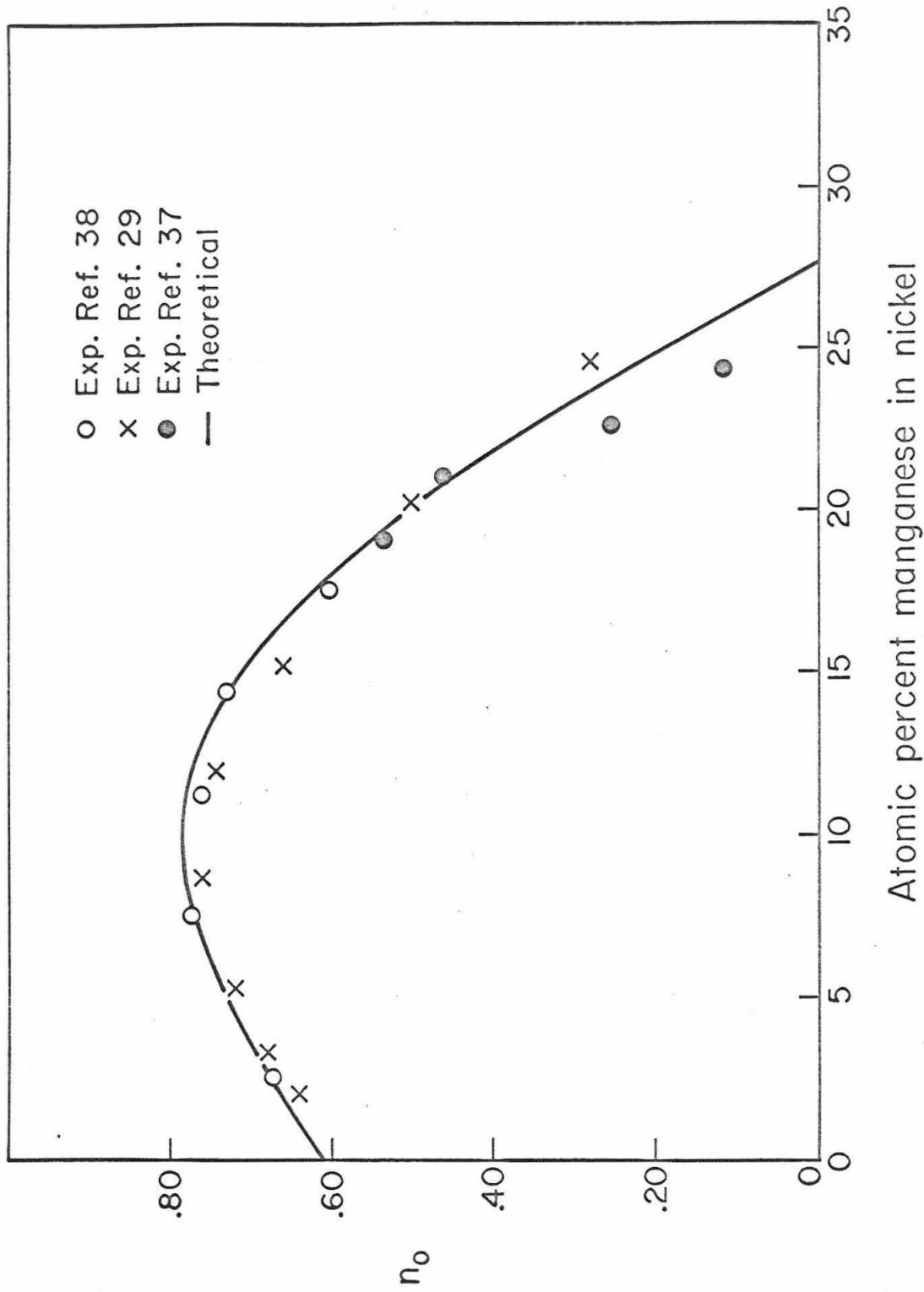


Fig. 23. Saturation moments of disordered nickel-manganese alloys

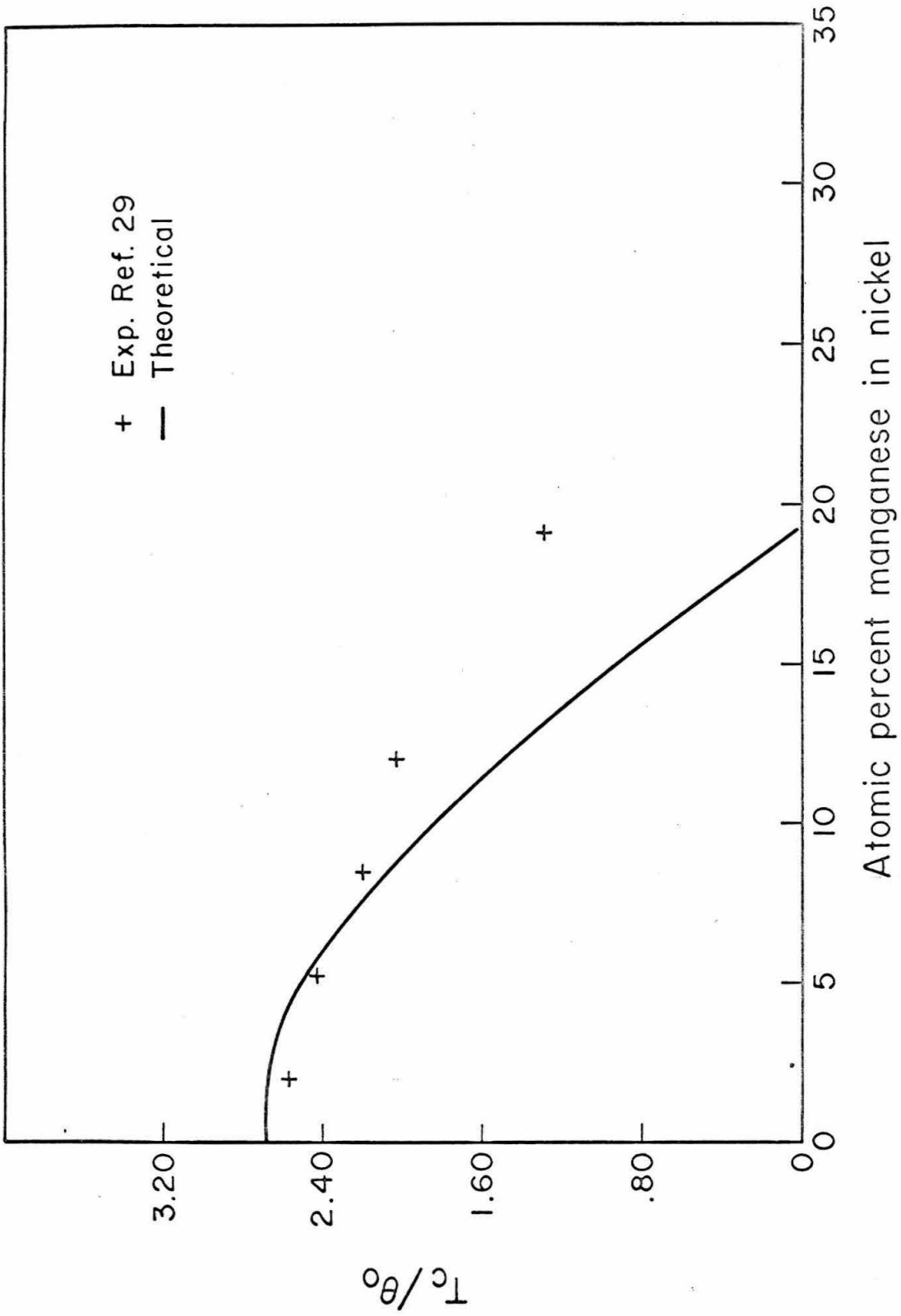
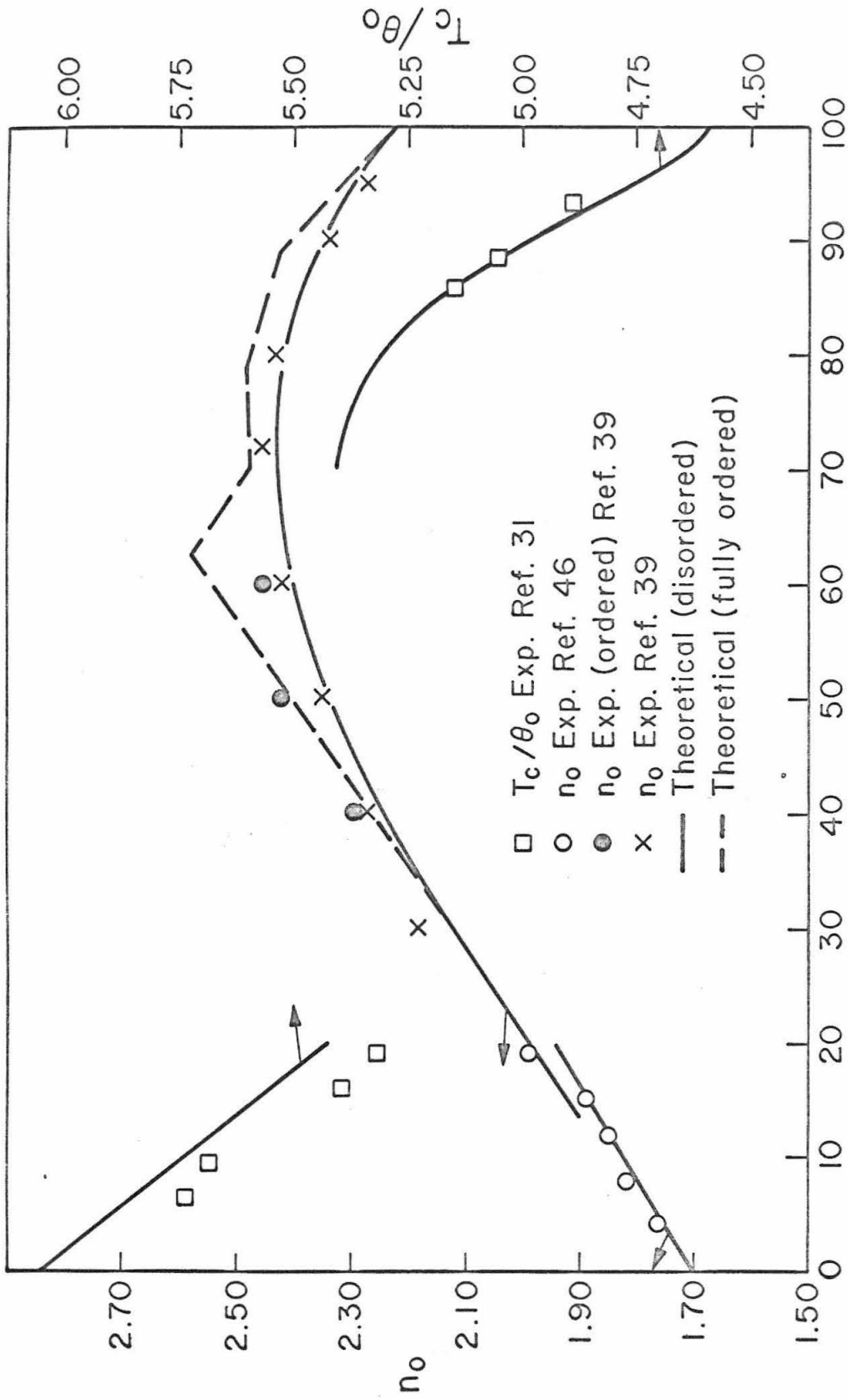
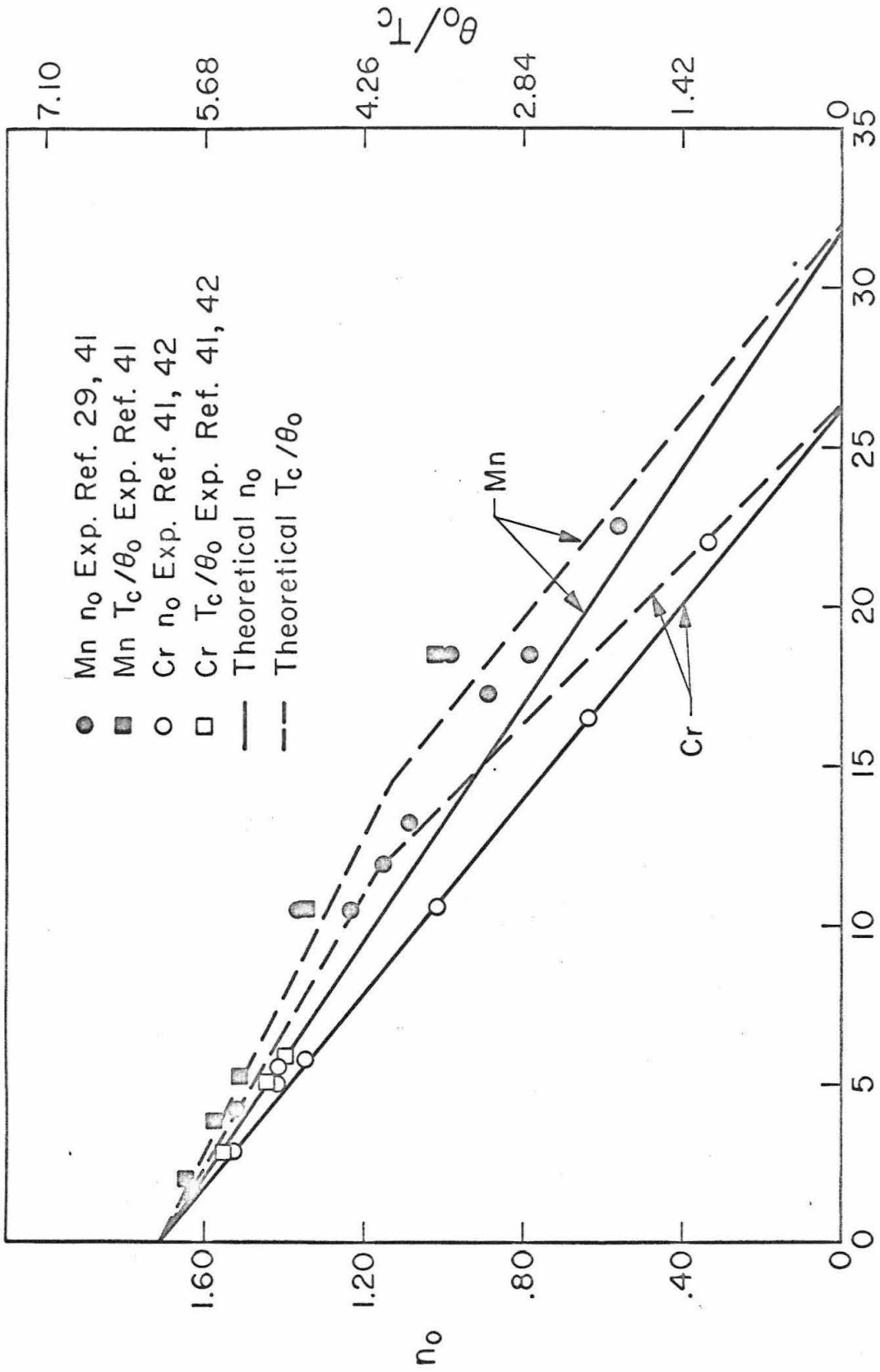


Fig. 24. Curie temperature of disordered nickel-manganese alloys



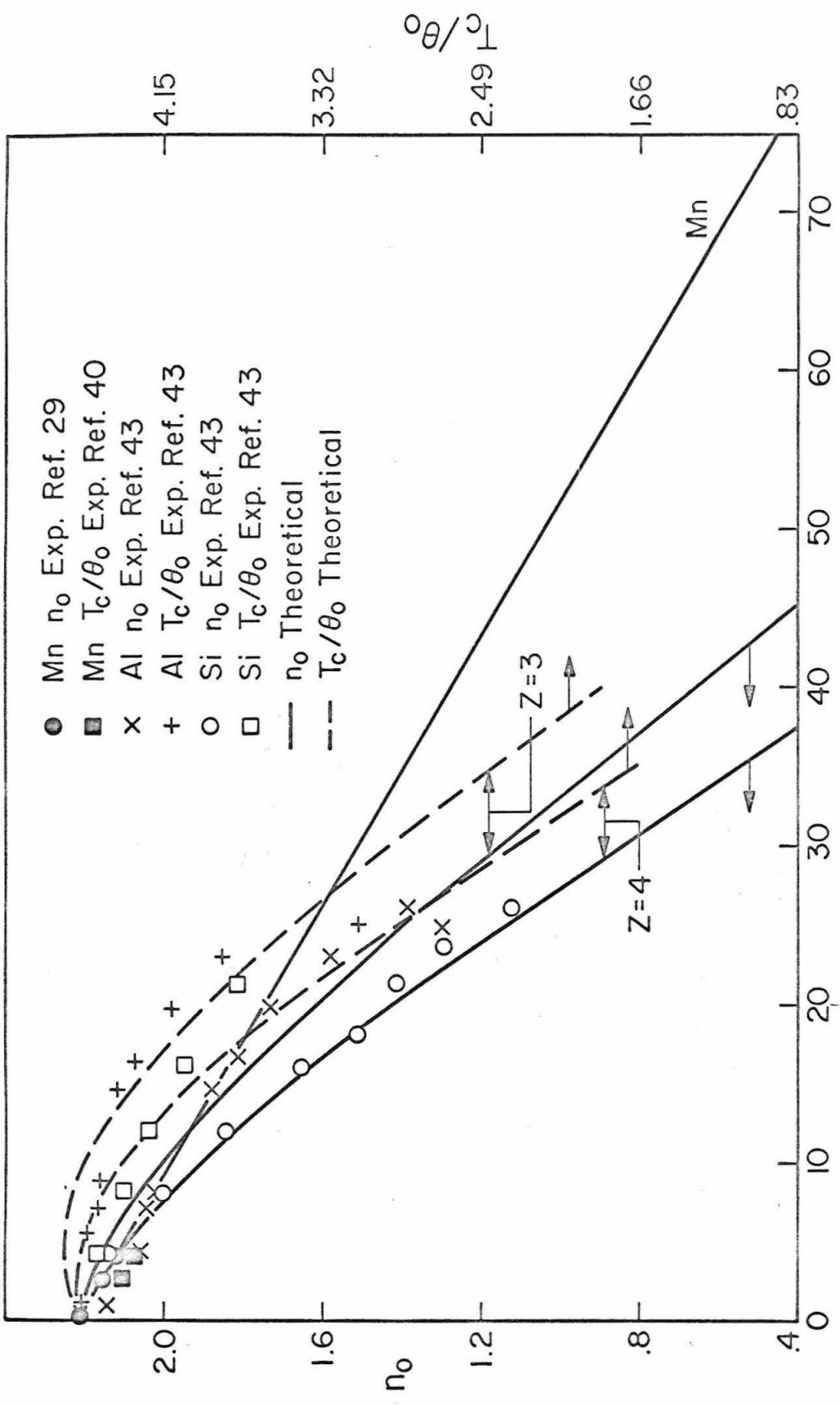
Atomic percent iron in cobalt

Fig. 25. Saturation moments and Curie temperatures for the iron-cobalt alloy



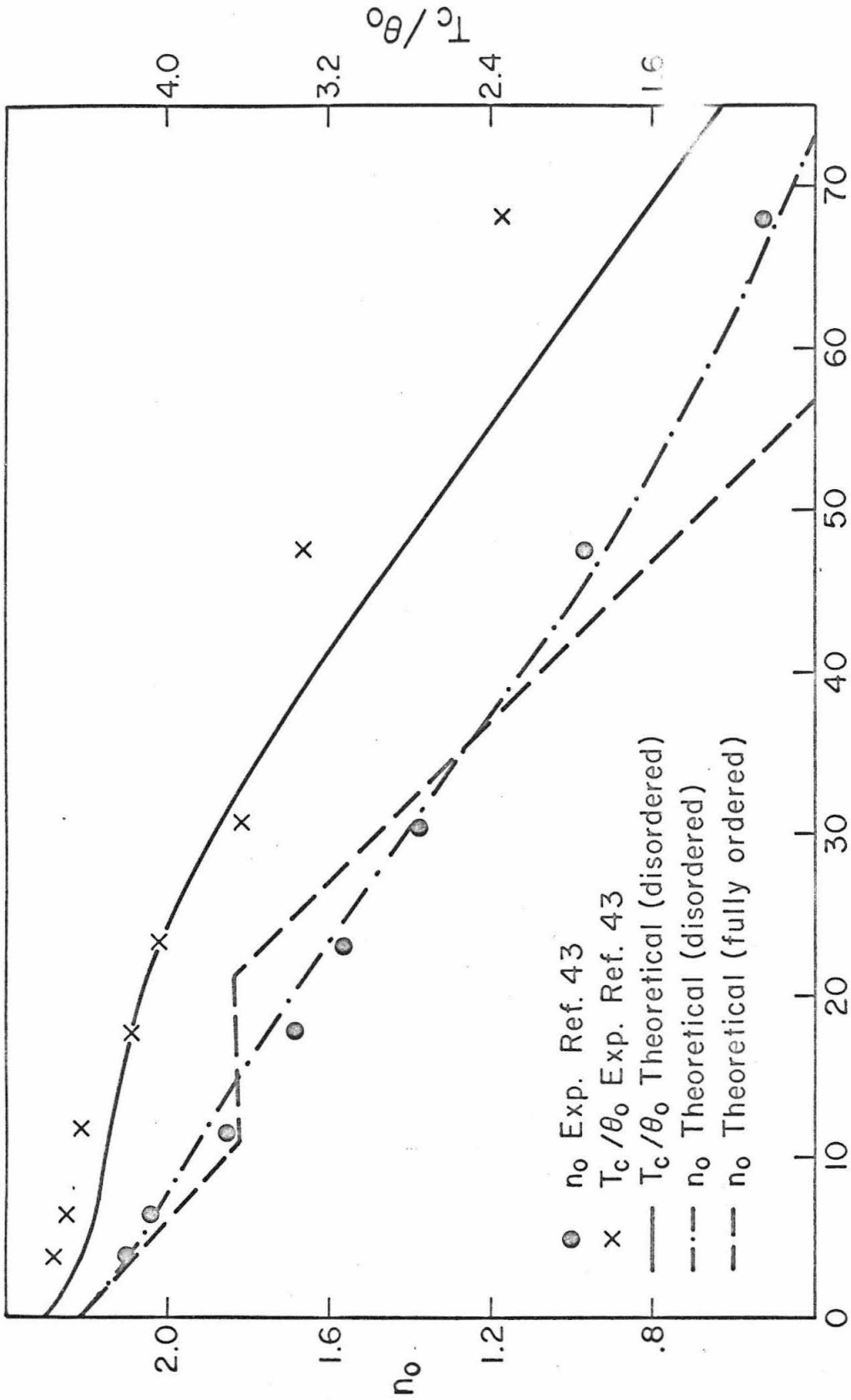
Atomic percent element in cobalt

Fig. 26. Saturation moments and Curie temperatures of cobalt alloys



Atomic percent element in iron

Fig. 27. Saturation moment and Curie temperature of iron alloys



Atomic percent chromium in iron

Fig. 28. Saturation moments and Curie temperatures for the iron-chromium alloys

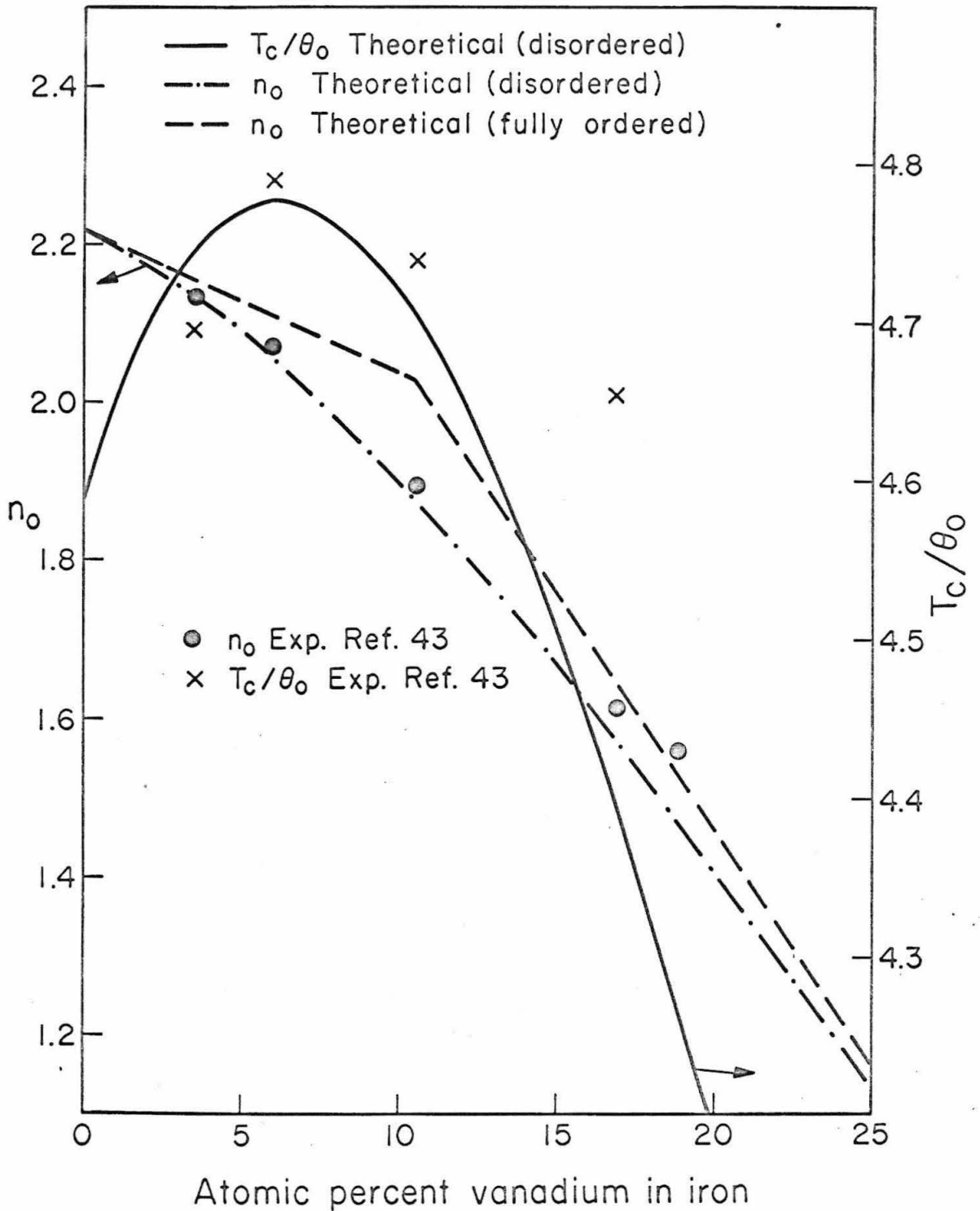


Fig. 29. Saturation moments and Curie temperatures of iron-vanadium alloys

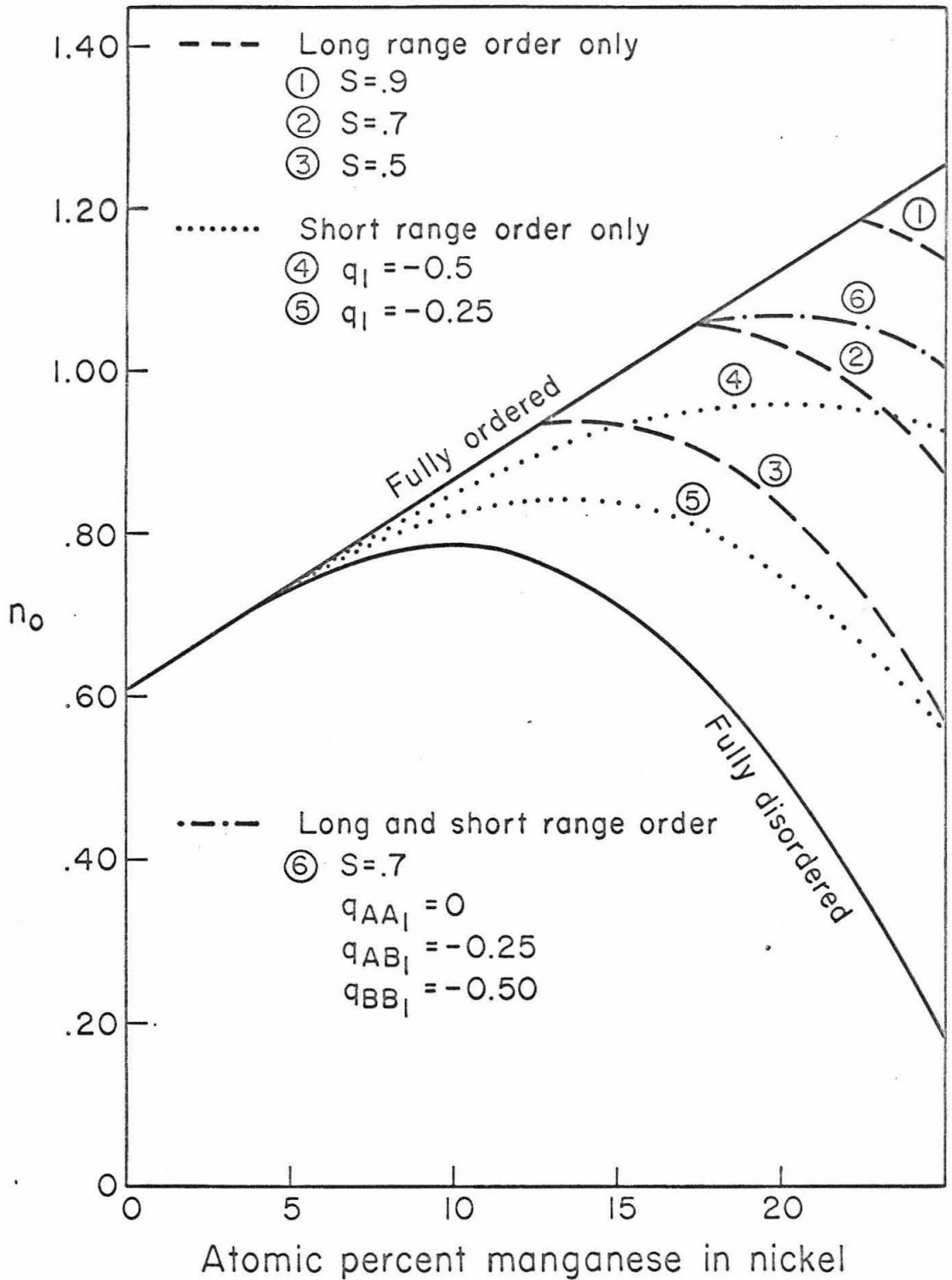
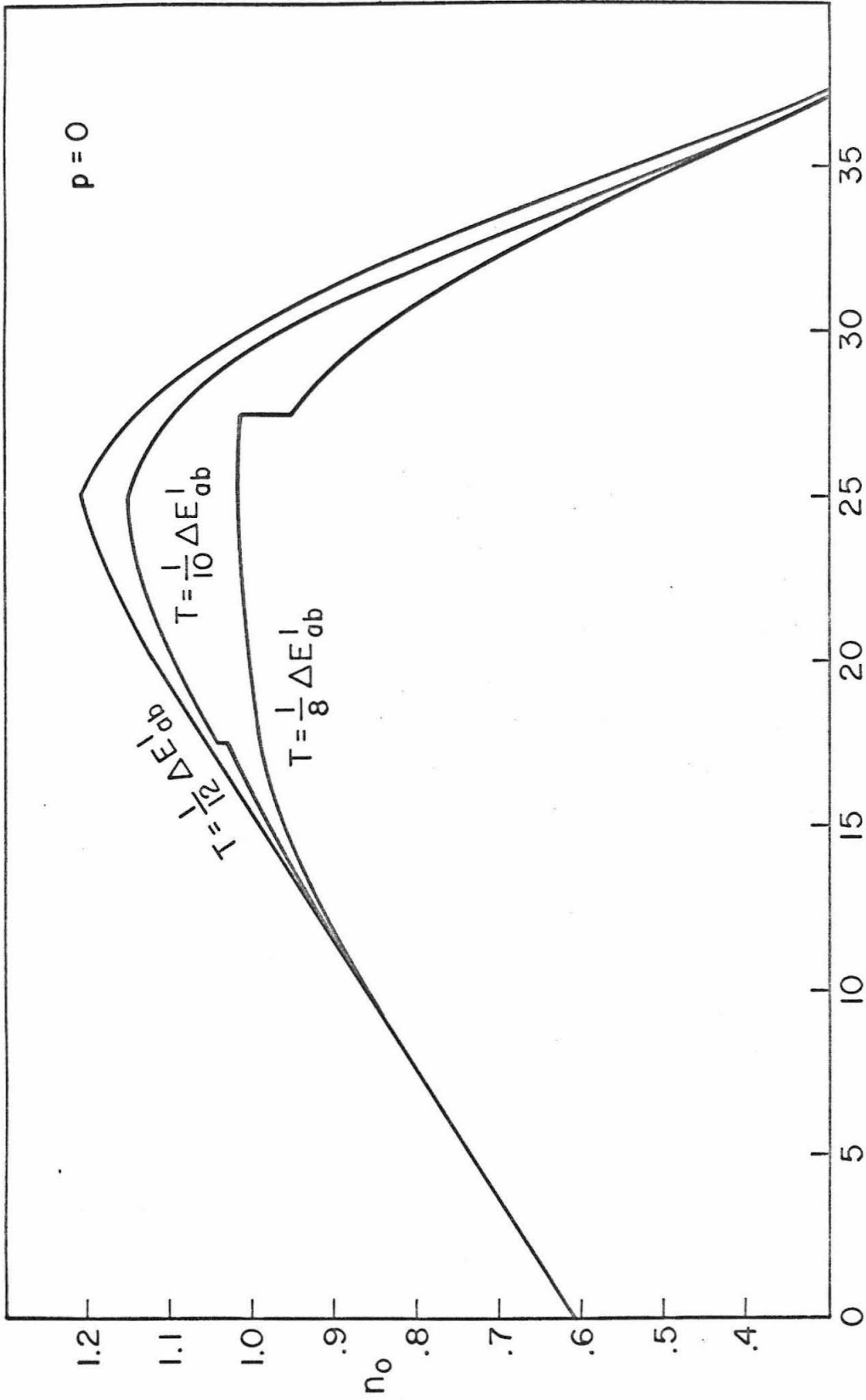
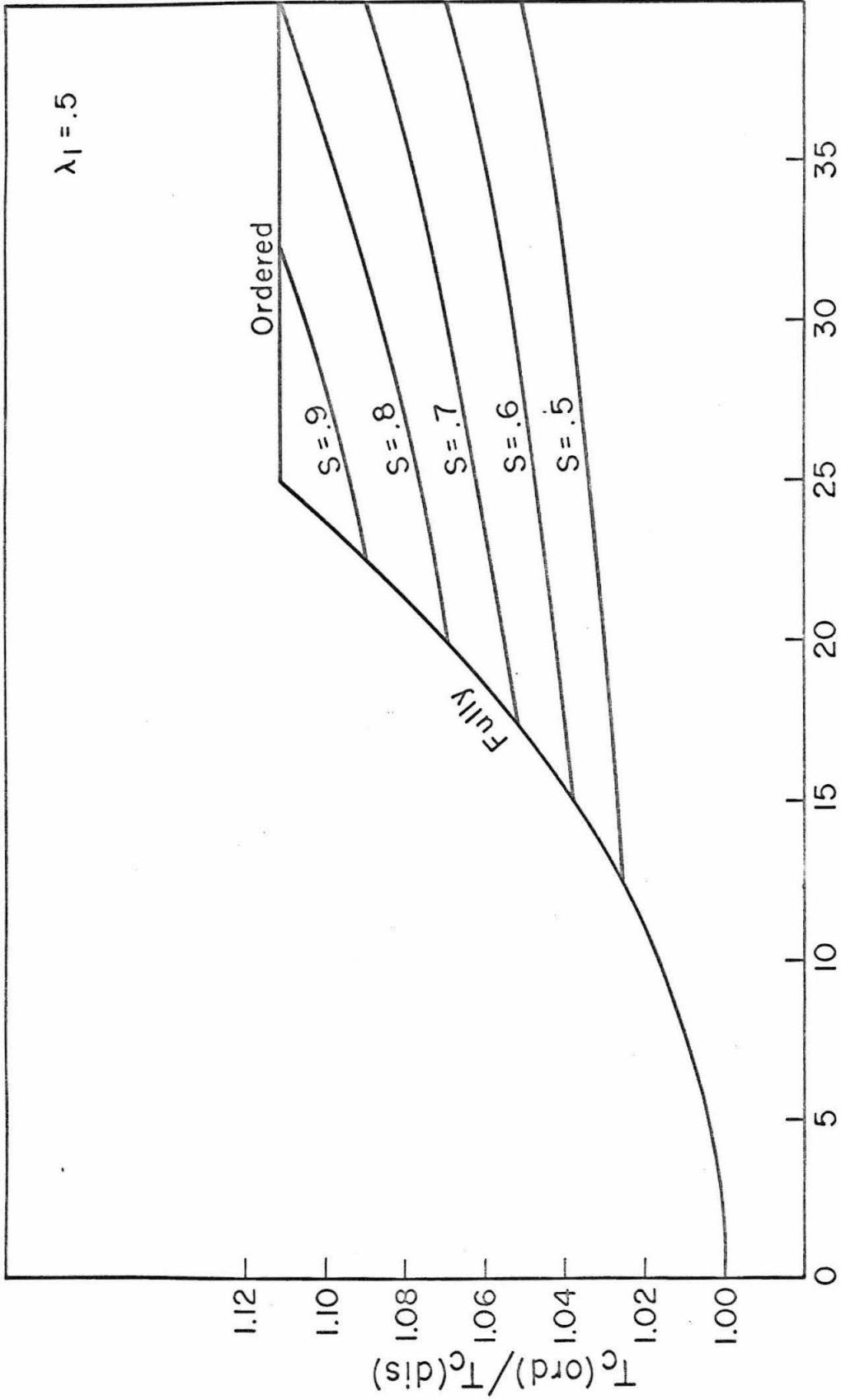


Fig. 30. Theoretical values of the saturation moments of nickel-manganese alloys for various degrees of long range order, S , and short range order, q_{AA_1} , q_{AB_1} , q_{BB_1} , $q_1 = q_{AA_1} = q_{AB_1} = q_{BB_1}$.



Atomic percent manganese in nickel

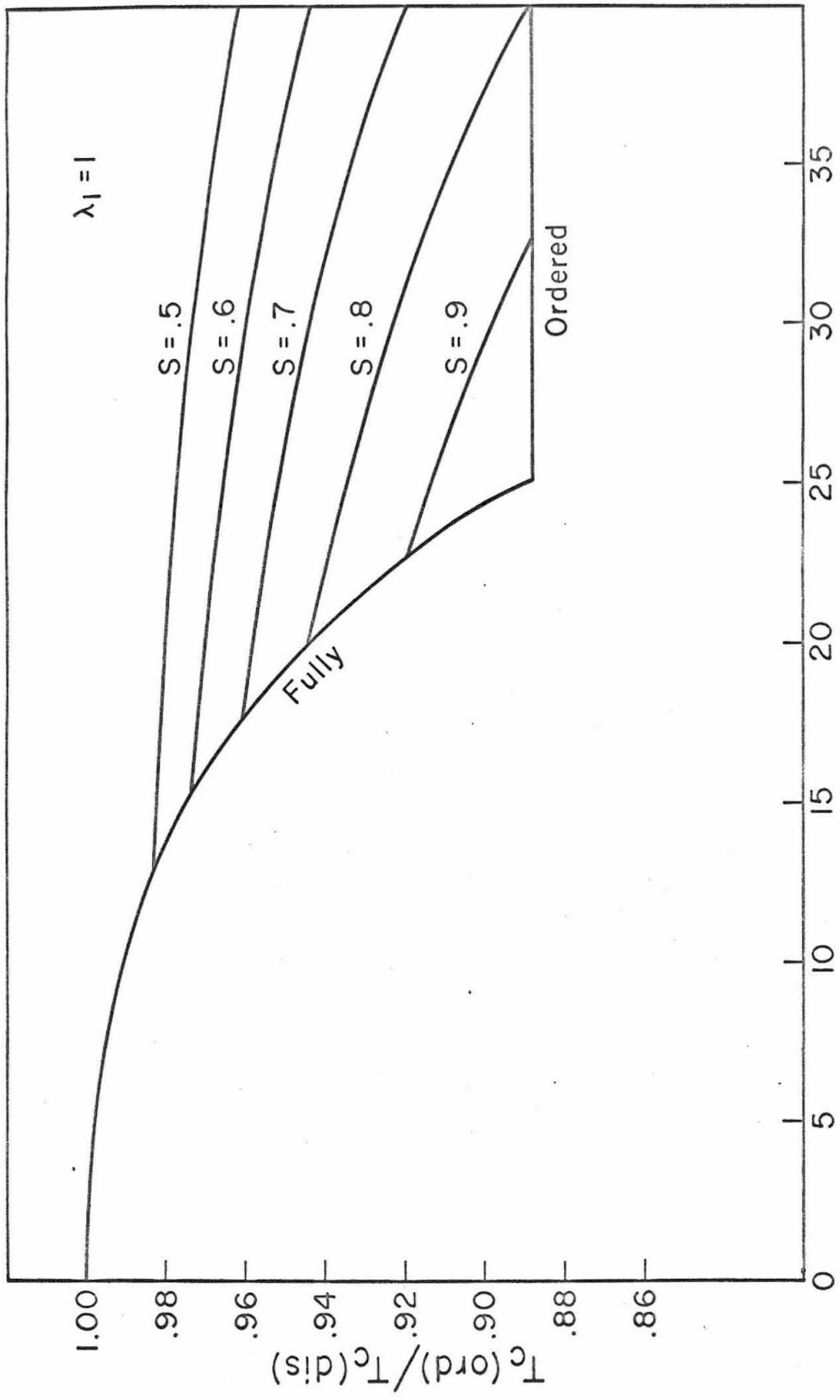
Fig. 31. Saturation magnetization of nickel manganese alloys quenched from various temperatures, T



$\lambda_1 = .5$

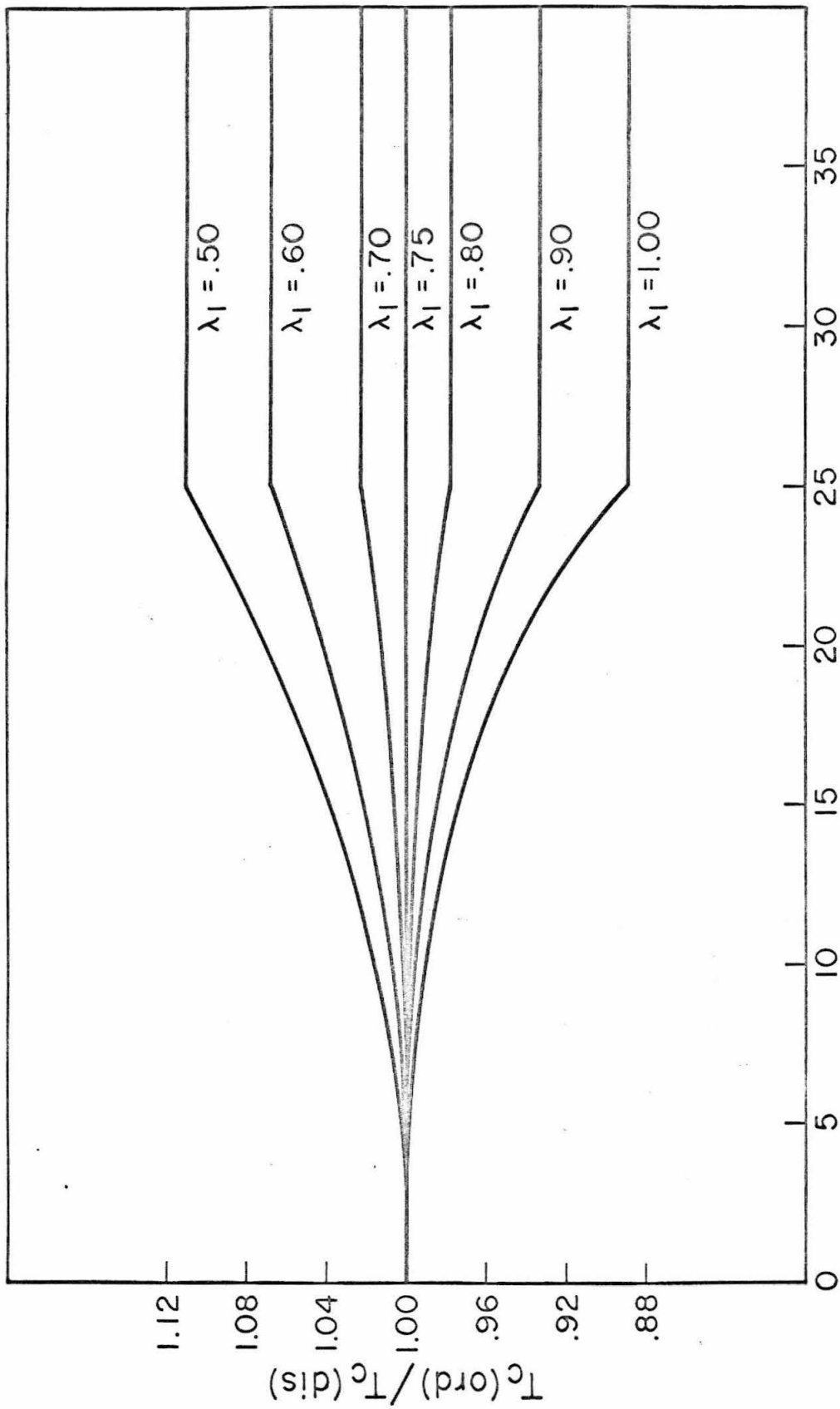
Atomic percent element in nickel

Fig. 32. Curie temperatures of nickel alloys with various degrees of long range order, S .



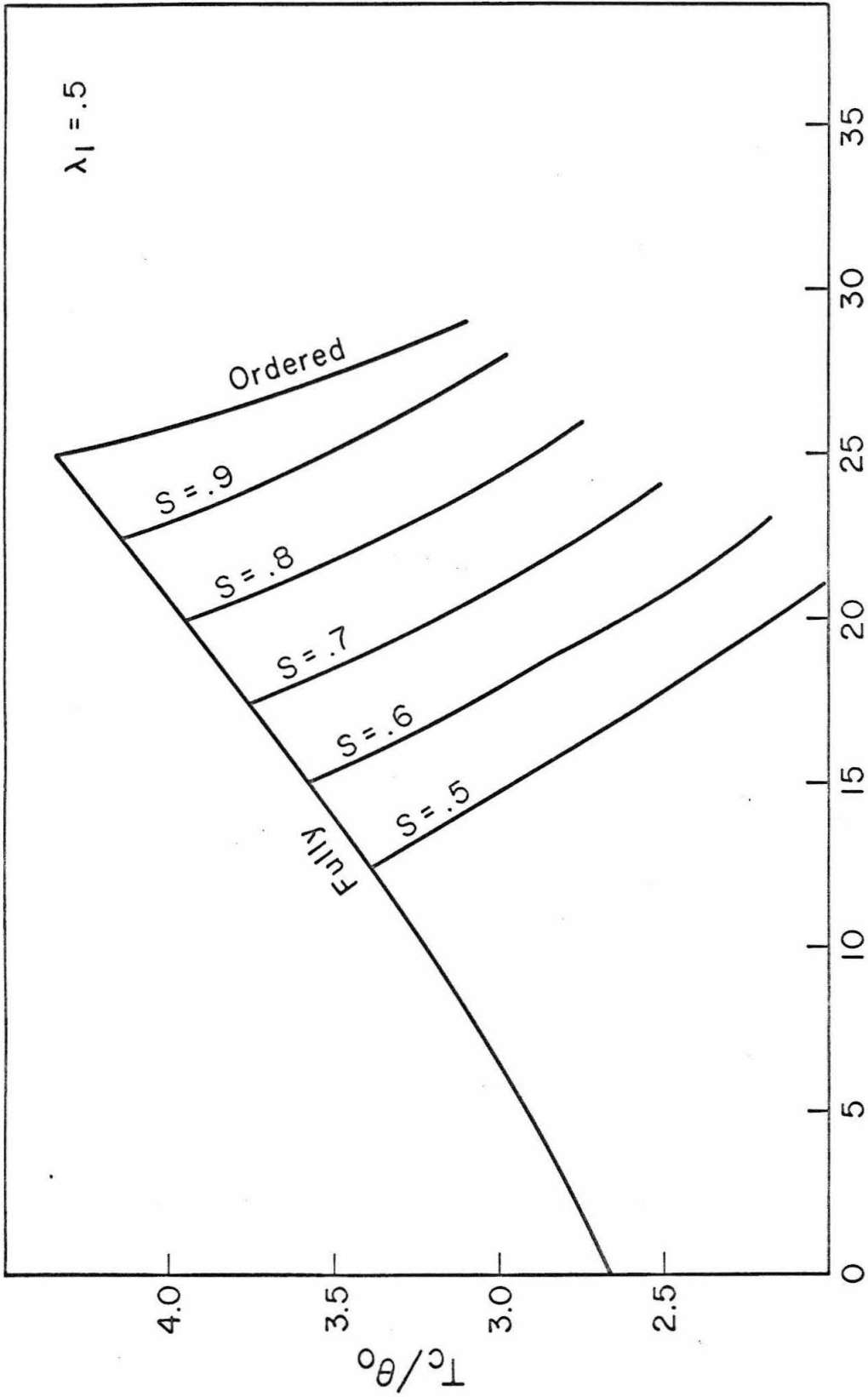
Atomic percent element in nickel

Fig. 33. Curie temperatures of nickel alloys with various degrees of long range order, S



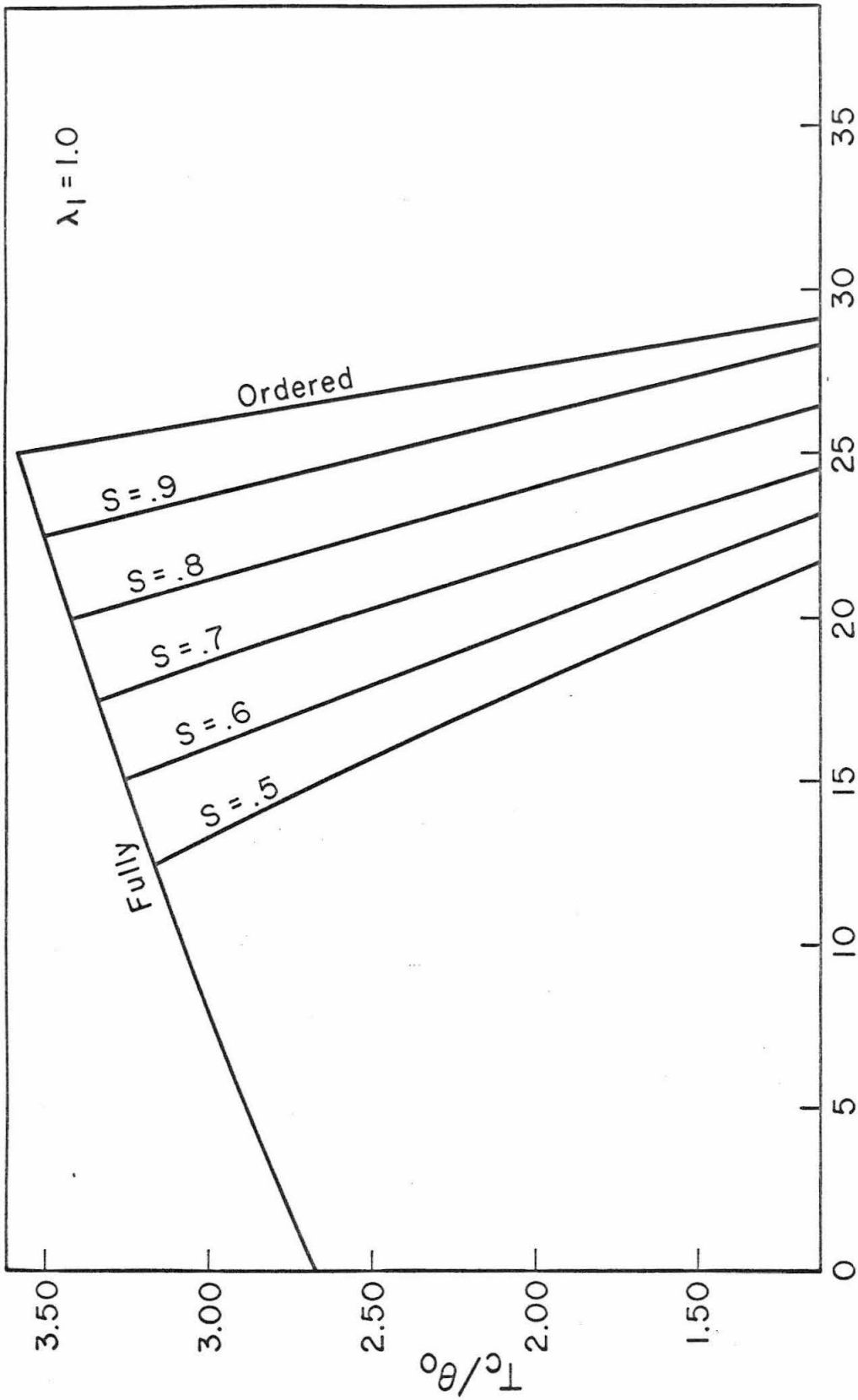
Atomic percent element in nickel

Fig. 34. Curie temperatures of fully ordered nickel alloys for various values of the magnetic interaction parameter, λ_I



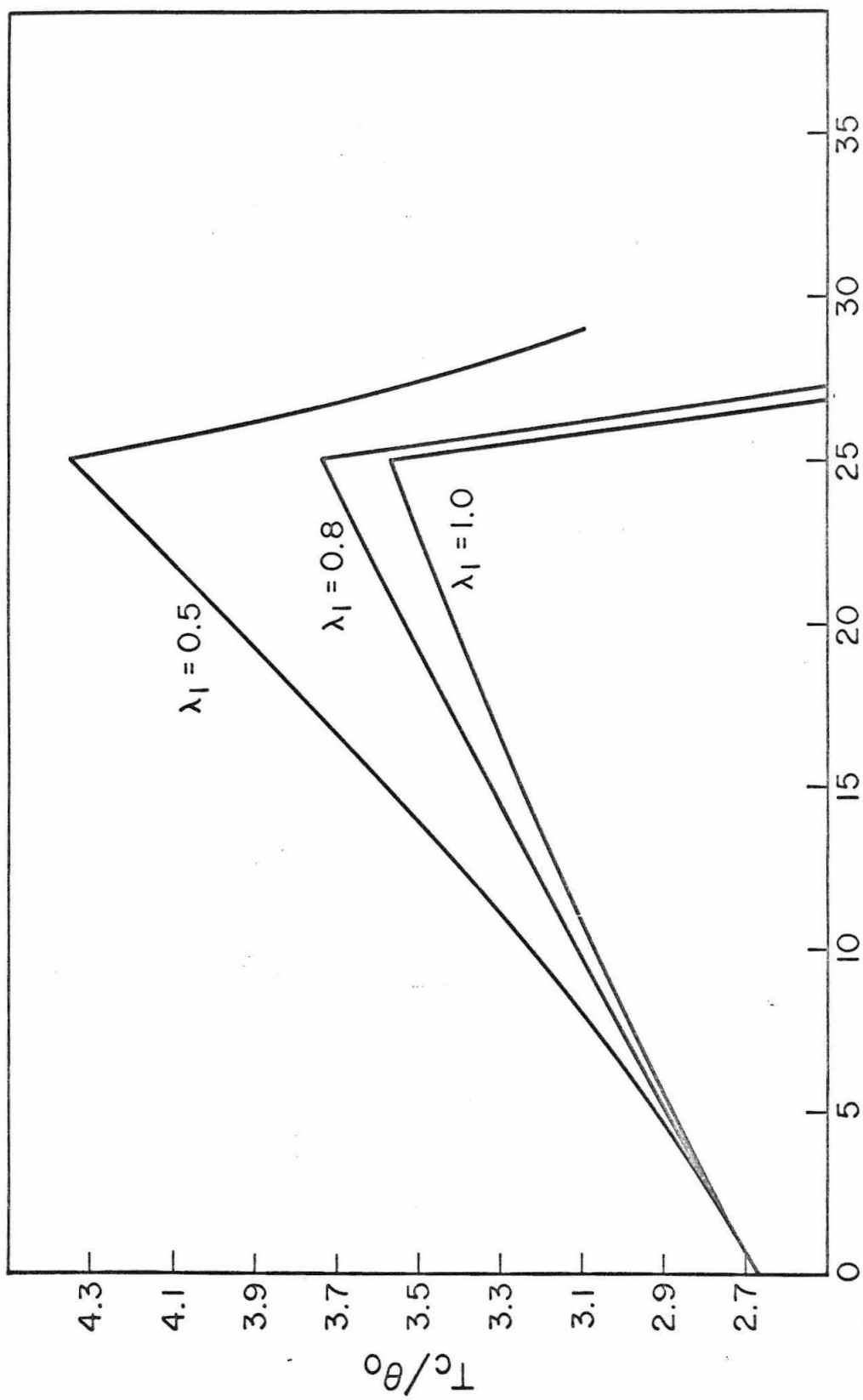
Atomic percent manganese in nickel

Fig. 35. Curie temperatures of nickel manganese alloys with various degrees of long range order, S



Atomic percent manganese in nickel

Fig. 36. Curie temperatures of nickel manganese alloys with various degrees of long range order, S



Atomic percent manganese in nickel

Fig. 37. Curie temperatures of fully ordered nickel manganese alloys for various values of the magnetic interaction parameter, λ_I

Conclusion

A theory of the order disorder transformation has been developed that considers all atomic interactions. The generality of the theory permits treatment of alloys of arbitrary composition in multi-component systems. The theory is applicable to virtually any crystal structure and superlattice.

The theory has been applied to a binary face centered cubic alloy assuming the possibility of A_3B , AB , and AB_3 superlattices. There were two arbitrary constants to be determined. One can be determined by comparison with the experimental critical temperature at one composition. The behavior of the alloy was examined as a function of the other parameter p , which may be determined by comparison with experimental determinations of three phase equilibria.

It was not possible to determine p by examining the energy of the alloys. The energy of alloys with the AB superlattice showed little variation as a function of p . The same may be said for the AB_3 and A_3B superlattices except for a small change in the energy given off on the formation of long range order.

The long range order of AB alloys decreased continuously to zero as the temperature was increased, while the AB_3 and A_3B alloys showed a discontinuity. The long range order changed very little with p except for the case of $p = .05$ in the AB_3 alloys, where the discontinuity in order was much greater than the other cases.

In all cases the short range order increased as the long range order decreased. The short range order reached a maximum at the critical temperature and decreased at higher temperatures. This

behavior of the short range order is a consequence of the definitions used in this treatment.

The most dramatic effect of p was seen in the phase diagrams. For $p = 0$ and $p = .025$ three maxima (25%, 50%, 75%) were predicted. For $p = 0$ two eutectoids were predicted. For $p = -.025$ one maximum (50%) was predicted. Two peritectoids were also predicted for this value of p .

The above results were compared with the experimental determination of the copper gold system. Best agreement with the experimental results was obtained for p between $-.005$ and $-.01$ and $\Delta E_{ab}^1 (m_{Cu} = .5) / k = 4430^\circ K$. This value of p would indicate a .5 to 1.0 percent energy contribution from the even shells as compared to the odd shells. The negative value of p indicates that like neighbors are favored in even shells, while unlike neighbors are favored in odd shells.

A theory to explain the magnetic properties of alloys has been developed. The theory is able to predict the magnetic moments and Curie temperatures of pure iron, cobalt, and nickel as well as many of their alloys in both the ordered and disordered states. The agreement with experiment in almost all cases is very good. The theory points out the importance of the electrons in the unfilled 3d subshell in determining both the magnetic moment and Curie temperature. The constant, θ_0 , needed to determine the magnitude of the Curie temperatures was determined to be equal to $230^\circ K$.

It was found that the state of order in an alloy may affect the magnetic properties, i. e. magnetic moment and Curie temperature, in two ways: 1) by changing the magnetic species present; and 2) by

changing the form of the equation for the Curie temperature. The alloy Ni_3Mn was found to have a critical dependence on long range order. By comparison of the experimental and theoretical properties it was possible to obtain a value for the magnetic interaction parameter, $\lambda_1 \approx 1$. This value of λ_1 means that the magnetic interaction is confined almost completely to the atoms in odd shells.

References

1. G. Tammann, Z. Anorg. Chem. 107, 1 (1919).
2. C. H. Johansson and J. O. Linde, Ann. Physik [4] 78, 439 (1925).
3. F. C. Nix, H. G. Beyer, and J. R. Dunning, Phys. Rev. 58, 1031 (1940).
4. L. H. Germer, F. E. Howarth, and J. J. Lander, Phys. Rev. 61, 614 (1942).
5. D. T. Keating and B. E. Warren, J. Appl. Phys. 22, 286 (1951).
6. J. M. Contey, J. Appl. Phys. 21, 24 (1950).
7. W. Gorsky, Z. Physik 50, 64 (1928).
8. G. Borelius, C. M. Johansson, and J. O. Linde, Ann. Physik [4] 86, 291 (1928).
9. C. Wagner and W. Schottky, Z. Physik. Chem. B11; 163 (1931).
10. U. Dehlinger and L. Graf, Z. Physik 64, 359 (1930).
11. W. L. Bragg and E. J. Williams, Proc. Roy. Soc. A145, 699 (1934); A151, 540 (1935); E. J. Williams, Proc. Roy. Soc. A152, 231 (1935).
12. H. Bethe, Proc. Roy. Soc. A150, 552 (1935).
13. R. Peierls, Proc. Roy. Soc. A154, 207 (1936).
14. T. S. Chang, Proc. Roy. Soc. A161, 546 (1937); Proc. Cambridge Phil. Soc. 34, 224 (1938); 35, 265 (1939).
15. E. E. Easthope, Proc. Cambridge Phil. Soc. 33, 502 (1937).
16. J. M. Cowley, Phys. Rev. 77, 669 (1950); 120, 1648 (1960).
17. G. Fournet, Compt. rend. reunion ann. avec Comm. Thermodynam. Union intern. phys. (Paris). Changements de phases, p. 199, 1952; J. phys. radium 14; 226 (1953).
18. E. M. Grabbe, Phys. Rev. 57, 728 (1940).
19. L. Pauling, Phys. Rev. 54, 899 (1938).
20. D. H. Martin, Magnetism in Solids, 30 (1967).
21. J. E. Goldman and R. Smoluchowski, Phys. Rev. 75, 140 (1949).

References, (Cont'd).

22. R. Smoluchowski, Phys. Rev. 84, 511 (1951).
23. H. Soto, Nippon Butsuri Gakkai-Shi 3, 1, 8, 16 (1958); J. Phys. Soc. Japan 6, 223 (1951); Sci. Repts. Research Insts. Tôhoku Univ. A3, 13 (1951); H. Soto and H. Yamamoto, J. Phys. Soc. Japan 6, 65 (1951).
24. T. Muto, T. Eguchi, and M. Shibuya, J. Phys. Soc. Japan 3, 277, 284 (1948).
25. Bell, Lavis, and Fairburn, Phil. Mag. 11, 937; 13, 477, 15, 587.
26. Stoner, E. C. Phil. Mag. [7] 15, 1018-34. (1933).
27. Marian, V. Ann. physique [11] 7, 349-527 (1937).
28. Weiss, P., Foëx, G. Intl. Crit. Tables 6, 366 (1929).
29. Sadron, C. Ann. physique [10] 17, 371-452 (1932).
30. Schramm, J., Z. Metallkunde 33, 347-55 (1941).
31. Masumoto, H., Sci. Repts. Tôhoku Imp. Univ., Sendai, 449-77 (1926).
32. Weiss, P., Forrer, M., Birch, F., Compt. rend. 189, 789-91 (1929).
33. Broniewski, W., Pietrek, W., Compt. rend. 201, 206-8 (1935).
34. Merica, P., Chem. and Metallurgical Eng. 24, 377 (1921).
35. Bando, Y., J. Phys. Soc. Japan 19, 237 (1964).
36. Crangle, J. and Hallam, G.C., Proc. Roy. Soc. 272, 119 (1963).
37. Hahn, R., and Kneller, E., Z. Metallkunde 49, 426 (1958).
38. Piercy, G. R. and Morgan, E. R., Cand. J. of Phys. 31, 529 (1953).
39. Bardos, D. I., J. Appl. Phys. 40, 1372 (1969).
40. Bozorth, R. M., Ferromagnetism, D. Van Nostrand Co. (1951).
41. Crangle, J., Phil. Mag. 2, 659 (1957).
42. Farcas, J., Ann. physique [11] 8, 146-52 (1937).
43. Fallot, M., Ann. physique [11] 6, 305-87 (1936).

References, (Cont'd.)

44. Shull, C. G. and Wilkinson, M. K., Phys. Rev. 97, 304 (1955).
45. Marcinkowski, M. J., and Brown, N., J. Appl. Phys. 32, 375 (1961).
46. Weiss, P. and Forrer, R., Ann. Phys. 12, 279 (1929).
47. Anderson, P.W., Phys. Rev., 124, 41 (1961).

Appendix I

Values of $N(H, i, I, k, J, j) / N_{IH}^i$

for various lattice structures and sublattices

Face centered cubic AB_3

$k=1$

i	j	H I J	H I J	H I J	H I J	H I J
		ABA	ABB	BBA	BBB	BAB
1	1	0	4	2	2	4
	2	2	0	0	2	2
	3	0	4	2	2	4
	4	1	0	0	1	1
3	1	0	2	1	1	2
	2	1	0	0	1	1
	3	0	2	1	1	2
	4	2	0	0	2	2
	5	0	2	1	1	2
	6	1	0	0	1	1
	7	0	2	1	1	2
5	2	1	0	0	1	1
	3	0	2	1	1	2
	4	1	0	0	1	1
	5	0	2	1	1	2
	7	0	2	1	1	2
	8	1	0	0	1	1
7	3	0	1	.5	.5	1
	4	1	0	0	1	1
	5	0	1	.5	.5	1
	6	1	0	0	1	1
	7	0	2	1	1	2
9	4	1	0	0	1	1
	7	0	4	2	2	4
	11	2	0	0	2	2
	10	5	0	2	1	1
10	7	0	2	1	1	2
	8	1	0	0	1	1
	11	2	0	0	2	2

i	j	H I J	H I J	H I J
		BBA	BBB	AAB
2	1	$\frac{4}{3}$	$\frac{8}{3}$	4
	3	$\frac{4}{3}$	$\frac{8}{3}$	4
	5	$\frac{4}{3}$	$\frac{8}{3}$	4
4	1	$\frac{1}{3}$	$\frac{2}{3}$	1
	3	$\frac{4}{3}$	$\frac{8}{3}$	4
	5	$\frac{2}{3}$	$\frac{4}{3}$	2
	7	$\frac{4}{3}$	$\frac{8}{3}$	4
	9	$\frac{1}{3}$	$\frac{2}{3}$	1
6	3	1	2	3
	7	2	4	6
8	5	$\frac{4}{3}$	$\frac{8}{3}$	4
	10	$\frac{4}{3}$	$\frac{8}{3}$	4
11	5	$\frac{1}{3}$	$\frac{2}{3}$	1
	7	$\frac{2}{3}$	$\frac{4}{3}$	2
	9	$\frac{1}{3}$	$\frac{2}{3}$	1
	10	$\frac{2}{3}$	$\frac{4}{3}$	2

Note: All values not listed equal 0.

$$i, j = 9 \Rightarrow (x, y, z) = (\frac{3}{2}, \frac{3}{2}, 0)$$

$$i, j = 10 \Rightarrow (x, y, z) = (2, \frac{1}{2}, \frac{1}{2})$$

Face centered cubic AB_3 (cont'd.)

k = 2

i	j	HIJ	HIJ	HIJ	i	j	HIJ	HIJ																																																									
		ABB	BBB	BAA			AAA	BBB																																																									
1	1	2	2	2	2	4	4	4																																																									
	3	2	2	2		8	1	1																																																									
	5	2	2	2	4	2	2	2																																																									
3	1	1	1	6		2	2																																																										
	3	2	2	11		2	2																																																										
	7	2	2	2	6	4	3	3																																																									
10	1	1	1	5		1	1	1	1	8	2	1	1	5	1	1	1	11	4	4	7	2	2	2	11	4	1	1	9	1	1	1	8	1	1	7	3	1	1	1	11	8	1	1	5	1	1	1	7	1	1	1	9	5	2	2	2	10	3	1	1	1	10	2	2
5	1	1	1		1	8	2	1	1																																																								
	5	1	1		1		11	4	4																																																								
	7	2	2	2	11		4	1	1																																																								
9	1	1	1	8		1	1																																																										
7	3	1	1	1		11	8	1	1																																																								
	5	1	1	1																																																													
	7	1	1	1																																																													
9	5	2	2	2																																																													
10	3	1	1	1																																																													
	10	2	2	2																																																													

Face centered cubic AB

k = 1

k = 2

k = 1					k = 2									
i	j	HIJ	HIJ	HIJ	HIJ	i	j	HIJ	HIJ	i	j	HIJ	HIJ	
		AAA	BAA	ABA	BBA			AAA	BBA			AAA	BAA	
		BBB	ABB	BAB	AAB			BBB	AAB			BBB	ABB	
1	1	0	2	2	4	2	1	$\frac{4}{3}$	$\frac{8}{3}$	1	1	2	2	
	2	2	0	2	0		3	$\frac{4}{3}$	$\frac{8}{3}$		3	2	2	
	3	0	2	2	4		5	$\frac{4}{3}$	$\frac{8}{3}$		5	2	2	
	4	1	0	1	0						2	4	0	
3	1	0	1	1	2	4	1	$\frac{1}{3}$	$\frac{2}{3}$	3	1	1	1	
	2	1	0	1	0		3	$\frac{4}{3}$	$\frac{8}{3}$		3	2	2	
	3	0	1	1	2		5	$\frac{2}{3}$	$\frac{4}{3}$		7	2	2	
	4	2	0	2	0		7	$\frac{4}{3}$	$\frac{8}{3}$		10	1	1	
	5	0	1	1	2	6	3	1	2	4	2	2	0	
	6	1	0	1	0		7	2	4		6	2	0	
	7	0	1	1	2						11	2	0	
5	2	1	0	1	0	8	5	$\frac{4}{3}$	$\frac{8}{3}$	5	1	1	1	
	3	0	1	1	2		10	$\frac{4}{3}$	$\frac{8}{3}$		5	1	1	
	4	1	0	1	0	11	5	$\frac{1}{3}$	$\frac{2}{3}$		7	2	2	
	5	0	1	1	2		7	$\frac{2}{3}$	$\frac{4}{3}$		9	1	1	
	7	0	1	1	2		9	$\frac{1}{3}$	$\frac{2}{3}$		6	4	3	0
	8	1	0	1	0		10	$\frac{2}{3}$	$\frac{4}{3}$			3	1	1
7	3	0	.5	.5	1	7	5	1	1	7	5	1	1	
	4	1	0	1	0		7	1	1		7	1	1	
	5	0	.5	.5	1		0	0	0		8	2	1	0
	6	1	0	1	0		0	1	1		11	4	0	
	7	0	1	1	2		0	0	1		9	5	2	2
	9	0	0	1	1		0	1	1		10	3	1	1
	10	0	1	0	1		0	1	0			10	2	2
9	4	1	0	1	0	9	4	1	0	11	4	1	0	
	7	0	2	2	4		11	2	0		8	1	0	
	11	2	0	2	0									
10	5	0	1	1	2	10	5	0	1	2	10	5	0	1
	7	0	1	1	2		7	0	1	2		7	0	1
	8	1	0	1	0		8	1	0	1		0	1	0
	11	2	0	2	0		11	2	0	2		0	2	0

Note: All values not listed equal 0. $i, j = 9 \Rightarrow (x, y, z) = (\frac{3}{2}, \frac{3}{2}, 0)$;

$i, j = 10 \Rightarrow (x, y, z) = (2, \frac{1}{2}, \frac{1}{2})$

Body centered cubic AB

k = 1						k = 2						
i	j	HIJ	i	j	HIJ	i	j	HIJ	i	j	HIJ	
		ABA			AAB			AAA			BAA	
		BAB			BBA			BBB			ABB	
1	2	3	2	1	4	2	3	4	1	1	3	
	3	3		4	4		4	4		3		
	5	1		4	4		1	3				
4	2	1	3	1	2	3	3	2	4	1	1	
	3	2		4	4		4	4		1	2	
	5	1	7	2	7	2	7	2	11	2	1	
	6	1	5	1	1	5	3	3	7	4	2	
	8	2		4	3		7	1		7	1	
9	1	11	1	1	11	1	4	11	1	1		
7	3	1	6	4	4	6	2	1	10	4	1	
	5	1		10	4		4	8		1	10	2
	8	2		4	2		2	9		2	7	3
9	2	2	8	7	2	8	1	11	7	3		
10	6	1	8	4	2	8	6	1	9	5	1	
	8	2		7	2		5	2				
	9	1		10	2		8	2				
11	5	1	9	4	1	9	5	1	9	8	2	
	9	3		7	2		8	2				
				10	1							
				11	1							

Note: $i, j = 10 \Rightarrow (x, y, z) = (5/2, 1/2, 1/2)$; $i, j = 11 \Rightarrow (x, y, z) = (3/2, 3/2, 3/2)$

Appendix II

Energy of a binary alloy on two sublattices

Equation (15) states

$$\begin{aligned}
 E_{\text{LRO}} &= \frac{1}{2} N \sum_{n\beta\gamma IJ} n_I X_{\beta}^{(I)} X_{\gamma}^{(J)} w_{JI}^n E_{\beta\gamma}^n \\
 &= \frac{1}{2} N \sum_{n\beta\gamma IJ} n_I w_{JI}^n (X_{\beta}^{(I)} - m_{\beta}) (X_{\gamma}^{(J)} - m_{\gamma}) E_{\beta\gamma}^n \\
 &\quad + \frac{1}{2} N \sum_{n\beta\gamma IJ} n_I w_{JI}^n (m_{\beta} X_{\gamma}^{(J)} + m_{\gamma} X_{\beta}^{(I)} - m_{\beta} m_{\gamma}) E_{\beta\gamma}^n
 \end{aligned}$$

Using equations (1), (2), (5), and (13)

$$E_{\text{LRO}}/N = \frac{1}{2} \sum_{n\beta\gamma} m_{\beta} m_{\gamma} E_{\beta\gamma}^n + \frac{1}{2} \sum_{n\beta\gamma IJ} n_I w_{JI}^n (X_{\beta}^{(I)} - m_{\beta}) (X_{\gamma}^{(J)} - m_{\gamma}) E_{\beta\gamma}^n$$

Let $E_{\beta\gamma} = \frac{1}{2} \sum_n E_{\beta\gamma}^n$ = energy of a β atom in pure γ .

$$\begin{aligned}
 E_{\text{LRO}}/N &= \sum_{\beta\gamma} m_{\beta} m_{\gamma} E_{\beta\gamma} + \frac{1}{2} \sum_{n\beta\gamma IJ} n_I w_{JI}^n (X_{\beta}^{(I)} - m_{\beta}) (X_{\gamma}^{(J)} - m_{\gamma}) (E_{\beta\gamma}^n - E_{\gamma\gamma}^n) \\
 &\quad + \frac{1}{2} \sum_{n\beta\gamma IJ} n_I w_{JI}^n (X_{\beta}^{(I)} - m_{\beta}) (X_{\gamma}^{(J)} - m_{\gamma}) E_{\gamma\gamma}^n
 \end{aligned}$$

Using equations (3) and (4):

$$\begin{aligned}
E_{\text{LRO}/N} &= \sum_{\beta\gamma} m_{\beta} m_{\gamma} E_{\beta\gamma} + \frac{1}{2} \sum_{n\beta\gamma IJ} n_I w_{JI}^n (X_{\beta}^{(I)} - m_{\beta})(X_{\gamma}^{(J)} - m_{\gamma})(E_{\beta\gamma}^n - E_{\gamma\gamma}^n) \\
&= \sum_{\beta\gamma} m_{\beta} m_{\gamma} E_{\beta\gamma} + \frac{1}{4} \sum_{nIJ\beta\gamma} n_I w_{JI}^n (X_{\beta}^{(I)} - m_{\beta})(X_{\gamma}^{(J)} - m_{\gamma})(E_{\beta\gamma}^n - E_{\gamma\gamma}^n) \\
&\quad + \frac{1}{4} \sum_{nIJ\beta\gamma} n_I w_{JI}^n (X_{\gamma}^{(I)} - m_{\gamma})(X_{\beta}^{(J)} - m_{\beta})(E_{\gamma\beta}^n - E_{\beta\beta}^n)
\end{aligned}$$

Using equations (13) and (14) and interchanging dummy indices:

$$E_{\text{LRO}/N} = \sum_{\beta\gamma} m_{\beta} m_{\gamma} E_{\beta\gamma} + \frac{1}{4} \sum_{nIJ\beta\gamma} n_I w_{JI}^n (X_{\beta}^{(I)} - m_{\beta})(X_{\gamma}^{(J)} - m_{\gamma})(2E_{\beta\gamma}^n - E_{\beta\beta}^n - E_{\gamma\gamma}^n)$$

$$\text{Let } \Delta E_{\beta\gamma}^n = \frac{1}{2}(E_{\beta\beta}^n + E_{\gamma\gamma}^n - 2E_{\beta\gamma}^n)$$

$$E_{\text{LRO}/N} = \sum_{\beta\gamma} m_{\beta} m_{\gamma} E_{\beta\gamma} - \frac{1}{2} \sum_{nIJ\beta\gamma} n_I w_{JI}^n (X_{\beta}^{(I)} - m_{\beta})(X_{\gamma}^{(J)} - m_{\gamma}) \Delta E_{\beta\gamma}^n$$

Consider the case of two sublattices. From equations (1) and (5):

$$n_A (X_{\beta}^{(A)} - m_{\beta}) = n_B (m_{\beta} - X_{\beta}^{(B)})$$

$$\begin{aligned}
E_{\text{LRO}/N} &= \sum_{\beta\gamma} m_{\beta} m_{\gamma} E_{\beta\gamma} - \frac{1}{2} \sum_{n\beta\gamma J} \Delta E_{\beta\gamma}^n \left\{ n_J w_{JJ}^n (X_{\beta}^{(J)} - m_{\beta})(X_{\gamma}^{(J)} - m_{\gamma}) \right. \\
&\quad \left. + \sum_{I \neq J} n_I w_{JI}^n (X_{\beta}^{(I)} - m_{\beta})(X_{\gamma}^{(J)} - m_{\gamma}) \right\} \\
&= \sum_{\beta\gamma} m_{\beta} m_{\gamma} E_{\beta\gamma} + \frac{1}{2} \sum_{n\beta\gamma J} \Delta E_{\beta\gamma}^n \sum_{I \neq J} n_I (w_{JJ}^n - w_{JI}^n) (X_{\beta}^{(I)} - m_{\beta})(X_{\gamma}^{(J)} - m_{\gamma})
\end{aligned}$$

Using equation (13):

$$E_{LRO/N} = \sum_{\beta\gamma} m_{\beta} m_{\gamma} E_{\beta\gamma} + \frac{1}{2} \sum_{n\beta\gamma} \Delta E_{\beta\gamma}^n (w_{AA}^n - w_{AB}^n) \left\{ n_B (X_{\beta}^{(B)} - m_{\beta}) (X_{\gamma}^{(A)} - m_{\gamma}) \right. \\ \left. + n_A (X_{\beta}^{(A)} - m_{\beta}) (X_{\gamma}^{(B)} - m_{\gamma}) \right\}$$

Using equations (1), (3), and (4) for a binary alloy:

$$E_{LRO/N} = m_a E_{aa} + m_b E_{bb} - m_a m_b (E_{aa} + E_{bb} - 2E_{ab}) \\ + \sum_n \Delta E_{ab}^n (w_{AA}^n - w_{AB}^n) (X_a^{(A)} - m_a) (m_a - X_a^{(B)}) \quad (19)$$

Equation (12) states:

$$E_{SRO} = \frac{1}{2} \sum_{ijk\alpha\beta\gamma HIJ} n_H N(H, i, I, k, J, j) X_{\alpha}^{(H)} X_{\beta}^{(I)} X_{\gamma}^{(J)} q_j(\beta I | \alpha H) q_j(\gamma J | \alpha H) E_{\beta\gamma}^{(r_k)}$$

For the case of a binary alloy, equations (9ab) yield:

$$E_{SRO} = \frac{1}{2} \sum_{ijk\alpha HIJ} n_H N(H, i, I, k, J, j) X_{\alpha}^{(H)} \\ \left\{ X_a^{(I)} X_a^{(J)} q_j(aI | \alpha H) q_j(aJ | \alpha H) E_{aa}^{(r_k)} \right. \\ \left. + X_a^{(I)} X_b^{(J)} q_j(aI | \alpha H) \left[- \frac{X_a^{(J)}}{X_b^{(J)}} q_j(aJ | \alpha H) \right] E_{ab}^{(r_k)} \right. \\ \left. + X_b^{(I)} X_a^{(J)} \left[- \frac{X_a^{(I)}}{X_b^{(I)}} q_j(aI | \alpha H) \right] q_j(aJ | \alpha H) E_{ba}^{(r_k)} \right. \\ \left. + X_b^{(I)} X_b^{(J)} \left[- \frac{X_a^{(I)}}{X_b^{(I)}} q_j(aI | \alpha H) \right] \left[- \frac{X_a^{(J)}}{X_b^{(J)}} q_j(aJ | \alpha H) \right] E_{bb}^{(r_k)} \right\} \\ = \sum_{ijk\alpha HIJ} n_H N(H, i, I, k, J, j) X_{\alpha}^{(H)} X_a^{(I)} X_a^{(J)} q_j(aI | \alpha H) q_j(aJ | \alpha H) \frac{\Delta E_{ab}^{(r_k)}}{N^k}$$

where $\Delta E_{ab}(r_k) = \frac{1}{2}N^k (E_{aa}(r_k) + E_{bb}(r_k) - 2E_{ab}(r_k))$

and $E_{ab}(r_k) = E_{ba}(r_k)$

Using equations (10a), (9a), and (4):

$$E_{SRO} = \sum_{ijkHIJ} n_H N(H,i,I,k,J,j) \frac{X_a(H)}{X_b(H)} X_a(I) X_a(J) q_{IH}^i q_{JH}^j \frac{\Delta E_{ab}(r_k)}{N^k}$$

where

$$q_{IH}^i = q_i(aI|aH) \quad \text{and} \quad q_{JH}^j = q_j(aJ|aH)$$

It is convenient to perform the summations for $i=0$ and for $j=0$.

$$\begin{aligned} E_{SRO} &= \sum'_{iIJ} n_J N_{IJ}^i X_a(I) X_a(J) q_{IJ}^i \frac{\Delta E_{ab}(r_i)}{N^i} \\ &+ \sum'_{jIJ} n_I N_{JI}^j X_a(I) X_a(J) q_{JI}^j \frac{\Delta E_{ab}(r_j)}{N^j} \\ &+ \sum'_{ijkHIJ} n_H N(H,i,I,k,J,j) \frac{X_a(H)}{X_b(H)} X_a(I) X_a(J) q_{IH}^i q_{JH}^j \frac{\Delta E_{ab}(r_k)}{N^k} \end{aligned}$$

where \sum' is for $i, j, k > 0$. Using equations (2) and (10a) and changing dummy indices:

$$\begin{aligned} E_{SRO} &= 2 \sum'_{iIJ} n_J N_{IJ}^i X_a(I) X_a(J) q_{IJ}^i \frac{\Delta E_{ab}(r_i)}{N^i} \\ &+ \sum'_{ijkHIJ} n_H N(H,i,I,k,J,j) \frac{X_a(H)}{X_b(H)} X_a(I) X_a(J) q_{IH}^i q_{JH}^j \frac{\Delta E_{ab}(r_k)}{N^k} \quad (20) \end{aligned}$$

Equation (17) may be simplified in much the same way as equation (12).

For a binary alloy equations (9ab) and (10ab) yield:

$$\begin{aligned}
 E'_{SRO} &= \frac{1}{2}N(1-f) \sum_{nIJ} n_I w_{JI}^n \left\{ X_a(I) X_a(J) q_n(aJ|aI) E_{aa}^n \right. \\
 &\quad + X_a(I) X_b(J) \left[-\frac{X_a(J)}{X_b(J)} q_n(aJ|aI) \right] E_{ab}^n \\
 &\quad + X_b(I) X_a(J) \left[-\frac{X_a(I)}{X_b(I)} q_n(aJ|aI) \right] E_{ba}^n \\
 &\quad \left. + X_b(I) X_b(J) \left[-\frac{X_a(I)}{X_b(I)} \frac{X_a(J)}{X_b(J)} q_n(aJ|aI) \right] E_{bb}^n \right\} \\
 &= N(1-f) \sum_{nIJ} n_I w_{JI}^n X_a(I) X_a(J) q_{IJ}^n \Delta E_{ab}^n \tag{21}
 \end{aligned}$$

Appendix III

Entropy of a binary alloy on two sublattices

From equation (22):

$$\ln W = \frac{1}{N} \sum_{i\alpha\beta HI} \ln \left(\begin{array}{c} N_{IH}^i X_{\alpha}^{(H)} n_H N \left(1 - \sum_{\gamma=1}^{\beta-1} p_i(\gamma I | \alpha H) \right) \\ N_{IH}^i X_{\alpha}^{(H)} n_H N p_i(\beta I | \alpha H) \end{array} \right)$$

Using Stirling's formula for factorials:

$$\ln \binom{AB}{AC} = A \left[B \ln B - C \ln C - (B-C) \ln(B-C) \right]$$

and

$$\begin{aligned} \ln W = \sum_{i\alpha\beta HI} n_H N_{IH}^i X_{\alpha}^{(H)} & \left\{ \left[1 - \sum_{\gamma=1}^{\beta-1} p_i(\gamma I | \alpha H) \right] \ln \left[1 - \sum_{\gamma=1}^{\beta-1} p_i(\gamma I | \alpha H) \right] \right. \\ & \left. - p_i(\beta I | \alpha H) \ln p_i(\beta I | \alpha H) - \left[1 - \sum_{\gamma=1}^{\beta} p_i(\gamma I | \alpha H) \right] \ln \left[1 - \sum_{\gamma=1}^{\beta} p_i(\gamma I | \alpha H) \right] \right\} \end{aligned}$$

For the case of a binary alloy:

$$\begin{aligned} \ln W = \sum_{iHI} n_H N_{IH}^i \left[X_a^{(H)} \right. & \left. \left\{ -p_i(aI | aH) \ln p_i(aI | aH) - \left[1 - p_i(aI | aH) \right] \ln \left[1 - p_i(aI | aH) \right] \right. \right. \\ & \left. \left. + \left[1 - p_i(aI | aH) \right] \ln \left[1 - p_i(aI | aH) \right] - p_i(bI | aH) \ln p_i(bI | aH) \right\} \right] \end{aligned}$$

$$\begin{aligned}
& - \left[1-p_i(aI|aH)-p_i(bI|aH) \right] \ln \left[1-p_i(aI|aH)-p_i(bI|aH) \right] \Big\} \\
& + X_b(H) \left\{ -p_i(aI|bH) \ln p_i(aI|bH) - \left[1-p_i(aI|bH) \right] \ln \left[1-p_i(aI|bH) \right] \right. \\
& + \left[1-p_i(aI|bH) \right] \ln \left[1-p_i(aI|bH) \right] - p_i(bI|bH) \ln p_i(bI|bH) \\
& \left. - \left[1-p_i(aI|bH) - p_i(bI|bH) \right] \ln \left[1-p_i(aI|bH) - p_i(bI|bH) \right] \right\} \Big] \\
= & - \sum_{iHI} n_H N_{IH}^i \left[X_a(H) \left\{ p_i(aI|aH) \ln p_i(aI|aH) + p_i(bI|aH) \ln p_i(bI|aH) \right\} \right. \\
& \left. + X_b(H) \left\{ p_i(aI|bH) \ln p_i(aI|bH) + p_i(bI|bH) \ln p_i(bI|bH) \right\} \right]
\end{aligned}$$

Using equations (8a), (9a), and (10a):

$$\begin{aligned}
\ln W = & - \sum_{iHI} n_H N_{IH}^i \left\{ X_a(H) G \left[X_a(I)(1+q_{IH}^i) \right] \right. \\
& \left. + X_b(H) G \left[X_a(I) \left(1 - \frac{X_a(H)}{X_b(H)} q_{IH}^i \right) \right] \right\}
\end{aligned}$$

where $G(X) = X \ln X + (1-X) \ln (1-X)$. Changing dummy indices:

$$\begin{aligned}
\ln W = & - \sum_{iIJ} n_J N_{IJ}^i \left\{ X_a(J) G \left[X_a(I)(1+q_{IJ}^i) \right] \right. \\
& \left. + X_b(J) G \left[X_a(I) \left(1 - \frac{X_a(H)}{X_b(H)} q_{IJ}^i \right) \right] \right\}
\end{aligned}$$

Appendix IV

Minimization of the free energy of short range order

From equation (20):

$$\begin{aligned} \frac{\partial E_{SRO}}{\partial q_{IJ}^i} = & \left\{ 2n_J N_{IJ}^i X_a(I) X_a(J) \frac{\Delta E_{ab}(r_i)}{N^i} \right. \\ & + \sum'_{jkH} n_J \frac{X_a(J)}{X_b(J)} X_a(I) N(J,i,I,k,H,j) X_a(H) q_{JH}^j \frac{\Delta E_{ab}(r_k)}{N^k} \\ & \left. + \sum'_{jkH} n_I \frac{X_a(I)}{X_b(I)} X_a(J) N(I,j,H,k,J,i) X_a(H) q_{IH}^j \frac{\Delta E_{ab}(r_k)}{N^k} (2-\delta_{IJ}) \right\} \end{aligned}$$

where

$$\delta_{IJ} = \begin{cases} 0 & I \neq J \\ 1 & I = J \end{cases}$$

From equation (23):

$$\begin{aligned} \frac{\partial S}{\partial q_{IJ}^i} = & -\kappa N_{IJ}^i n_J \left\{ X_a(J) X_a(I) G' \left[X_a(I) (1+q_{IJ}^i) \right] \right. \\ & \left. - X_a(J) X_a(I) G' \left[X_a(I) \left(1 - \frac{X_a(J)}{X_b(J)} q_{IJ}^i \right) \right] \right\} (2-\delta_{IJ}) \end{aligned}$$

where $G'(X) = \frac{dG}{dX} = \ln \frac{X}{1-X}$

$$\frac{\partial S}{\partial q_{IJ}^i} = -\kappa N_{IJ}^i n_J X_a(I) X_a(J) \ln \frac{X_a(I) (1+q_{IJ}^i) \left[1 - X_a(I) \left(1 - \frac{X_a(J)}{X_b(J)} q_{IJ}^i \right) \right]}{\left[1 - X_a(I) (1+q_{IJ}^i) \right] X_a(I) \left(1 - \frac{X_a(J)}{X_b(J)} q_{IJ}^i \right)}$$

(2- δ_{IJ})

$$= -\kappa N_{IJ}^i n_J X_a(I) X_a(J) \ln \frac{(1+q_{IJ}^i) \left[1 + \frac{X_a(I) X_a(J)}{X_b(I) X_b(J)} q_{IJ}^i \right]}{\left[1 - \frac{X_a(I)}{X_b(I)} q_{IJ}^i \right] \left[1 - \frac{X_a(J)}{X_b(J)} q_{IJ}^i \right]} (2-\delta_{IJ})$$

$$\frac{\partial F}{\partial q_{IJ}^i} = (2-\delta_{IJ}) n_J N_{IJ}^i X_a(I) X_a(J)$$

$$\left\{ 2 \frac{\Delta E_{ab}(r_i)}{N^i} + \sum'_{jkH} \left[\frac{N(J,i,I,k,H,j)}{N_{IJ}^i} \frac{X_a(H)}{X_b(J)} q_{JH}^j \frac{\Delta E_{ab}(r_k)}{N^k} + \frac{N(I,j,H,k,J,i)}{N_{JI}^i} \frac{X_a(H)}{X_b(I)} q_{IH}^j \frac{\Delta E_{ab}(r_k)}{N^k} \right] + \kappa T \ln \frac{(1+q_{IJ}^i) \left[1 + \frac{X_a(I) X_a(J)}{X_b(J) X_b(I)} q_{IJ}^i \right]}{\left[1 - \frac{X_a(I)}{X_b(I)} q_{IJ}^i \right] \left[1 - \frac{X_a(J)}{X_b(J)} q_{IJ}^i \right]} \right\} = 0$$

Dividing out terms and using the symmetry of $N(I, j, H, k, J, i)$:

$$\frac{2\Delta E_{ab}(r_i)}{N \kappa T} + \ln \frac{(1+q_{IJ}^i) \left[1 + \frac{X_a(I) X_a(J)}{X_b(I) X_b(J)} q_{IJ}^i \right]}{\left[1 - \frac{X_a(I)}{X_b(I)} q_{IJ}^i \right] \left[1 - \frac{X_a(J)}{X_b(J)} q_{IJ}^i \right]} + \sum'_{jkH} \frac{\Delta E_{ab}(r_k)}{N^k \kappa T} X_a(H) \left[\frac{N(J,i,I,k,H,j)}{N_{IJ}^i} \frac{q_{JH}^j}{X_b(J)} + \frac{N(I,i,J,k,H,j)}{N_{JI}^i} \frac{q_{IH}^j}{X_b(I)} \right] = 0$$

(25)